71-28,099

McKELVEY, Jr., John Murray, 1937-
KINETICS OF IODINATION OF METHYL SUBSTITUTED BENZENES.

Georgia Institute of Technology, Ph.D., 1971
Chemistry, organic

University Microfilms, A XEROX Company, Ann Arbor, Michigan

Reproduced with permission of the copyright owner. Further reproduction prohibited without permission.

KINETICS OF IODINATION OF METHYL SUBSTITUTED BENZENES

A THESIS

Presented to

The Faculty of the Graduate Division

by

John Murray McKelvey, Jr.

In Partial Fulfillment

of the Requirements for the Degree

Doctor of Philosophy

in the School of Chemistry

Georgia Institute of Technology

April, 1971

Reproduced with permission of the copyright owner. Further reproduction prohibited without permission.

KINETICS OF IODINATION OF METHYL SUBSTITUTED BENZENES

Approved:

Chairman

Date approved by Chairman: 4-15-71

Reproduced with permission of the copyright owner. Further reproduction prohibited without permission.

In presenting the dissertation as a partial fulfillment of the requirements for an advanced degree from the Georgia Institute of Technology, I agree that the Library of the Institute shall make it available for inspection and circulation in accordance with its regulations governing materials of this type. I agree that permission to copy from, or to publish from, this dissertation may be granted by the professor under whose direction it was written, or, in his absence, by the Dean of the Graduate Division when such copying or publication is solely for scholarly purposes and does not involve potential financial gain. It is understood that any copying from, or publication of, this dissertation which involves potential financial gain will not be allowed without written permission.

John Murray McKelvey Jr.

7/25/68

Reproduced with permission of the copyright owner. Further reproduction prohibited without permission.

ACKNOWLEDGMENTS

I am indebted to Dr. E. Grovenstein, Jr. for his advice and assistance during the course of this work, and for financial assistance as derived from research assistantships. I am grateful to Drs. R. A. Pierotti and H. M. Neumann for serving on the reading committee and for giving additional advice. Dr. W. H. E. provided much encouragement. I am also indebted to fellow graduate students for their assistance. The staff of the School of Chemistry (especially E.B., D.L., M.R., and G.O.) gave many hours of their time.

The award of an American Chemical Society Petroleum Research Foundation Fellowship is thankfully acknowledged.

Drs. J. E. Bloor and Bruce Gilson of the Chemistry Department, University of Virginia, and Dr. Paul Dobosh of Carnegie Mellon University kindly provided the molecular orbital programs used in this study. The assistance of the Rich Electronic Computer Center is acknowledged, as well as a few frustrations.

The families of Drs. R. J. Sullivan and T. H. Longfield provided many hours of enjoyment and assistance. The assistance of Mr. James B. Ramage, Sr. of Atlanta, and Mr. Don Everett of Rome, Georgia in the early part of my college education is acknowledged.

The help of Miss Mary Ann Gruters in preparing the rough draft of this thesis is happily acknowledged. Mrs. Lydia Geeslin is to be thanked for her assistance in editing and typing the final draft.

Most of all I am indebted to my family, especially my parents, for their faith, encouragement, and prayers during this effort.

Reproduced with permission of the copyright owner. Further reproduction prohibited without permission.

TABLE OF CONTENTS

	Page
ACKNOWLEDGMENTS	ii
LIST OF TABLES	v
LIST OF FIGURES	vii
SUMMARY	viii
Chapter	
I. INTRODUCTION	1
Background	1
Hydrogen Isotope Effects	4
Correlation of Structure with Reactivity	9
Solvents	12
Purpose of This Thesis	12
II. PREPARATION AND PURIFICATION OF MATERIALS USED	14
Hydrocarbons	14
Other Materials Used	18
III. GENERAL PROCEDURE FOR STUDY OF REACTION KINETICS	20
Kinetic Measurements	20
Preparation of Solutions	21
Calculation of Rate Constants	23
IV. IODINATION OF MESITYLENE, ANISOLE, AND m-XYLENE	29
Introduction	29
New Experimental Results	35
Discussion of Possible Mechanisms	42
Mechanism I	42
Mechanism II	43
Mechanism III	44
Mechanism IV	44
Mechanism V	45
Possible Dependence of k*I on Ionic Strength	48

Reproduced with permission of the copyright owner. Further reproduction prohibited without permission.

TABLE OF CONTENTS (Concluded)

Chapter		Page
	Discussion	51
	The Dependence on Silver Ion	53
	The Effect of Temperature on Silver Ion Dependence	
	The Effect of Silver Ion on the Isotope Effect	
	The Influence of Variations in Iodine Concentration	61
	The Influence of Variation in Ionic Strength	61
	Conclusions from the Study of Mesitylene, Anisole, and m-Xylene	62
V.	KINETICS AND RELATIVE REACTIVITIES OF BENZENE AND OTHER METHYLATED DERIVATIVES	64
	Introduction	64
	Experimental Results	66
	Discussion	78
	Isotope Effects	78
	Product Isolation and Partial Rate Factors	83
	Thermodynamic Parameters	98
	Molecular Orbital Calculations	107
	Conclusions	115
VI.	RECOMMENDATIONS FOR FUTURE WORK	118
APPENDICES		119
A.	SOLUTION TO GENERAL RATE EQUATION	120
B.	SOLUTION TO BLANK REACTION EQUATION	123
C.	SAMPLE CALCULATION	124
D.	METHYL GROUP GEOMETRIES	126
BIBLIOGRAPHY		128
VITA		133

Reproduced with permission of the copyright owner. Further reproduction prohibited without permission.

LIST OF TABLES

Table		Page
1..	Mesitylene Rate Constants Determined at 25.0° in the Presence of Ag^+ and 0.10 M $HClO_4$.	30
2.	Mesitylene-d_3 Rate Constants Determined at 25.0° in the Presence of Ag^+ and 0.10 M $HClO_4$.	31
3.	Mesitylene Rate Constants Determined at 35.0° in the Presence of Ag^+ and 0.10 M $HClO_4$.	31
4.	m-Xylene Rate Constants Determined in the Presence of Ag^+ and 0.10 M $HClO_4$	32
5.	Anisole Rate Constants Determined at 25.0° in the Presence of Ag^+ and 0.10 M $HClO_4$.	33
6.	Mesitylene Rate Constants Determined at 25.0° in the Presence of Ag^+ and $HClO_4$	33
7.	Benzene Rate Constants Determined in the Presence of Ag^+ and $HClO_4$.	67
8.	Toluene Rate Constants Determined in the Presence of Ag^+ and 0.1 M $HClO_4$.	68
9.	p-Xylene Rate Constants Determined in the Presence of Ag^+ and 0.1 M $HClO_4$.	69
10.	o-Xylene Rate Constants Determined in the Presence of Ag^+ and 0.1 M $HClO_4$.	70
11.	Durene Rate Constants Determined in the Presence of Ag^+ and 0.1 M $HClO_4$.	71
12.	Prehnitene Rate Constants Determined in the Presence of Ag^+ and 0.1 M $HClO_4$.	72
13.	Pentamethylbenzene Rate Constants Determined in the Presence of Ag^+ and 0.1 M $HClO_4$	73
14.	Thermodynamic Properties of Kinetic Studies Done in the Presence of Ag^+.	76
15.	Isotope Effects Determined in 0.1 M $HClO_4$.	79

Reproduced with permission of the copyright owner. Further reproduction prohibited without permission.

LIST OF TABLES (Concluded)

Table		Page
16.	Observed and Calculated Rate Constants Relative to Benzene.	88
17.	Comparison of Observed and Calculated Rate Constants at 60° Calculated from Partial Rate Factors of Ogata and Aoki.	93
18.	Hammett Data for Iodination and Bromination in H_2O	96
19.	Correlation of $(\Delta S^{\ddagger})_{obs}$ with a Dipole Model.	103
20.	Relative Proton Affinities and Relative Rate	106
21.	Ground State (G.S.) and Proton Complex (P.C.) Properties from CNDO Calculations.	112

Reproduced with permission of the copyright owner. Further reproduction prohibited without permission.

LIST OF FIGURES

Figure		Page
1.	Plots of 1/k*I Versus (ArH).	34
2.	Plot of $\log_{10}$ (k*I/T) Versus 1/T	36
3.	Plots of k*I Versus Time of Reaction	37
4.	Plot of k*I for Mesitylene Versus Initial (I_2)	38
5.	Plot of Dependence of k*I on Quarter-life of I_2.	41
6.	Plot of Observed Relative Rates for Iodination in H_2O Versus Those Calculated from Partial Rate Factors.	90
7.	Comparison of Partial Rate Factors Determined in H_2O and HOAC-HO_2AH.	92
8.	Hammett Plots for Iodination and Bromination in H_2O	95
9.	Comparison of Partial Rate Factors for Iodination and Bromination with Equilibrium Constants for Proton Complex Formation	97
10.	Correlation of $(\Delta S^{\ddagger})_{obs}$ with Dipole Model.	104
11.	Plot of Log (Partial Rate Factors) for Iodination in H_2O Versus Calculated Proton Affinities.	105
12.	Additivity Principle Correlations.	110

Reproduced with permission of the copyright owner. Further reproduction prohibited without permission.

SUMMARY

The kinetics of the iodination of benzene, toluene, o-xylene, m-xylene, p-xylene, prehnitene, mesitylene, and pentamethylbenzene in aqueous solution have been studied as a function of the concentration of iodine, iodide ion, and hydrocarbon.

A major purpose of this research was to elucidate the kinetic behavior of mesitylene in the presence of silver ion. Previous studies near 10^{-6} M iodide ion concentration in the absence of silver ion indicated the following mechanism

$$I_2 + H_2O \underset{k_{-1}}{\overset{k_1}{\rightleftharpoons}} H_2OI^+ + I^-$$

$$H_2OI^+ + ArH \underset{k_{-3}}{\overset{k_3}{\rightleftharpoons}} ArHI^+ + H_2O$$

$$ArHI^+ + H_2O \xrightarrow{k_5} ArI + H_3O^+$$

The previous studies also showed the rate law

$$\frac{-d[I_2]}{dt} = k^*I \frac{(ArH)(I_2)}{(I^-)}$$

where

$$k^*I = \frac{k_1 k_3 k_5}{k_{-1}(k_{-3} + k_5)}$$

The expression for k*I was derived from the application of the steady

Reproduced with permission of the copyright owner. Further reproduction prohibited without permission.

state approximation and the assumption that

$$k_{-1}(I^-) \gg k_3(ArH)$$

A proton isotope effect of 2.3 showed that k_3 was important in the rate determining process.

The use of silver ion to lower the iodide ion concentration both accelerates the reaction and makes questionable the above inequality involving $k_{-1}(I^-)$. The above rate law, in view of the expected attainment of the silver iodide equilibrium

$$Ag^+ + I^- \rightleftarrows AgI \qquad K_{sp} = (Ag^+)(I^-)$$

may be rewritten as:

$$\frac{-d[I_2]}{dt} = \frac{k^*I}{K_{sp}}(ArH)(I_2)(Ag^+)$$

For mesitylene, m-xylene, and anisole it was found that the numerical value of k*I was dependent on the concentration of the above three reactants.

From the kinetic results it is suggested that the more important source of H_2OI^+ in the presence of silver ion is via the processes:

$$I_2 + Ag^+ \rightleftharpoons AgI_2^+ \qquad K = \frac{(AgI_2^+)}{(Ag^+)(I_2)}$$

$$AgI_2^+ + H_2O \underset{k_{-2}}{\overset{k_2}{\rightleftharpoons}} H_2OI^+ + AgI$$

The experimental data are consistent with the results of the steady

Reproduced with permission of the copyright owner. Further reproduction prohibited without permission.

state treatment upon both H_2OI^+ and $ArHI^+$ for a mechanism involving the two sources of H_2OI^+. This gives

$$\frac{1}{k^*I} = \frac{k_{-1}\ (k_{-3} + k_5)}{k_1\ k_3\ k_5} + \frac{(Ag^+)}{K_{sp}} \frac{(ArH)}{\{k_1 + k_2 K\ (Ag^+)\}}$$

This expression predicts the observed inverse dependence of k*I on the hydrocarbon concentration at constant silver ion concentration. The second term in this expression is required because $k_{-1}(I^-)$ may be approximately equal to $k_3(ArH)$ at high concentrations of the more reactive hydrocarbons used herein. This term also requires that k*I decrease with respect to silver ion concentration but in fact the opposite effect was observed, which requires that the term becomes

$$\frac{(ArH)}{K_{sp}\ k_2 K}$$

A negative activation energy has been found for k_2K. The small decrease in k*I with silver ion concentration is due to the decreased fraction of silver ion complexed with silver iodide as AgI_2^+.

An increase of k*I with iodine concentration was found and is due to the increase of $k_{-1}(I^-)$ with respect to $k_3(ArH)$.

Through the principle of microscopic reversibility and on the assumption that the hydrolysis of AgI_2^+ is at equilibrium, it may be shown that

$$k^*I = \frac{k_2 K\ k_3\ k_5}{k_{-2}\ (k_{-3} + k_5)} = \frac{k_1\ k_3\ k_5}{k_{-1}\ (k_{-3} + k_5)}$$

Rate constants may then be compared both in the presence (first term) and

Reproduced with permission of the copyright owner. Further reproduction prohibited without permission.

in the absence (second term) of silver ion.

The presence of silver ion does not affect the isotope effect when k*I is independent of the reactant concentrations. Over the iodide ion concentration range from 10^{-11} M to 10^{-4} M the isotope effect is ca. 2.3 for mesitylene.

The second purpose of this research was to study the overall effect of structure upon the reactivity of methyl substituted benzene molecules toward H_2OI^+. The reactivity was found to parallel that for other electrophilic substitution reactions such as chlorination, bromination, iodination by AcOI, and oxygenation by $O(^3P)$. The reaction of H_2OI^+ with a methyl substituted hydrocarbon is characterized by a primary isotope of 2.3 which is increased to 2.9 when steric hindrance is apparent at the reaction center. Where the isotope effect is approximately constant, then the relative reactivity is due solely to the relative rate of attack of H_2OI^+ on the hydrocarbon.

The 10^6 fold range of relative reactivities of the methyl substituted benzene derivatives is readily estimated from relative energies of the respective proton complexes as obtained from CNDO/2 molecular orbital calculations. These calculations give a good account of the stabilization of the transition state by the participation of the methyl group through hyperconjugation.

Water has been found to be a suitable solvent in which nonpolar hydrocarbons may be studied. As water allows some characterization of the ionic inorganic chemistry involved, more understanding of the organic portion is available.

Reproduced with permission of the copyright owner. Further reproduction prohibited without permission.

CHAPTER I

INTRODUCTION

Background

Electrophilic halogenation of aromatic compounds has been studied by many workers and from these studies a review[1] of the relative reactivities of various halogenating reagents has recently been made by Berliner. Following the work of Melander[2] the mechanism of aromatic halogenation has been generally accepted as a two step mechanism. One such mechanism may be represented by

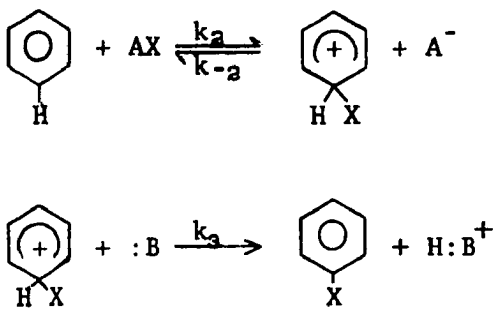

where A is a halogen atom different from or the same as X. In the case where molecular halogen is not effective, a reagent containing positively charged halogen may be involved, and the mechanism must be different.

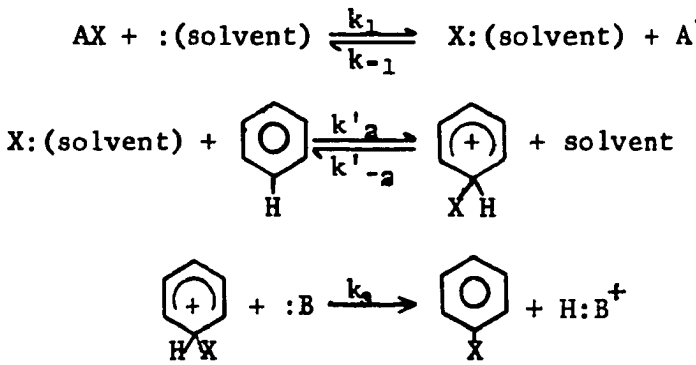

Reproduced with permission of the copyright owner. Further reproduction prohibited without permission.

A third, more general type, mechanism would be one in which the two mechanisms given above are limiting cases and in which both mechanisms can be simultaneously operative. On the basis of previous work on the kinetics of iodination of phenoxide anion, Grovenstein and coworkers[3,4] concluded that no differentiation between the first two mechanisms could be made, i.e., it could only be stated that the transition state is positively charged and contains a halogen atom. Grovenstein and Aprahamian,[5] however, were able to make such a distinction for p-nitrophenol. Very recently Sullivan and Grovenstein[6] have amplified the work on the p-nitrophenoxide anion and phenoxide anion and in addition studied the 2,4-dinitrophenoxide anion and were able to distinguish between the two mechanisms.

The experimental rate law

$$-\frac{d[I_2]}{dt} = \frac{dx}{dt} = k_{app}\,[(ArH)_0 - X][(I_2)_0 - X]$$

gives at zero percent reaction

$$k^* \equiv k^0_{app}\,\frac{(I_2)_0}{(I_2)_0 - (HOI)_0 - (I_3^-)_0}$$

where HOI represents the amount of iodine hydrolyzed and I_3^- represents any I_2 present as the triiodide anion at zero percent reaction. Here k_{app} is an apparent rate constant. The concentration of a reagent at zero percent reaction is denoted by $(\ )_0$ throughout this thesis. The value of k_{app} extrapolated to zero percent reaction is denoted a k^0_{app}. The first mechanism, involving I_2 as the halogenating agent and water as

Reproduced with permission of the copyright owner. Further reproduction prohibited without permission.

the base B then gives

$$\frac{1}{k^*} = \frac{k_{-2}}{k_2 k_3} (I^-) + \frac{1}{k_2}$$

where here (I^-) is the actual iodide ion concentration at zero percent reaction, i.e., the sum of $[(HOI) - (I_3^-)]$ and any I^- added initially as NaI. The following is obtained for the second mechanism on the assumption that an equilibrium concentration of halogenating agent prevails.

$$\frac{1}{k^*} = \frac{k_{-1}}{k_1 k'_2} \left(1 + \frac{k'_{-2}}{k_3}\right) (I^-)$$

The differentiation between the two mechanisms is easily made theoretically as a plot of 1/k versus (I^-) has a positive intercept for the first mechanism, while for the second the plot goes through the origin. If both mechanisms are operative then possibly 1/k versus (I^-) would have two linear portions, one at lower iodide concentrations passing through the origin, and the other at higher iodide concentrations, which when extrapolated to zero iodide concentration would have a non zero intercept.

Sullivan found that above 10^{-5} M iodide the first mechanism was important for 2,4-dinitrophenoxide anion while below 10^{-6} M the second mechanism becomes increasingly important. For p-nitrophenoxide anion the change between mechanisms appeared to occur at 10^{-6} M (I^-). For phenoxide anion, which is more reactive than the p-nitrophenoxide anion, the plot of $1/k^*$ versus (I^-) appears to go through the origin. This, nevertheless, is taken to mean that the first mechanism is operating, since the iodide term may be much larger than the second term. The work of

Reproduced with permission of the copyright owner. Further reproduction prohibited without permission.

Gnanapragasam[7] with that of Aprahamian and that of Sullivan indicates that near 10^{-7} M iodide anisole is less reactive than 2,4-dinitrophenoxide anion and that both mechanisms might possibly be operating. Near 10^{-11} M iodide the H_2OI mechanism is highly favored. Gnanapragasam found that, for mesitylene and mesitylene-$\underline{d}_3$ which are comparable in reactivity to anisole, a plot $1/k^*$ versus iodide goes through the origin and over the range of 10^{-8} to 10^{-4} M iodide is linear within experimental error. Here the second mechanism is thought to apply and further it should be applicable for all compounds of lesser reactivity. In order to study mesitylene at 10^{-11} M iodide, Gnanapragasam carried out kinetic studies at 25° in the presence of 4.24×10^{-6} M Ag^+ and found that, as the mesitylene concentration was varied from (1 to 35) $\times 10^{-6}$ M, k^*I decreased by 50 percent and at 35° the decrease was 75 percent. For mesitylene-$\underline{d}_3$ at 25° over the hydrocarbon concentration range of (1 to 33) $\times 10^{-6}$ M, k^*I decreased 45 percent. For anisole there was a drop of 33 percent over a range of (2 to 45) $\times 10^{-6}$ M while from (4 to 232) $\times 10^{-6}$ M for m-xylene the decrease was 30 percent.

Hydrogen Isotope Effects

It is important in any reaction to determine the various rate determining processes or steps. In the case of substitution reactions as opposed to addition reactions, it is significant to differentiate between an initial attack by a reagent and the subsequent loss of any fragment of the substrate. In the case of aromatic electrophilic substitution, a proton is often lost. The importance of the participation of proton motion in a rate determining process may be investigated by the

Reproduced with permission of the copyright owner. Further reproduction prohibited without permission.

substitution of a deuterium atom for a proton atom at the reaction center. By separately considering the potential function of a proton, $V(r,\theta)$, where r is the C-H bond distance and θ represents an angular deviation from equilibrium, as being parabolic in the ground state reactant and in the transition state, it may be readily shown that, when the Arrhenius expression for k* is used, the isotope effect k_h^*/k_d^* may be expressed in the form

$$\ell n \left(\frac{k_h^*}{k_d^*}\right) = \frac{h}{2\pi kT}\left[(k^o)^{\frac{1}{2}} - (k^{\ddagger})^{\frac{1}{2}}\right]\left[(\mu_h)^{\frac{1}{2}} - (\mu_d)^{\frac{1}{2}}\right]$$

where h is the Planck constant, k is the Boltzman constant, and T is the absolute temperature. The effective reduced mass for the ground state and transition state is represented by μ. The force constants k^o and $k^{\ddagger}$ are defined for the ground state and the transition state as

$$k^i_{bend} = \left(\frac{\partial^2 V(r,\theta)}{\partial\theta^2}\right)_{r_e;\theta_e=0}$$

$$k^i_{vib} = \left(\frac{\partial^2 V(r,\theta)}{\partial r^2}\right)_{r_e;\theta_e=0}$$

where r_e is the appropriate equilibrium C-H bond distance. The relationship above gives in terms of algebraic signs of the three component terms the following

$$\ell n \left(\frac{k_h^*}{k_d^*}\right) = + \; [\pm][+]$$

A change in hybridization of the C-H bond from sp^2 to sp^3 at the reaction center during the course of the reaction is accompanied by a decrease in

Reproduced with permission of the copyright owner. Further reproduction prohibited without permission.

the C-H stretching force constant and an increase in the C-H bending force constant. While the environment of the proton will change during the course of the reaction there should be no large effect on the relative reduced masses and hence the reduced masses of the proton bearing substrate should remain the smaller, and the related term in the above expression should remain positive. If proton removal from the transition state is solely rate determining, then the second term is positive, and (k_h^*/k_d^*) is greater than 1.0. If a bending mode is predominantly involved in the rate determining process the second term will be negative and there will be an inverse isotope effect, i.e., (k_h^*/k_d^*) will be less than 1.0. The realistic point of view shows that both types of modes can be of importance and thence a more general expression may be formulated

$$\ln\left(\frac{k_h^*}{k_d^*}\right) = \frac{h}{2\pi kT}\left\{\alpha\left[(k_v^0)^{\frac{1}{2}} - (k_v^{\ddagger})^{\frac{1}{2}}\right] + (1-\alpha)\left[(k_b^0)^{\frac{1}{2}} \quad (k_b^{\ddagger})^{\frac{1}{2}}\right]\right\} \times \left[(\mu_h)^{-\frac{1}{2}} - (\mu_d)^{-\frac{1}{2}}\right]$$

where α is a weighing factor between 0 and 1.0 and the subscripts k_b and k_v refer to bending and stretching modes, respectively. Coincident assumptions are that all force constants are independent of isotopic substitution and that they are independent of each other.

It is necessary to consider the reversibility ratio k_{-2}/k_3 obtained from the I_2 mechanism in light of the above discussion; there must be consistency between experiment and theory. Since $k_{-2}\ (I^-)/k_3$ is the ratio of the fraction of molecules reverting to reactants and the fraction going to products, this ratio must in turn be related to some sort of average geometry at the reaction center in the transition state.

It is notable that the reversibility ratio k_{-2}/k_3 and the acidity

Reproduced with permission of the copyright owner. Further reproduction prohibited without permission.

of the intermediate are not independent but are mutually dependent on the electronegativity of other substituents or atoms on the phenoxide anion. Phenoxide, p-nitrophenoxide, and 2,4-dinitrophenoxide give intermediates of increasing acidity in the order listed; the corresponding reversibility ratios are observed to be 1.4×10^6, 2.1×10^4, and 4.2×10^3. The isotope effects at 50° of these three phenoxide anions are 6.5, 5.6, and 4.5, respectively, as determined for the I_2 mechanism, and are defined as the ratios of the reversibility ratios,

$$(k^d_{-2}/k^d_3)/(k^h_{-2}/k^h_3) \approx k^h_3/k^d_3$$

of the respective protium and deuterium labeled ions. The transition state, ‡, is thought to arise from the reaction of a stable intermediate, a σ complex, with a base, B, in the manner

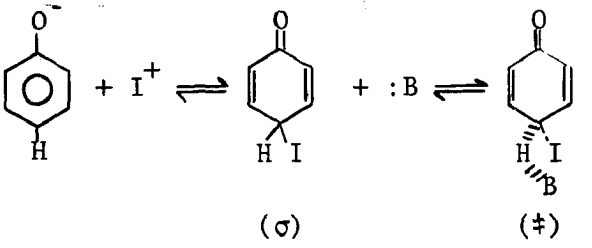

Now $-RT\,\ell n(k_{-2}/k_3)$ reflects the difference in the free energy of activation required for an intermediate to revert to reactant versus going to the transition state. Substitution of nitro groups for hydrogen atoms at positions meta to the reaction center should increase the acidity of the proton at the reaction center and the activation required to form the transition state should be lowered. The decrease in the isotope effect for the three anions would then be a function of the acidity of the

Reproduced with permission of the copyright owner. Further reproduction prohibited without permission.

corresponding intermediate.

The relationship of acidity to the geometry of the transition state can be explained in terms of a change of hybridization of the C-H bond as previously mentioned. Physically this requires that, as the C-H bond weakens, the cause must be an increasing change in hybridization from sp^3 toward sp^2; therefore, in structure, the transition state must be increasingly similar to the product.

The isotope effect defined in terms of k* from the I_2 mechanism has the form

$$\frac{k_h^*}{k_d^*} = \frac{\left[1 + \frac{k_{-2}}{k_3^d}(I^-)\right]}{\left[1 + \frac{k_{-2}}{k_3^h}(I^-)\right]}$$

while for the H_2OI^+ mechanism

$$\frac{k_h^*}{k_d^*} = \frac{\left(1 + \frac{k_{-2}}{k_3^d}\right)}{\left(1 + \frac{k_{-2}}{k_3^d}\right)}$$

These forms are taken as the ratios for the protium and deuterium cases of the appropriate expressions of k* and it has been assumed that k_2 and k_{-2} are independent of isotopic substitution on the aromatic ring.

In the case of the I_2 mechanism k_h^*/k_d^* may be a function of iodide ion concentration, and may not be constant. The value of k_3^h/k_3^d for the I_2 mechanism is taken as the ratio of the slopes of $1/k_d^*$ and $1/k_h^*$ plotted against iodide ion concentration. In the case of the H_2OI^+ mechanism the ratio k_h^*/k_d^* is independent of iodide ion concentration and is constant.

Reproduced with permission of the copyright owner. Further reproduction prohibited without permission.

It is possible, therefore, to differentiate between the two mechanisms by noting the variance of k_h^*/k_d^* with respect to iodide ion concentration.

It is important to note for 2,4-dinitrophenoxide that below 10^{-5} M iodide where H_2OI^+ is the effective halogenating agent the observed isotope effect at 50° is 2.3 and in contrast to the I_2 mechanism the ratio of k_3^h/k_3^d is not determined directly. By letting

$$\alpha = k_3^h/k_3^d$$

however and noting the value[8] of 0.43 ± 0.04 for k_{-2}/k_3^h then

$$2.3 = \frac{1 + 0.43\ \alpha}{1 + 0.43}$$

or including reasonable error estimates

$$\alpha = 5.3 \pm 1$$

The difference between this value for the true isotope effect and the observed isotope effect, 2.3, reflects the extent to which proton loss is not totally rate determining in the H_2OI^+ mechanism.

Correlation of Structure with Reactivity

The dependence of reaction rates and isotope effects upon structure has been assessed in the case of the phenoxide anions. The effect of structure on rates of reactions for methyl substituted benzenes has been studied in the cases of chlorination,[9,10] bromination,[11] oxidation[12] by $O(^3P)$, and protiodeuteration.[13] The iodination of the same substrates dissolved in peracetic acid has also been studied.[14] There have been

Reproduced with permission of the copyright owner. Further reproduction prohibited without permission.

several studies[15,16,17] on the effect of methyl substitution on the basicity of benzene towards HF. In all of these efforts the rates of reaction increased monotonically, as did the basicity, with the number of methyl groups. While there has been no observed isotope effect in chlorination there has recently been found a small isotope effect 1.14 ± 0.04 for the reaction of $O(^3P)$ with benzene as well as a more sizable isotope effect (near 1.5) in the case of bromination[18] of highly substituted, sterically hindered benzenes such as 3-methoxydurene, 3-bromodurene, and 5-t-butyl-1,2,3-trimethyl benzene (5-t-butylhemimelitine).

The rate determining steps of several of the above reactions have been considered as the formation of the halogenating agent[19] in the case of chlorination by positive chlorine, the formation of a sigma complex for bromination,[20] and, as mentioned previously, proton removal in the case of iodination of phenoxide anions. It is not intended, as the case for bromination previously mentioned indicates, that these steps be understood as being solely rate determining for a mixture of rate determining steps can be involved. It is apparent, then, that structure can play a part in the determination of the slow step.

An explanation of the participation of a methyl group via resonance in an electrophilic reaction has been offered by Dewar in terms of hyperconjugation,[21] and is best described qualitatively by comparing the $C{\equiv}H_3$ group to a C≡N group. In both groups there are two sets of orbitals that have p type symmetry and one that has s symmetry with respect to the bond axis. Quantitatively the H_3 molecular orbital having the same symmetry as the ring π system may be arbitrarily represented[22] as

Reproduced with permission of the copyright owner. Further reproduction prohibited without permission.

$$6^{-\frac{1}{2}} [2\Phi_2 - (\Phi_1 + \Phi_3)]$$

where the Φ's are hydrogen 1s atomic orbitals. This hydrogenic molecular orbital has p symmetry as well as the same linear combination of the three sp^3 hybrid orbitals on the H_3 bearing carbon. The combination

$$2^{-\frac{1}{2}} (\Phi_1 - \Phi_3)$$

also has p type symmetry but can be thought of as being parallel to the aromatic ring plane and hence interacts in the most part with the sigma framework of the ring. Dewar points out that, in a neutral species such as toluene, the resonance interaction between the methyl group and π system is small while in positively charged systems such as the isopropyl and t-butyl carbonium ions methyl resonance is very important in stabilizing the ion. It is therefore reasonable to consider the same phenomena as participating when a methyl group is present in a positively charged system such as

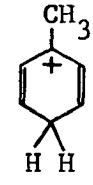

Prior to 1965 molecular orbital calculations were for the most part restricted to π systems and methyl substituents were commonly reflected by small corrections in the Hückel matrix diagonal element corresponding to the carbon in the π system to which the methyl group was bonded. The direct resonance interaction of a methyl group with such a Wheland inter-

Reproduced with permission of the copyright owner. Further reproduction prohibited without permission.

mediate is now readily investigated economically via complete valence shell molecular orbital schemes[23,24] such as CNDO/2 and MINDO/2 in which bonding interaction between each of the methyl hydrogens and the 2s and 2p atomic orbitals on the proton bearing carbon are specifically incorporated. While these two schemes adequately treat the orbitals of interest, the methods are semi-empirical and use numerical parameters obtained from neutral molecules. Recently, some work,[25] employing several MO schemes, has been done correlating reactivity rates for several methyl bearing hydrocarbons.

For molecules bearing a formal charge it has been suggested that the atomic orbital electronegativity of the hydrogen 1s orbitals as well as the carbon 2s and 2p orbitals be represented as a quadratic function of the charge on the parent atom. The one center repulsion integrals have been observed to be a linear function of the charge on each center.[26]

Solvents

In nearly all the halogenation studies on non-polar compounds to date organic solvents such as CCl_4 and acetic acid[27] have been used due to the very low solubility of non-polar aromatic compounds in water. There have been reported recently, however, two studies of the bromination of methylated benzenes in water.[28,29] The rates of bromination of methyl-substituted benzenes in acetic acid,[30] trifluoroacetic acid,[31] and water parallel the dielectric constants of the solvents used 6.2, 39.5, and 78.4, respectively.

Purpose of This Thesis

The purpose of this thesis is to present a study of the kinetics

Reproduced with permission of the copyright owner. Further reproduction prohibited without permission.

of iodination in water of the methylated benzene series, in addition to the parent compound, toluene, p-xylene, o-xylene, m-xylene, durene, prehnitene, mesitylene, and pentamethylbenzene. Utilizing the deuterated analogues the isotope effect of benzene, toluene, p-xylene, durene, mesitylene, and pentamethylbenzene have been studied to help elucidate the mechanism of the reaction. The reaction products for toluene and o-xylene were isolated and analyzed so that partial rate factors could be determined. Valence bond calculations were made utilizing the CNDO/2 scheme, with the parameters of Wiberg[32] being chosen to take into account molecules bearing a formal charge. An effort was made to calculate the product distribution observed for toluene and o-xylene as well as the relative rates of reaction for the entire series of hydrocarbons studied.

Reproduced with permission of the copyright owner. Further reproduction prohibited without permission.

CHAPTER II

PREPARATION AND PURIFICATION OF MATERIALS USED

Hydrocarbons

Benzene

Phillips Research grade (99.9 percent min.) benzene (50 ml) was treated with ICl (0.05 molar ratio) in the presence of 10 ml of water and silver nitrate (5 g) by shaking for 24 hours. The solution was decanted from the residual solid material, washed with five percent KOH saturated with KCl, washed with brine, and then dried over Drierite. It was distilled under atmospheric conditions in a specially designed still having in contact with the vapor a single smooth wall 24/40 tapered joint which obviated the need for grease. There was no provision for the distillation temperature to be determined but approximately 10 percent of the contents of the still was discarded as a forerun.

Benzene-d_6

Benzene-d_6 (99.5 percent d) was obtained from Mallinckrodt Chemical Company and was purified exactly as the protium analogue.

1,2-Dimethylbenzene (o-xylene)

Phillips Research grade (99.97 percent) hydrocarbon was purified exactly as benzene.

1,3-Dimethylbenzene (m-xylene)

The purification of m-xylene was carried out by Gnanapragasam[33] by reacting 1.5 moles of m-xylene with 0.75 mole of Br_2 over a period of five

Reproduced with permission of the copyright owner. Further reproduction prohibited without permission.

days. After washing with 3 N NaOH and with water, the reaction mixture was dried over Drierite and distilled through a 14 inch vigreaux column. The fraction boiling at 61-62° (49 mm) was collected. This fraction was then distilled through a two-foot, spinning band column. The fraction boiling at 137° (737 mm) was collected. The refractive index at 20° was 1.4977 (lit. 1.4972).

1,4-Dimethylbenzene (p-xylene)

Phillips Research grade hydrocarbon (99.95 percent) was purified exactly as benzene.

1,4-Dimethylbenzene-d_4

This was prepared from the parent hydrocarbon in the same fashion as toluene-d_5. NMR analysis revealed 92.3 percent exchange of ring protons.

2,3-Dimethyliodobenzene

This was synthesized from 2,3-dimethylaniline via the Sandmeyer reaction. The published procedure[34] was modified as follows. The product was extracted from the aqueous reaction mixture with benzene. The benzene was removed by distillation at atmospheric pressure and the residue steam distilled to give a colorless product. The product was extracted from the distillate with benzene and dried with calcium chloride. The benzene was again removed by distillation at atmospheric pressure and the residue was distilled from a Hickman still under reduced pressure (water aspirator).

3,4-Dimethyliodobenzene

This compound was purchased from Eastman Kodak and used as received.

Iodotoluenes

The three iodotoluene derivatives, ortho-, meta-, and para-

Reproduced with permission of the copyright owner. Further reproduction prohibited without permission.

iodotoluene, were Eastman Kodak White Label grade and were distilled at a boiling point near 80° and near 10 mm pressure. They were subsequently stored at -20°.

Pentamethylbenzene

Zone refined pentamethylbenzene from Columbia Chemical Company was used without further purification.

Pentamethylbenzene-$\underline{d}_1$

This compound was prepared in identical fashion to that for durene-$\underline{d}_2$ except that the solution was kept at room temperature for two weeks. The red solution was poured over aqueous base plus ice, filtered, and sublimed at 40° and atmospheric pressure. NMR analysis showed 92 percent exchange of the ring proton. The compound melted over a range from 47.5-49° (lit. 51.5°).[35] A vpc analysis showed less than 1.0 percent total impurities (a tetramethyl substituted benzene and hexamethylbenzene). Of the three possible tetramethylbenzene impurities the 1,2,3,4 and 1,2,4,5 tetramethyl isomers are insignificantly reactive when compared to pentamethylbenzene; the 1,2,3,5 tetramethyl isomer is of comparable reactivity however. Since 25 percent of the pentamethylbenzene is consumed in the course of a kinetic run, less than 0.5 percent of an impurity of comparable reactivity is not significant.

1,2,3,4-Tetramethylbenzene (Prehnitene)

Aldrich Chemical Company was the source of this compound. It was purified exactly as benzene except that it was distilled under vacuum in a Hickman still (bath temperature of 80°, 10.0 mm pressure). A 10 percent forerun was discarded. After distillation the pot residue partially

Reproduced with permission of the copyright owner. Further reproduction prohibited without permission.

solidified after cooling, yielding yellow needles which were not isolated but were probably the monoiodo derivative.

1,2,4,5-Tetramethylbenzene (Durene)

Zone refined durene (mp 79.5° uncorrected) obtained from Aldrich Chemical Company was used without further purification.

1,2,4,5-Tetramethylbenzene-$\underline{d}_2$ (Durene-$\underline{d}_2$)

Zone refined durene (mp 79.5° uncorrected) was treated with a 100-fold excess of deuterotrifloroacetic acid in a sealed ampoule placed in refluxing acetone. After one week the ampoule was cooled in ice, opened, and the contents poured onto aqueous KOH and ice. The deuterated product was filtered, dried, and distilled in a sublimation apparatus at 100° and atmospheric pressure. White needles were obtained (mp 79.5° uncorrected). NMR analysis showed 90.6 percent exchange.

Toluene

Baker Analyzed Reagent toluene was first distilled on a spinning band column and then treated by shaking vigorously for eight hours with each of eight portions of 49.5 mole percent H_2SO_4, washed with five percent water saturated with KCl, then washed with brine, dried over sodium, and distilled on a four-foot column packed with glass helices.

Toluene-$\underline{d}_5$

A portion of the first distilled toluene was treated with six 49.5 mole percent portions D_2SO_4 in D_2O. By NMR analysis the ring protons were 80 percent exchanged. Three more exchanges were done and NMR analysis showed 92 percent exchange. The remaining ring protium content was assumed to be in the meta positions and to be unimportant. This premise

Reproduced with permission of the copyright owner. Further reproduction prohibited without permission.

is supported by considering molecular orbital calculations on the relative stabilities of the three possible intermediate proton sigma complexes as well as the very small meta partial rate factors for bromination and iodination (this work).

1,3,5-Trimethylbenzene (Mesitylene)

This compound was purified by Gnanapragasam like toluene except that 39.1 mole percent sulfuric acid was used.

Other Materials Used

Calcium Sulfate

"Drierite" was used without further purification.

Carbon Tetrachloride

See Sullivan.[36]

Deuterium Oxide

See Sullivan.[37]

Deuterosulfuric Acid

See Sullivan.[38]

Iodine

Baker Analyzed Reagent grade was used as received.

Perchloric Acid

See Sullivan.[39]

Potassium Biphthalate

Baker Analyzed Reagent grade was used as received.

Potassium Dichromate

Baker Analyzed Reagent grade was used as received.

Reproduced with permission of the copyright owner. Further reproduction prohibited without permission.

Potassium Permanganate

Baker Analyzed Reagent grade was used as received.

Sodium Bicarbonate

Baker Analyzed Reagent grade was used as received.

Sodium Carbonate

Baker Analyzed Reagent grade was used as received.

Sodium Iodide

Fisher certified Reagent grade granular sodium iodide was used without further purification. As finely divided material readily absorbs moisture, the much higher surface to weight ratio of the granular form is preferred.

Sodium Metal

Baker Analyzed Reagent grade was used as received.

Sodium Perchlorate

G. Frederick Smith Company was the supplier of sodium perchlorate (tetrahydrate) and it was used as received.

Sulfuric Acid

Baker Analyzed Reagent grade was used as received.

Trifluoroacetic Acid-d

This reagent was prepared by reacting equimolar amounts of trifluoroacetic acid anhydride and D_2O at zero degrees and allowing it to stand for two days at room temperature. It was used without further purification.

Water

The water purification is described by Sullivan.[40]

Reproduced with permission of the copyright owner. Further reproduction prohibited without permission.

CHAPTER III

GENERAL PROCEDURE FOR STUDY OF REACTION KINETICS

Kinetic Measurements

The spectrophotometric technique used in this work was developed by N. S. Gnanapragasam and is discussed in detail by Sullivan.[41] To a 50.0 ml low-actinic volumetric flask having a hand-lapped glass stopper were added water, solutions of hydrocarbon, and solutions of silver nitrate so that the resulting volume was 35.0 ml. To start the reaction 5.0 ml of an iodine-perchloric acid was added, the final volume being 40.0 ml. If a reaction was found to be sufficiently slow, a set of blank reaction flasks were prepared as described above except that water was substituted for the hydrocarbon solution. The 50.0 ml flasks, as well as the acid-iodine stock solution, were all equilibrated in a constant temperature bath set at $25.00^{\circ} \pm 0.02^{\circ}$. The same thermometer was used throughout this work. It was calibrated by a platinum resistive thermometer and showed an error of $+ 0.20^{\circ}$ over the range of 25° to 40°. The zero time was taken to occur when one-half the acid-iodine solution had been added to the flask. (The normal time for addition was three seconds.) The flask was shaken vigorously and returned immediately to the thermostat. The reaction was stopped by the addition of standardized sodium carbonate solution to render the solution to a pH of 6.5-7.5. This usually required for complete reaction of the base a number of equivalents 1.1 times the number of equivalents of acid in each flask. The time was noted

Reproduced with permission of the copyright owner. Further reproduction prohibited without permission.

when half the base was added. As neutralization of the kinetic solution at very low iodide concentration converts the unreacted iodine to hypoiodous acid, 1.0 ml of a solution of sodium iodide (1.0 g/ml) stored at -20° in a refrigerator freezer compartment was then added. This addition served two purposes: first, the hypoiodous acid is converted to the triiodide anion in a known quantitative manner and second, the silver ion present is converted to silver diiodide anion. A lesser amount of sodium iodide is insufficient to effect the latter conversion and the resulting solution would accordingly be cloudy and unfit for optical determination of the triiodide ion.

Preparation of Solutions

The hydrocarbon stock solutions were prepared by the addition of a known amount of hydrocarbon to water in a volumetric flask (usually about 90 percent filled) and the resulting solution was shaken on a highly efficient mechanical shaker for at least six hours. There have been reported solubility studies[42,43] of several of the present hydrocarbons in water; these studies reported a good direct linear correlation of the pK_s, where K_s is the hydrocarbon solubility expressed in g/ℓ versus the solute molar volume. For the stock solution used in the kinetic studies the amount of pure hydrocarbon added to a given volume of water was kept near three-quarters the estimated (where unknown) solubility. The solution was inspected for cloudiness after shaking. If for any reason cloudiness was present after shaking, the solution was discarded; the flask was baked at 150° for one hour, and the process was repeated with a smaller amount of hydrocarbon. The solubilities of the hydrocarbons

Reproduced with permission of the copyright owner. Further reproduction prohibited without permission.

varied from 1.75 g/ℓ for benzene to 5.0 mg/ℓ for pentamethylbenzene. In certain cases the extinction coefficient for optical absorption of the hydrocarbon in the stock solution was determined; thus the same solution could be used later, the concentration being determined from the absorbance and the extinction coefficient.

The iodine solutions were prepared by aqueous extraction of a saturated carbon tetrachloride-iodine solution, the fourth extract being kept and filtered through glass wool to remove any remaining carbon tetrachloride solution. The aqueous solutions were found to be 1.30×10^{-3} M in iodine.

The silver nitrate solutions were prepared fresh each day that kinetic runs were made. A stock solution was made sufficiently concentrated (typically 0.25 g/250.0 ml) to minimize weighing errors and then a second stock solution prepared from the first by dilution. An aliquot of 5.0 ml of the second solution was added to each flask so that the known final silver concentration was $(4 \text{ to } 32) \times 10^{-6}$ M.

The quenching procedure must be done with caution as 40.0 ml of 0.1 N acid is capable of liberating 50 ml of CO_2 when sodium carbonate is used or 100 ml when sodium bicarbonate is used. Subsequent to this realization, solely sodium carbonate was used.

Schmalsteig[44] found that, at temperatures near -20°, concentrated solutions (1.0 g/ml) of sodium iodide were not oxidized readily and did not freeze due to the high ionic strength. It was necessary to wash the sodium iodide delivery pipette immediately to preclude contamination of subsequent reaction flasks with traces of iodine from air oxidation of iodide ion to iodine as the iodide to iodine concentration ratio under

Reproduced with permission of the copyright owner. Further reproduction prohibited without permission.

quenching conditions was near 10^6. Since under quenching conditions this ratio also held for $(I^-)/(Ag^+)$ and since the pK_{sp} of AgI is near 16, the need for washing of all glassware with care is obvious. To this end each reaction flask, which initially had been pretreated under kinetic conditions, was cleaned after each use by washing with 50 ml of water in five equal portions. Then the flasks were filled to the brim, stoppered for one hour, emptied and washed again with an additional 10 ml portion of water. This washing procedure was found to be sufficient for all studies where silver ion was used.

The pipettes, burettes, and volumetric flasks used were all Corning class A. They were not checked for calibration.

Calculation of Rate Constants

The high molecular coefficient of absorption of the triiodide ion (26,400 at 3530 Å) in conjunction with a 10.0 cm optical quartz cell, gave for 2×10^{-6} M iodine solutions an absorbance near 0.6 absorbance units on the Cary 14 spectrometer used in this study. The ranges of the spectrometer were calibrated in units of 0.005 times full range deflection in absorbance units and absorbance readings were typically read to ± 0.0002 absorbance units for the more sensitive range and to ± 0.002 for the less sensitive one. This results in an error of less than two percent in the reading of absorbance. The absorption observed was corrected by a reduction of 0.002 times the cell pathlength in cm due to background absorption caused by silver diiodide anion and the excess sodium iodide.

The concentration of unreacted iodine was determined from the absorbance by the relationship

Reproduced with permission of the copyright owner. Further reproduction prohibited without permission.

$$(I_2) = (E)(Abs)$$

where E is a constant[45] for a given cell pathlength, triiodide extinction coefficient, and reaction and quenching volumes. For 40.0 ml of reaction solution, 1.0 ml of iodide solution, 2.5 ml of sodium carbonate, and a 10.0 cm cell E is determined to be 4.1543×10^{-6}.

The rate constants studied herein can be derived from the exact solution of the observed rate law

$$\frac{dx}{dt} = \frac{-d[I_2]}{dt} = k_{obs} \frac{(ArH)(I_2)}{(I^-)}$$

The subscript zero will denote a concentration at zero time. It is necessary to correct for the hydrolysis of I_2

$$I_2 + H_2O \underset{}{\overset{K_h}{\rightleftharpoons}} HOI + H^+ + I^-$$

since the high acidity (0.10 M H^+) used is incapable of completely suppressing the hydrolysis of iodine (10^{-6} M) because of the very low iodide ion concentration (typically 10^{-11} M).

$$\frac{-d[I_2]}{dt} = k_{obs} \frac{[(ArH)_o - x][(I_2)_o - x - (HOI)]}{[x + (HOI)]}$$

where (I^-) has been redefined in terms of the iodide produced during the course of the reaction and x is defined as the amount of reacted hydrocarbon.

It is experimentally necessary at 25° to use silver ion to acceler-

Reproduced with permission of the copyright owner. Further reproduction prohibited without permission.

ate the reaction by lowering the iodide ion so that the reaction to be studied will occur at a practical rate.

$$\frac{dx}{dt} = \frac{-d[I_2]}{dt} = \frac{k_{obs}}{K_{sp}} [(ArH)_o - x][(I_2)_o - (x + HOI)][(Ag^+)_o - (x + HOI)]$$

When using silver ion (4×10^{-6} M) with mesitylene (3×10^{-5} M), for example, a half-life for iodine of 200 seconds can be attained but with benzene (0.01 M) the iodine has a half-life of 6×10^5 seconds. If the solubility product of AgI is divided by the final expression for K_h

$$\frac{K_{sp}}{K_H} = \frac{(Ag^+)(I^-)\ \gamma \pm^2\ (I_2)}{(H^+)(I^-)(HOI)\ \gamma \pm^2} = \frac{[(Ag^+)_o - (x + HOI)][(I_2)_o - (x + HOI)]}{(H^+)(HOI)}$$

and if from the result HOI is determined to be solely a function of a single variable, x, the rate law after a suitable change of variables may be solved in closed form using integration by parts. The solution is given in Appendix A.

In nearly all the studies the hydrocarbon and silver ion concentrations were greater than that of the iodine; hence a point by point plot of ℓn (Abs) for iodine versus time is approximately linear and gives a running progress report on the reaction being studied. This correlation served extremely well in rejecting data points and pointing out the need for various new reaction points to be taken. Points that deviated extremely from the linear rough plot always were found to give erratic values for the rate constants. For reaction conditions where there was consumption of iodine in the blank flasks, the log plot of the blank

Reproduced with permission of the copyright owner. Further reproduction prohibited without permission.

absorbances versus time was always linear. Further, the slope varied monotonically with the silver ion concentration. This leads to a corrected rate law

$$\frac{-d[I_2]}{dt} = \frac{k_r}{K_{sp}}[(ArH)_o - x][(I_2)_o - (x' + HOI)][(Ag^+)_o - (x' + HOI)]$$

$$+ k_b[(I_2)_o - (x' + HOI)][(Ag^+)_o - (x' + HOI)]$$

where x' is the loss of I_2 by both blank reaction and the reaction of interest and where k_r is the rate constant of main interest and k_b is the rate constant for the blank drop. Further x'-x = Δx represents the iodine consumed by the <u>in situ</u> blank reaction. On comparing the blank reaction to the main reaction

$$\frac{d(\Delta x)}{dx} = \frac{k_b(Ag^+)(I_2)}{k_r(ArH)(Ag^+)(I_2)} = \frac{k_b}{k_r[(Ar)_o - x]}$$

or

$$\Delta x = \frac{k_b}{k_r} \ell n \left[\frac{(ArH)_o}{(ArH)_o - x}\right]$$

so that

$$x' = x + \Delta x = x + \frac{k_b}{k_r} \ell n \left[\frac{(ArH)_o}{(ArH)_o - x}\right]$$

or

$$x' = x - \frac{k_b}{k_r} \ell n \left[1 - \frac{x}{(ArH)_o}\right]$$

If $x/(ArH)_o$ is sufficiently small compared to unity, as it is expected to be under pseudo zero order conditions for the hydrocarbon, only the first term of a series expansion of the ℓn function need be retained to give

Reproduced with permission of the copyright owner. Further reproduction prohibited without permission.

$$x' = x - \frac{k_b}{k_r}\left[\frac{-x}{(ArH)_o}\right] = x\left[1 + \left(\frac{k_b}{k_r\ (ArH)_o}\right)\right]$$

For benzene, the least reactive of the hydrocarbons studied, $\frac{k_b}{k_r\ (ArH)_o} \approx$ 0.8. The term in the rate law containing $(ArH)_o - x$ must now be replaced by $(ArH)_o - x'/1.8$; however, $x'/1.8$ still remains much less than $(ArH)_o$ under experimental conditions employed and further replacing x by x' still leaves the reaction near a pure pseudo zero order reaction with respect to hydrocarbon, and it is therefore reasonable as an approximation where

$$(ArH)_o - x \approx (ArH)_o - x'$$

to write the rate law as

$$\frac{dx'}{dt} = \frac{-d[I_2]}{dt} = k_r\,[(ArH)_o - x'][(I_2)_o - (x' + HOI)][(Ag)_o - (x' + HOI)]$$

$$+ k_b\,[(Ag)_o - (x' + HOI)][(I_2)_o - (x' + HOI)]$$

for which the solution in Appendix A is applicable. The following is obtained on comparison with the observed rate law

$$k_{obs}\ (ArH)(I_2)(Ag^+) = k_r\ (ArH)(I_2)(Ag^+) + k_b\ (I_2)(Ag^+)$$

or for

$$(ArH)_o >> (I_2)_o \approx (Ag^+)_o$$

$$k_r = k_{obs} - \frac{k_b}{(ArH)_o}$$

Reproduced with permission of the copyright owner. Further reproduction prohibited without permission.

The value of k_b for each set of kinetic runs is determined independently from the blank reaction flasks and the slope of a least squares fit of the exact solution given in Appendix B for the blank reaction rate law

$$\frac{dx''}{dt} = \frac{-d[I_2]}{dt} = k_b\,[(Ag^+)_o - (x'' + HOI)][(I_2)_o - (x'' + HOI)]$$

where x'' is the iodine consumed in the independent blank reaction.

Reproduced with permission of the copyright owner. Further reproduction prohibited without permission.

CHAPTER IV

IODINATION OF MESITYLENE, ANISOLE, AND m-XYLENE

Introduction

In an effort to investigate for mesitylene, anisole, and m-xylene, the cause of the drop in the rate constant $k^*(I^-)$, with the increase of the hydrocarbon concentration, three of Gnanapragasam's experiments were repeated. His results are shown in Table 1 (Section A), Tables 2 and 3, Table 4 (Section A), and Table 5. Experiments 113 and 114 of Table 6 as well as experiment 124 of Table 4 (Section B) verify the type of results found in the first five tables. The rate constant $k^*(I^-)$, hereafter referred to as k*I, reproducibly drops as the initial (ArH) is increased at constant (Ag^+) and (I_2). It is noted in Table 1 (Section C) that, as the initial (Ag^+) is increased, while keeping the initial (ArH) and (I_2) approximately constant, the values for k*I appear to increase only slightly, if at all. The rate constant also increases as the initial iodine concentration is increased while keeping (ArH) and (Ag^+) constant, Table 1 (Section B).

In Figure 1 are found plots of 1/k*I vs. (ArH) at 4.24×10^{-6} M (Ag^+) and 2×10^{-6} M (I_2) as taken from Tables 1 (Section A), 2, 3, and 5. It is noted for both protio and deutero substituted mesitylene at 25° that 1/k*I appears to be linear in the region near zero hydrocarbon concentration and that the slopes in the lower concentration range appear to be the same. At 35° the plot appears to be linear throughout for mesitylene.

Reproduced with permission of the copyright owner. Further reproduction prohibited without permission.

Table 1. Mesitylene Rate Constants Determined at 25.0° in the Presence of (Ag^+) and 0.10 M $HClO_4$. Measured by N. S. Gnanapragasam

Experiment No.	ArH M x 10^6	I_2 M x 10^6	Ag^+ M x 10^6	$k^*(I^-)$ x 10^9 sec^{-1}
Section A				
98	1.039	1.754	4.245	6.96 ± 0.47
88	1.886	1.851	4.245	6.60 ± 0.33
83	4.102	2.101	4.245	6.56 ± 0.31
89	8.536	1.851	4.245	4.86 ± 0.24
85	16.61	2.053	4.245	4.09 ± 0.20
111	17.26	1.974	4.245	3.70 ± 0.65
90	33.22	1.851	4.245	3.32 ± 0.31
109	34.51	1.957	4.245	3.15 ± 0.39
110	34.51	2.002	4.245	4.86 ± 1.51
Section B				
113	4.171	0.506	4.245	4.95 ± 0.48
86	4.438	1.023	4.245	5.64 ± 0.24
(83)*	(4.102)	(2.101)	(4.245)	(6.56 ± 0.31)
112	4.171	3.522	4.245	7.05 ± 0.49
87	16.61	1.023	4.245	3.37 ± 0.14
Section C				
(83)*	(4.102)	(2.101)	(4.245)	(6.56 ± 0.31)
72	3.960	1.921	8.708	7.71 ± 0.53
84	4.102	2.062	15.49	8.52 ± 0.23
81**	5.601	1.833	25.84	7.49 ± 0.49

*From Section A

**H^+ = 0.30 M

Note: In all tables headings ArH, I_2, and Ag^+ refer to initial stochiometric concentrations, elsewhere denoted by $(\ )_o$.

Reproduced with permission of the copyright owner. Further reproduction prohibited without permission.

Table 2. Mesitylene-d_3 Rate Constants Determined at 25.0° in the Presence of (Ag^+) and 0.10 M $HClO_4$. Measured by N. S. Gnanapragasam

Experiment No.	ArH M × 10^6	I_2 M × 10^6	Ag^+ M × 10^6	$k^*(I^-) \times 10^8$ sec^{-1}
99	1.223	1.754	4.245	3.37 ± 0.15
91	1.619	2.215	4.245	3.50 ± 0.17
92	16.47	2.215	4.245	2.41 ± 0.15
93	32.94	2.215	4.245	1.71 ± 0.16
100	49.81	1.754	4.245	1.40 ± 0.25
78	5.028	2.406	8.807	3.40 ± 0.16

Table 3. Mesitylene Rate Constants Determined at 35.0° in the Presence of (Ag^+) and 0.10 M $HClO_4$. Measured by N. S. Gnanapragasam

Experiment No.	ArH M × 10^6	I_2 M × 10^6	Ag^+ M × 10^6	$k^*(I^-) \times 10^8$ sec^{-1}
118	1.092	1.763	4.245	2.73 ± 0.33
115	1.976	1.582	4.245	2.79 ± 0.16
119	4.534	1.710	4.245	2.23 ± 0.13
116	8.611	1.543	4.245	1.64 ± 0.15
120	17.47	1.675	4.245	1.16 ± 0.06
117	34.03	1.547	4.245	0.71 ± 0.05

Reproduced with permission of the copyright owner. Further reproduction prohibited without permission.

Table 4. m-Xylene Rate Constants Determined in the Presence of (Ag^+) and 0.10 M $HClO_4$. Measured by J. M. McKelvey

Experiment No.	ArH M x 10^6	I_2 M x 10^6	Ag^+ M x 10^6	k*(I^-) x 10^{10} sec^{-1}
Section A				
Temperature 25.0°				
101*	4.677	1.858	4.249	0.93 ± 0.02
102*	52.84	1.822	4.249	0.80 ± 0.02
104*	232.4	2.215	4.249	0.68 ± 0.05
Section B				
Temperature 25.0°				
124	816.5	3.165	4.300	0.73 ± 0.03
125	258.0	2.780	21.89	1.06 ± 0.05
131**	79.83	2.152	19.41	0.970 ± 0.05
132	80.15	2.567	20.45	1.11 ± 0.02
133	46.39	6.655	18.88	1.21 ± 0.05
147	59.04	2.975	13.22	0.967 ± 0.08
148	64.14	1.821	12.71	1.01 ± 0.04
149	64.99	4.686	21.16	0.96 ± 0.06
150	25.43	2.502	20.08	1.20 ± 0.09
Temperature 35.0°				
135	44.71	1.977	19.69	6.46 ± 0.41
136	45.06	2.373	18.92	6.71 ±

*These experiments were done by N. S. Gnanapragasam.

**(H^+) = 0.20 M

Reproduced with permission of the copyright owner. Further reproduction prohibited without permission.

Table 5. Anisole Rate Constants Determined at 25.0° in the Presence of (Ag^+) and 0.10 M $HClO_4$. Measured by N. S. Gnanapragasam

Experiment No.	ArH M × 10^6	I_2 M × 10^6	Ag^+ M × 10^6	$k^*(I^-) \times 10^9$ sec^{-1}
106	2.867	2.116	4.248	2.25 ± 0.13
105	45.91	2.116	4.248	1.01 ± 0.13

Table 6. Mesitylene Rate Constants Determined at 25.0° in the Presence of (Ag^+) and 0.10 M $HClO_4$. Measured by J. M. McKelvey

Experiment No.	ArH M × 10^6	I_2 M × 10^6	Ag^+ M × 10^6	$k^*(I^-) \times 10^9$ sec^{-1}
113	31.51	2.298	5.082	3.79 ± 0.19
103	3.610	2.007	20.02	8.57 ± 0.72
110	4.718	1.861	26.61	8.67 ± 0.21
115	70.16	0.591	2.464	2.75 ± 0.51
123	42.69	2.355	5.042	4.44 ± 0.39
126	13.31	1.890	10.46	7.19 ± 0.25

Reproduced with permission of the copyright owner. Further reproduction prohibited without permission.

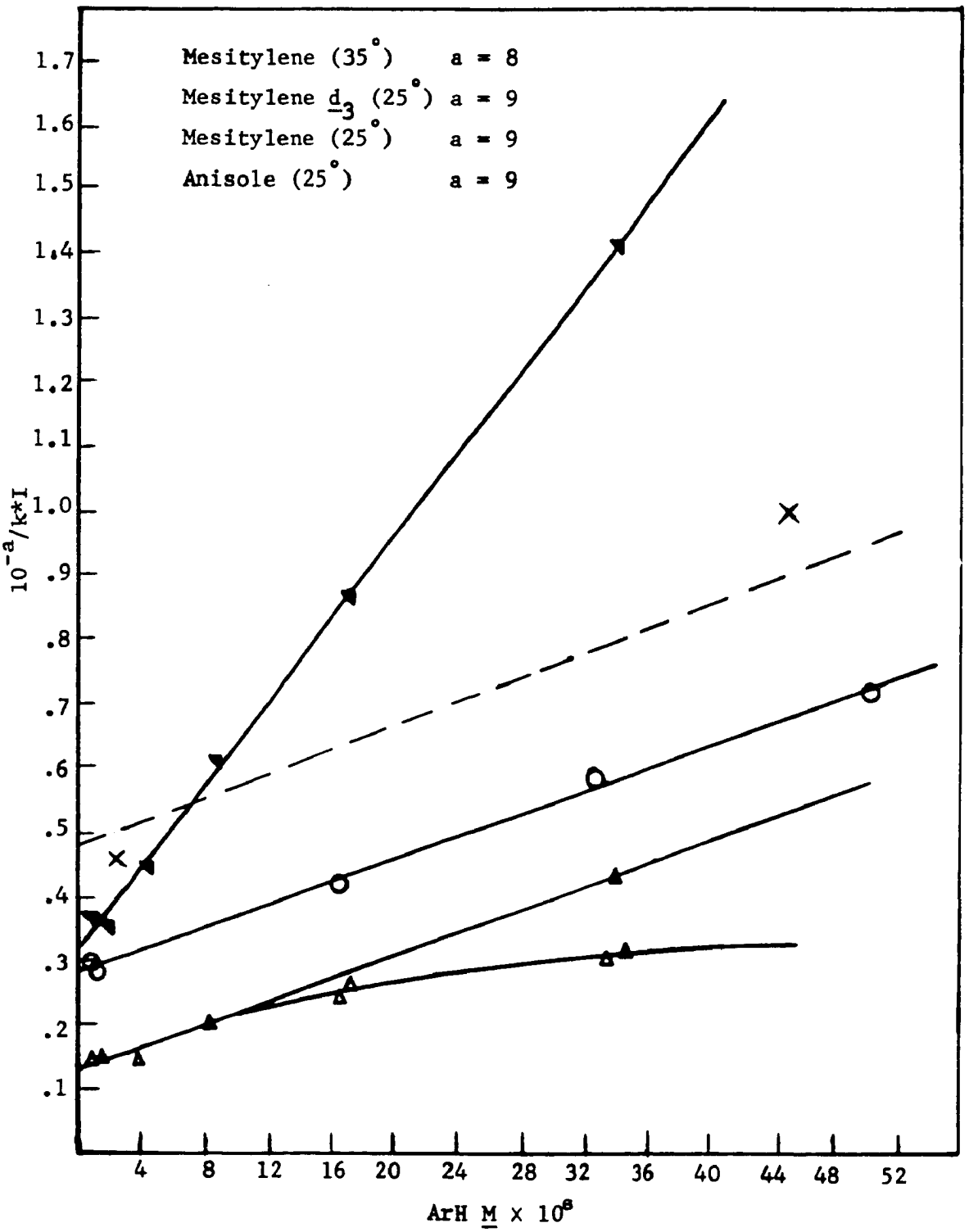

Figure 1. Plots of 1/k*I Versus (ArH). (Other concentrations are $(Ag^+) = 4.24 \times 10^{-6}$ $\underline{M}$ and $(I_2) = 1.9 \times 10^{-6}$ $\underline{M}$.)

Reproduced with permission of the copyright owner. Further reproduction prohibited without permission.

Figure 2 shows, for mesitylene, a plot of $\log_{10}$ (k*I/T) vs. 1/T. The three points at lower values of 1/T correspond from left to right to values of k*I, 12.4 ± 0.5, 3.79 ± 0.26, and 1.11 ± 0.04 x 10^{-7} sec^{-1} determined by Gnanapragasam at 60.0°, 50.0°, and 40.0°, respectively. They were measured in the absence of any silver ion. The two remaining points are 32.2 and 8.00 x 10^{-8}, the intercept values of k*I taken from Figure 1 for the temperatures 35.0° and 25.0°, respectively.

Figure 3 contains the rate constants as determined during an entire experiment. The experiments represented are 90, 100, and 105 of Tables 1, 2, and 5, respectively. They are correlated with the reaction time for each experimental point for which a value for k*I was determined. Each experiment shows a drop in k*I with time and, further, k*I appears to approach a limiting value in each case.

Figure 4 correlates the values of k*I (Table 1, Section B) measured at constant (ArH) and (Ag^+) but varying (I_2). The values of k*I increase as (I_2) is increased.

It is important to note that, at this point, all the above correlations are empirical but will be later shown to have some basis in theory.

New Experimental Results

The behavior of k*I as a function of hydrocarbon concentration might be accounted for by assuming storage of large amounts of the iodine by way of a prior equilibrium in the form of a σ complex according to the equation

$$ArH + I_2 \rightleftarrows ArHI^+ + I^-$$

Reproduced with permission of the copyright owner. Further reproduction prohibited without permission.

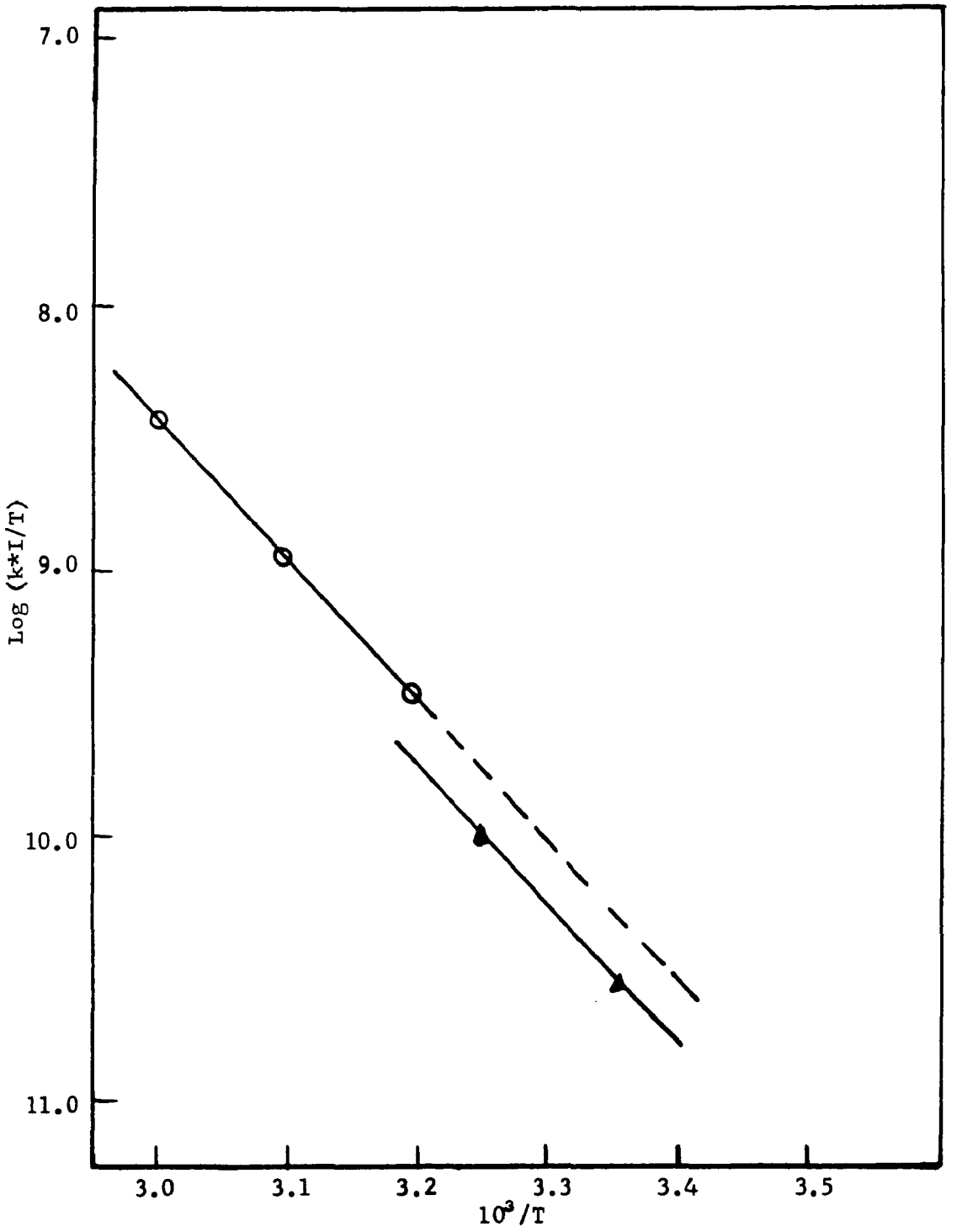

Figure 2. Plot of $\log_{10}$ (k*I/T) Versus 1/T. (Mesitylene data of N. S. Gnanapragasam.)

Reproduced with permission of the copyright owner. Further reproduction prohibited without permission.

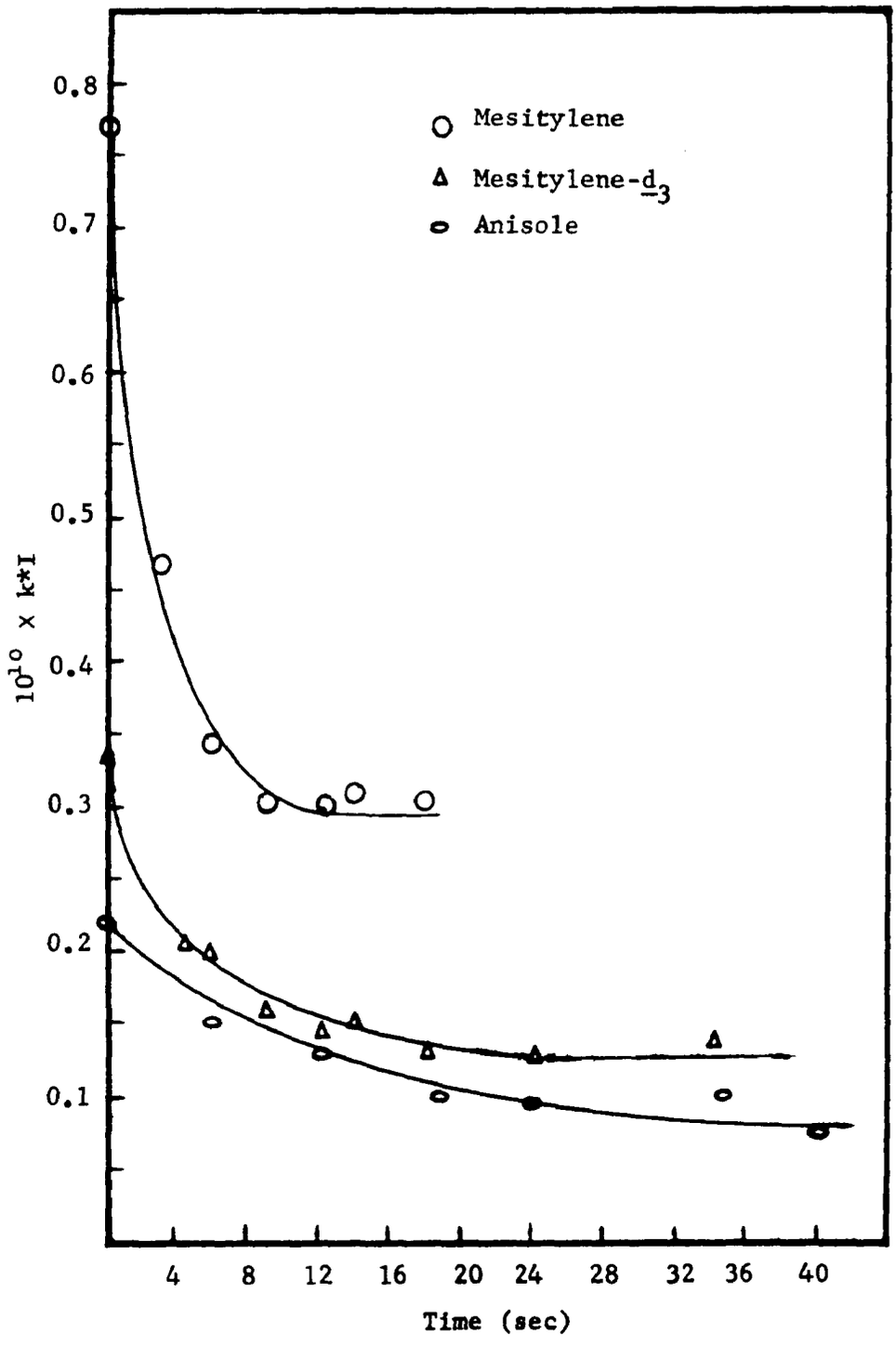

Figure 3. Plots of k*I Versus Time of Reaction. (Points at zero time are from the intercepts in Figure 1 or are estimated.)

Reproduced with permission of the copyright owner. Further reproduction prohibited without permission.

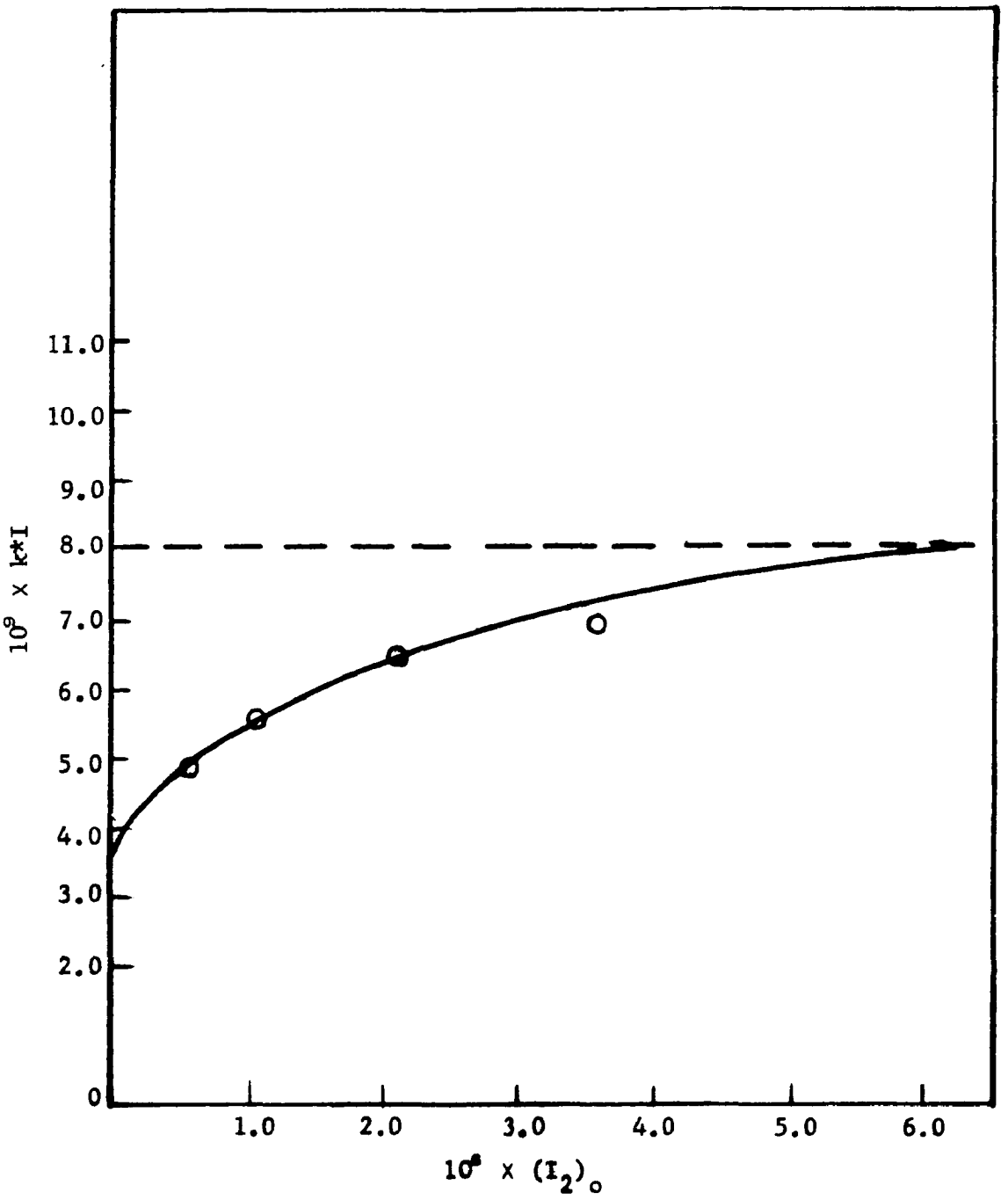

Figure 4. Plot of k*I for Mesitylene Versus Initial (I_2). $((Ag^+) = 4.24 \times 10^{-6}$ M and (ArH) = 4.1×10^{-6} M.)

Reproduced with permission of the copyright owner. Further reproduction prohibited without permission.

The equilibrium concentration of the σ complex should increase as (I^-) is decreased via larger amounts of Ag^+. Such a dependence is not borne out in fact. This is indicated by experiment 126 in Table 6 where k*I is $7.19 \pm 0.52 \times 10^{-9}$ at (Ag^+) of 10.46×10^{-6} M and (ArH) of 13.3×10^{-8} M while the expected value as determined from Figure 1 is 4.2×10^{-9} at (Ag^+) of 4.24×10^{-6} M and (ArH) of 13.3×10^{-6} ArH.

Dimerization or some other form of association of the hydrocarbon in aqueous solution might be possible. Results of the measurement of the partial pressure, p, of mesitylene over a solution of known concentration preclude this possibility. The solution was 1500 ml of 9.317×10^{-5} M mesitylene in a 2 liter volumetric flask fitted with a hollow, ground glass stopper equipped with a rubber septum for sampling the gas phase as well as the aqueous phase. From the application of Henry's law to a solution saturated by ArH and to a solution of lower (ArH), the vapor pressure of ArH over the latter is

$$p = p^* x \qquad (1)$$

Here p^* is the vapor pressure of mesitylene over the saturated solution and x is the ratio of the liquid phase concentration of the hydrocarbon solution of lower concentration divided by the concentration of the saturated solution. The value of p^*, 3.5 mm at 25°, was determined as described below utilizing a gas chromatograph for measuring the partial pressure over a saturated hydrocarbon solution. The solubility of mesitylene[46] at 25° is 5.4×10^{-4} M, and for the solution first mentioned, the cited data lead, via equation (1), to a calculated value of 0.60 mm for p. The gas phase over this same solution was studied on a vapor phase

Reproduced with permission of the copyright owner. Further reproduction prohibited without permission.

chromatograph and showed 8.45×10^{-9} moles present in 0.25 ml. When substituted into the ideal gas law, a value of 0.63 ± 0.04 mm for p is obtained. This value compares very well with that predicted by Henry's law. The ratio of the partial pressure for equivalent hydrocarbon concentrations (9.3×10^{-5} M) of mesitylene in 0.1 N $NaClO_4$ to that in pure water is 1.09 ± 0.05 and thus mesitylene appears to behave ideally in both pure water and solutions having an ionic strength of 0.10. It is concluded that association of the hydrocarbon in aqueous phase does not occur to a significant extent and, therefore, it cannot be the cause of the drop in the rate constant.

The similarity in the rate behavior of anisole to that of mesitylene as indicated in Table 5 is of interest here. The ability of water to hydrogen bond with the ether oxygen atom of anisole makes association much less likely than in the case of mesitylene. Since no association was found for mesitylene, it is also precluded here. It is noted that anisole dissolves in water much more rapidly than mesitylene.

The possibility that the solubility equilibrium for the reaction

$$Ag^+ + I^- \rightleftarrows AgI$$

had not been attained cannot be excluded completely. The rate of combination of Ag^+ and I^- is possibly that of the collision frequency; however, rapidly precipitated AgI may have a larger value of K_{sp} due to smaller particle size than that of slowly formed AgI to which the standard thermodynamic value[47] of K_{sp} pertains. Increasing the silver ion concentration in order to increase the rate of precipitation should increase the deviation in (I^-) from that expected from the standard value of K_{sp}. As a

Reproduced with permission of the copyright owner. Further reproduction prohibited without permission.

Reproduced with permission of the copyright owner. Further reproduction prohibited without permission.

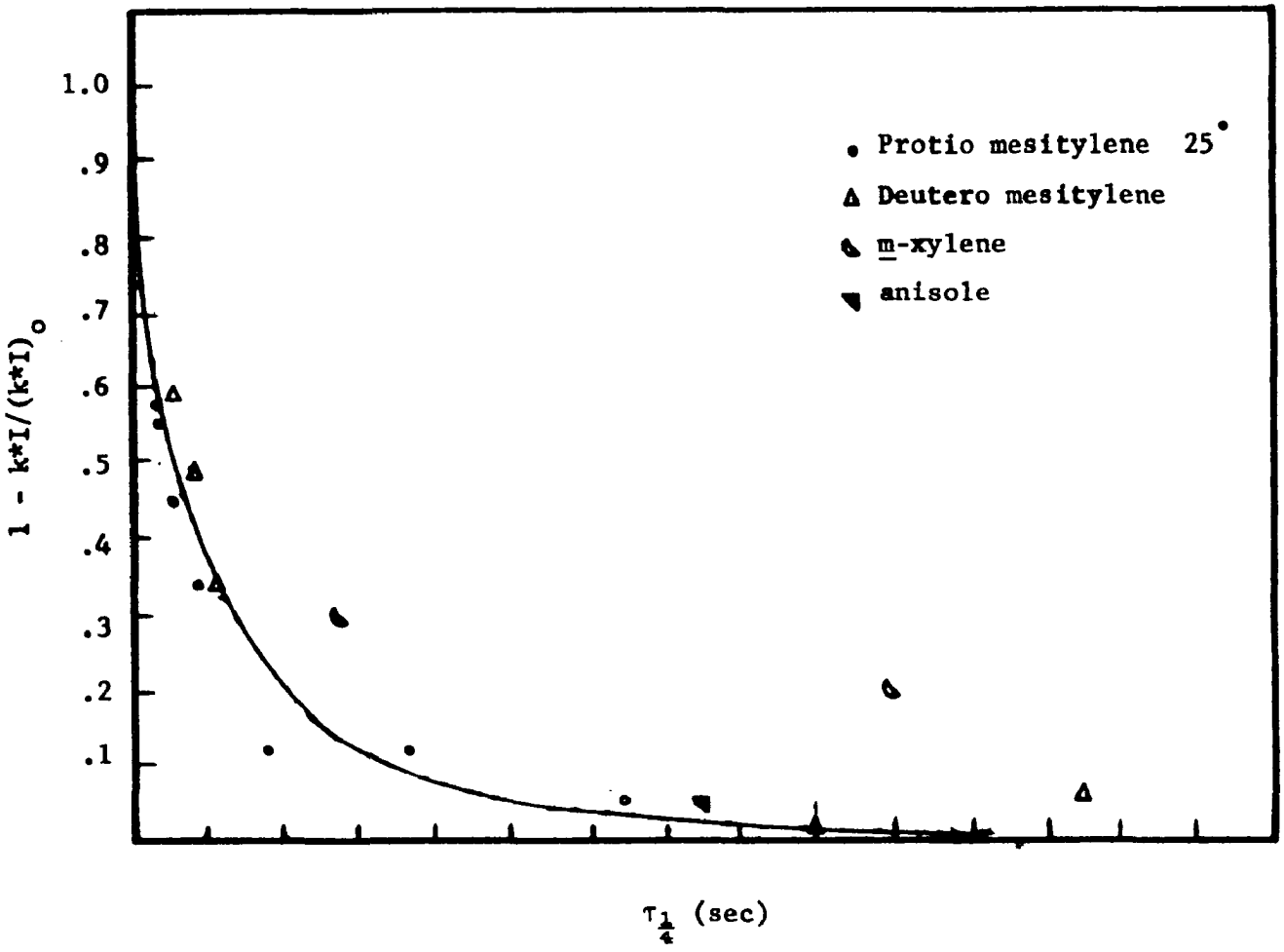

Figure 5. Plot of Dependence of k*I on Quarter-life of I_2

result, the true iodide ion concentration would be higher than expected and hence the apparent k*I would be lower than the true value. The increase of (Ag^+) had the opposite effect; the rate constant was larger.

In Figure 5 is seen a correlation of the drop in rate constants with respect to the velocity of the reaction represented by the quarter-life of iodine. Here the drop in the rate constant is defined in terms of the ratio of the rate constant for the initial hydrocarbon concentration of concern to that value derived from the intercept, (k*I), in Figure 1. All the data represented were taken by Gnanapragasam. The correlation of the data as a function of the reaction rate seems to indicate that factors related to the high rate of reaction rather than some specific property of the hydrocarbons are responsible for the deviations noted.

Often approximations are employed when using steady state treatments to derive expressions for rate constants once a mechanism is suggested. Often the approximations made are enlightening, simplifying, and useful; however, in this work they are felt to be tenuous, and so any mechanisms investigated and discussed will have as few approximations employed as possible. Where the approximations are used, an effort will be made to justify them.

Discussion of Possible Mechanisms

Mechanism I

In this mechanism H_2OI^+ is the halogenating agent.

$$I_2 + H_2O \underset{k_{-1}}{\overset{k_1}{\rightleftharpoons}} H_2OI^+ + I^- \qquad K_1 \equiv k_1/k_{-1}$$

Reproduced with permission of the copyright owner. Further reproduction prohibited without permission.

$$H_2OI^+ + ArH \underset{k_{-3}}{\overset{k_3}{\rightleftharpoons}} \sigma + H_2O$$

$$\sigma + H_2O \xrightarrow{k_5} ArI + H_3O^+$$

where σ represents the sigma complex between I^+ and ArH.

Detailed examination of this mechanism gives, for the most general case, the expression

$$\frac{1}{k^*I} = \frac{k_{-1}\ (k_{-3} + k_5)}{k_1\ k_3\ k_5} + \frac{(ArH)}{k_1\ (I^-)} \qquad (2)$$

In the presence of silver ion the expression may be rewritten as

$$\frac{K_{sp}}{k^*I} = \frac{k_{-1}\ (k_{-3} + k_5)\ K_{sp}}{k_1\ k_3\ k_5} + \frac{(ArH)(Ag^+)}{k_1} \qquad (3)$$

This mechanism suggests that, when $k_3(H_2OI^+)(ArH)$ is comparable to $k_1(I_2)$, then the rate of formation of halogenating agent becomes partially rate determining.

Mechanism II

In this mechanism AgI_2^+ is the effective halogenating agent

$$Ag^+ + I_2 \underset{}{\overset{fast}{\rightleftharpoons}} AgI_2^+ \qquad K \equiv \frac{(AgI_2^+)}{(Ag^+)(I_2)}$$

$$AgI_2^+ + ArH \underset{k_{-4}}{\overset{k_4}{\rightleftharpoons}} \sigma + AgI$$

$$H_2O + \sigma \xrightarrow{k_5} ArI + H_3O^+$$

Reproduced with permission of the copyright owner. Further reproduction prohibited without permission.

For this mechanism

$$k^*I = \frac{K\ k_4\ k_5\ K_{sp}}{k_{-4} + k_5} \qquad (4)$$

Here there is no dependence whatever upon the concentration of Ag^+ or ArH, hence, at least in theory this mechanism can be distinguished from Mechanism I.

Mechanism III

A third possible mechanism is the following

$$H_2O + Ag^+ + I_2 \underset{k'_{-1}}{\overset{k'_1}{\rightleftharpoons}} H_2OI^+ + AgI$$

$$H_2OI^+ + ArH \underset{k_{-3}}{\overset{k_3}{\rightleftharpoons}} \sigma\ H_2O$$

$$\sigma + H_2O \xrightarrow{k_5} ArI + H_3O^+$$

for which

$$\frac{K_{sp}}{k^*I} = \frac{k'_{-1}\ (k_{-3} + k_5)}{k'_1\ k_3\ k_5} + \frac{(ArH)}{k'_1} \qquad (5)$$

This mechanism cannot be distinguished from a fourth one (Mechanism IV)

Mechanism IV

$$Ag^+ + I_2 \underset{k''_{-1}}{\overset{k''_1}{\rightleftharpoons}} AgI_2^+$$

$$AgI_2^+ + ArH \underset{k_{-4}}{\overset{k_4}{\rightleftharpoons}} \sigma + AgI$$

$$\sigma + H_2O \xrightarrow{k_5} ArI + H_3O^+$$

Reproduced with permission of the copyright owner. Further reproduction prohibited without permission.

on the basis of the dependence on (ArH) since here

$$\frac{K_{sp}}{k^*I} = \frac{k''_{-4}\ (k_{-4} + k_5)}{k_1''\ k_4\ k_5} + \frac{(ArH)}{k_1''}$$

Mechanism V

The fifth mechanism combines some of the features of the above mechanisms.

$$I_2 + H_2O \underset{k_{-1}}{\overset{k_1}{\rightleftharpoons}} H_2OI^+ + I^- \qquad K_1 = (H_2OI^+)(I^-)/(I_2)$$

$$Ag^+ + I^- \rightleftharpoons AgI \qquad K_{sp} = (Ag^+)(I^-)$$

$$Ag^+ + I_2 \rightleftharpoons AgI_2^+ \qquad K = (AgI_2^+)/(Ag^+)(I_2)$$

$$H_2O + AgI_2^+ \underset{k_{-2}}{\overset{k_2}{\rightleftharpoons}} AgI + H_2OI^+ \qquad K_2 = (H_2OI^+)/(AgI_2^+)$$

$$H_2OI^+ + ArH \underset{k_{-3}}{\overset{k_3}{\rightleftharpoons}} \sigma + H_2O$$

$$H_2O + \sigma \xrightarrow{k_5} ArI + H_3O^+$$

Applying the steady state approximation to H_2OI^+ and σ

$$H_2OI^+ = \frac{k_1(I_2) + k_2\ (AgI_2^+) + k_{-3}\ \sigma}{k_{-1}\ (I) + k_{-2} + k_3\ (ArH)} \tag{6}$$

$$\sigma = \frac{k_3\ (ArH)(H_2OI^+)}{k_{-3} + k_5} \tag{7}$$

If x is the amount of iodine reacted to form products then

Reproduced with permission of the copyright owner. Further reproduction prohibited without permission.

$$\frac{dx}{dt} = k_5\ \sigma$$

or

$$\frac{dx}{dt} = \frac{\{k_1 (I_2) + k_2\ (AgI_2^+)\}\ k_3\ k_5\ (ArH)}{\{k_{-1}\ (I^-) + k_{-2}\}\ (k_{-3} + k_5) + k_3\ k_5\ (ArH)} \tag{8}$$

Substituting for (AgI_2^+) in terms of K and for (I^-) in terms of K_{sp} then

$$\frac{dx}{dt} = \frac{\{k_1 + k_2 K\ (Ag^+)\}\ k_3\ k_5\ (ArH)(I_2)(Ag^+)}{\{k_{-1}\ K_{sp} + k_{-2}\ (Ag^+)\}\ (k_{-3} + k_5) + k_3\ k_5\ (ArH)(Ag^+)} \tag{9}$$

but by definition

$$\frac{dx}{dt} = \frac{k^*I}{K_{sp}}\ (ArH)(I_2)(Ag^+)$$

and hence

$$\frac{K_{sp}}{k^*I} = \frac{\{k_{-1}\ K_{sp} + k_{-2}\ (Ag^+)\}\ (k_{-3} + k_5)}{\{k_1 + k_2 K\ (Ag^+)\}\ k_3\ k_5} + \frac{(ArH)(Ag^+)}{\{k_1 + k_2 K\ (Ag^+)\}} \tag{10}$$

Noting that equilibrium conditions require that

$$k_{-1}\ K_{sp} = \frac{k_1}{K_2 K}$$

and

$$\frac{K_1}{K_{sp}} = K_2 K$$

then the first term in equation (10) becomes

$$\frac{k_{-1}\ (k_{-3} + k_5)\ K_{sp}}{k_1\ k_3\ k_5} \tag{11}$$

or equivalently

Reproduced with permission of the copyright owner. Further reproduction prohibited without permission.

$$\frac{k_{-2}\ (k_{-3} + k_5)}{k_2 K\ k_3\ k_5} \tag{12}$$

Thus equation (10) becomes

$$\frac{K_{sp}}{k^*I} = \frac{K_{sp}\ k_{-1}\ (k_{-3} + k_5)}{k_1\ k_3\ k_5} + \frac{(ArH)(Ag^+)}{\{k_1 + k_2 K\ (Ag^+)\}} \tag{13}$$

This equation requires that a plot of K_{sp}/k^*I versus (ArH) be linear and have a slope of

$$(Ag^+)/\{k_1 + k_2 K\ (Ag^+)\}$$

The slope is inversely proportional to the net effective rate constant for the formation of H_2OI^+. This slope appears to be dependent upon (Ag^+), but in the limit that

$$k_2 K\ (Ag^+) \gg k_1$$

then the net rate equation is written

$$\frac{K_{sp}}{k^*I} = \frac{(k_{-3} + k_5)}{KK_2\ k_3\ k_5} + \frac{ArH}{k_2 K} \tag{14}$$

If the equilibrium concentration of H_2OI^+ is not maintained, it is not possible to maintain the equilibrium concentration of HOI as they are related by

$$K_a = \frac{(H^+)(HOI)}{(H_2OI^+)} \tag{15}$$

since proton transfer to oxygen is expected to be rapid compared to $k_1(I_2)$,

Reproduced with permission of the copyright owner. Further reproduction prohibited without permission.

or k_2 (AgI_2^+).

As in some of the previous mechanisms, plots of 1/k*I versus (ArH) give intercepts at (ArH) = 0 where the ratio for deuterium and protium compounds is given by equation (16) if isotope effects are neglected for k_3.

$$\frac{(k^*I)_h}{(k^*I)_d} = \frac{(1 + k_{-3}/k_5)_d}{(1 + k_{-3}/k_5)_h} \tag{16}$$

This expression is identical in form to that found for the H_2OI^+ mechanism in the absence of Ag^+.

Mechanism V indicates that, for sufficiently reactive hydrocarbons at very low (I^-), k*I may decrease to the point where the equilibrium concentration of H_2OI^+ is not maintained and therefore $\{k_{-1} K_{sp} + k_{-2} (Ag^+)\}$ is not significantly greater than k_3 (ArH).

Possible Dependence of k*I on Ionic Strength

The effect of ionic strength upon the rate of reaction of hydrocarbon with I_2 in the presence of Ag^+ is not predicted to be the same as in the absence of Ag^+. In the latter case it is found that

$$\frac{dx}{dt} = (k^*I)_{obs} \frac{(ArH)(I_2)}{(I^-)} = \frac{k^*I\ (ArH)(I_2)}{(I^-)\ \gamma_{\pm}\ \gamma^{\ddagger}} \tag{17}$$

when $(k^*I)_{obs}$ is the rate constant determined neglecting activity coefficients, whereas k*I is the rate constant determined using activity coefficients. Here $\gamma_{\pm}$ is the mean activity coefficient and $\gamma^{\ddagger}$ is the gross effective activity coefficient of the transition state. If the activity coefficients are equated then

Reproduced with permission of the copyright owner. Further reproduction prohibited without permission.

$$k^*I = (k^*I)_{obs}\ \gamma_{\pm}^2 \tag{18}$$

In the presence of (Ag^+), however, where $(I^-)\ \gamma_{\pm}^2 = K_{sp}/(Ag^+)$

$$\frac{dx}{dt} = \frac{(k^*I)_{obs}}{K_{sp}}\ (ArH)(I_2)(Ag^+) = \frac{k^*I}{K_{sp}}\ (ArH)(I_2)(Ag^+) \tag{19}$$

or

$$k^*I = (k^*I)_{obs}$$

If $\gamma_{\pm}$ and $\gamma^{\ddagger}$ are not equal in fact, then in the absence of (Ag^+) at low ionic strength, denoted by the subscript ℓ,

$$k^*I = (\gamma_{\pm})_{\ell}\ (\gamma^{\ddagger})_{\ell}\ [(k^*I)_{obs}]_{\ell} \tag{20}$$

while in the presence of Ag^+ and high ionic strength, denoted by h,

$$k^*I = \frac{(\gamma^{\ddagger})_h}{(\gamma_{\pm})_h}\ [(k^*I)_{obs}]_h \tag{21}$$

At a given temperature, however, the ratios of k*I should be unity if the treatment of activity coefficients is appropriate and, hence, from the ratio of equations (20) and (21)

$$\frac{[(k^*I)_{obs}]_{\ell}}{[(k^*I)_{obs}]_h}\ \frac{(\gamma_{\pm})_{\ell}\ (\gamma^{\ddagger})_{\ell}\ (\gamma_{\pm})_h}{(\gamma^{\ddagger})_h} = 1 \tag{22}$$

Since the non Ag^+ work was done at 10^{-5} M ionic strength $\gamma_{\pm}$ is near unity and

Reproduced with permission of the copyright owner. Further reproduction prohibited without permission.

$$\frac{(\gamma^{\ddagger})_h}{(\gamma_{\pm})_h\ (\gamma^{\ddagger})_\ell} = R$$

where R is the ratio of the observed rate constants shown in equation (22).

If $\gamma^{\ddagger}$ and $\gamma_{\pm}$ are independent of small changes in temperature, then they affect only ΔS type terms. From entropy arguments[48] it will be assumed that $\gamma^{\ddagger}$ may be interpreted as follows. Not only is the transition state charged but it may be polar. In order to obtain some estimate of the electronic properties of the transition state, a CNDO/2 calculation was done. Since it is not possible to do CNDO/2 calculations on molecules containing iodine atoms, a calculation for the para-toluene transition state using Cl^+ as the electrophile was considered. The result showed a dipole moment greater than ten Debeye for this transition state model. This suggests that the transition state for the analogous iodination reaction also has a very large dipole moment. Since the transition state also bears a charge, then two contributions to $\Delta S^{\ddagger}$, the entropy of activation, become apparent. One contribution is due to the "point charge" nature of the transition state. This property is usually associated with the mean activity coefficient $\gamma_{\pm}$. The second contribution is a correction to the first and takes into account the high polarity of the electrostatic nature of the transition state, and will be arbitrarily associated with $\delta^{\ddagger}$, a type of activity coefficient associated with non spherical electrostatic properties. The sum of these two contributions then allows $\gamma^{\ddagger}_{\pm}$ to be rewritten

$$\gamma^{\ddagger} \equiv \gamma^{\ddagger}_{\pm}\ \delta^{\ddagger} \qquad (23)$$

Reproduced with permission of the copyright owner. Further reproduction prohibited without permission.

Now equations (23) and (24) reduce to

$$\frac{(\delta^{\ddagger})_h}{(\delta^{\ddagger})_\ell} = R$$

In the case where the enthalpies of activation for a reaction under different ionic conditions are the same, then any difference in reaction rates must be due to differences in the entropies of activation to which R ln (γ) and R ln (δ) are related.

Discussion

It is felt that Mechanism V adequately describes the kinetic behavior for the aqueous iodination of mesitylene, anisole, and m-xylene in the presence of Ag^+. Figure 1 shows that the initial slope for mesitylene at 25° is 8.8×10^{12} ℓ-sec/m and the initial slope indicated appears to be the same for mesitylene-d_3 and anisole at 25°.

The data for mesitylene are not strictly linear. This can be accounted for quite easily. When the numerical value for k*I was calculated, it was assumed that (HOI) was an equilibrium[49] value. Figure 3 suggests that for the ordinary mesitylene where

$$(ArH) = 34 \times 10^{-6} \text{ M}$$

and

$$(Ag^+)_o = 4.24 \times 10^{-6} \text{ M}$$

the equilibrium concentration of HOI, and hence H_2OI^+, has dropped to a very low value after 100 sec, after which k*I becomes constant. This value of (HOI) must be near zero. The true value of k*I, $(k^*I)_t$, is thus

Reproduced with permission of the copyright owner. Further reproduction prohibited without permission.

$$(k^*I)_t = (k^*I)_{obs} \frac{\{(I_2)_o - (HOI) - x\}\{(Ag)_o - (HOI) - x\}}{\{(I_2)_o - x\}_t \{(Ag)_o - x\}_t} \quad (24)$$

The initial value of (HOI) is 20.0 percent of $(I_2)_o$ and, hence, the equilibrium amount of HOI would be approximately $0.2\{(I_2)_o - x\}$. A time of 100 seconds represents 30 percent reaction and, hence, HOI = $0.14\ (I_2)_o$. The correction factor is calculated for $(I_2)_o = 1.85 \times 10^{-6}$ M, from

$$(I_2) = (I_2)_o - 0.3(I_2)_o - 0.2\{(I_2)_o - 0.3(I_2)_o\} = 0.56(I_2)_o$$

$$= 1.04 \times 10^{-6} \text{ M}$$

$$(Ag^+) = (Ag^+)_o - 0.44(I_2)_o = 3.43 \times 10^{-6} \text{ M}$$

$$(I_2)_t = (I_2)_o - 0.3(I_2)_o = 0.7(I_2)_o = 1.30^{6}\ 10^{-}x \text{ M}$$

$$(Ag^+)_t = (Ag)_o - 0.3(I_2)_o = 3.70 \times 10^{-6} \text{ M}$$

to be

$$\frac{(I_2)(Ag^+)}{(I_2)_t(Ag^+)_t} = \frac{1.04 \times 3.43}{1.30 \times 3.70} = 0.74$$

The numerical value for k*I under these experimental conditions is 1/0.74 times too large and 1/k*I is too small by the same factor. This point is noted in Figure 1 and further, since the value of k*I at zero ArH should be k*I for equilibrium conditions, the slope throughout the low (ArH) range should be very close to that at zero (ArH). This appears to be the fact. It would be more difficult to assess a value of (HOI) at intermediate values of (ArH) between zero and 34×10^{-6} M.

The linearity in Figure 1 for mesitylene-$\underline{d}_3$ without the above correction suggests that the equilibrium values for HOI used in the numerical

Reproduced with permission of the copyright owner. Further reproduction prohibited without permission.

calculation of k*I were correct. The slope of the line drawn for anisole is 8.8×10^{12}, which is within experimental error of the slope allowed by 10 percent error in each of the points shown.

The explanation above of the curvature in Figure 1 obscures the possibility that a second halogenating agent, AgI_2^+, may also be reacting with the hydrocarbon. This reagent is known[50] to be a very reactive iodinating agent. A mechanism that has these two halogenating agents can be shown to allow a nonlinear functional dependence of 1/k*I upon (ArH). This mechanism is not given here since the more simple mechanism, Mechanism V, appears adequate to explain the data.

The Dependence on Silver Ion

Experimentally it was found that k*I varied with (Ag^+) under certain conditions.

The explicit dependence of 1/k*I upon (Ag^+) is from equation (10)

$$\frac{\partial \left(\frac{1}{k^*I}\right)}{\partial (Ag^+)} = \frac{k_1}{K_{sp}} \frac{(ArH)}{\{k_1 + k_2 K (Ag^+)\}^2}$$

This derivative is always positive and requires that k*I decrease with an increase in (Ag^+) or else remain constant if $k_2 K (Ag^+) \gg k_1$ according to equation (14). The data of Table 1 (Section C) show that k*I increases from 6.6 to 8.5×10^{-9} upon increasing (Ag^+) from 4.24 to 15.5×10^{-6} M. The value from the intercept of Figure 1 of k*I where all composite equilibria are assumed is 8.0×10^{-9}. Increasing (Ag^+) from 8.7 to 15.5×10^{-6} M causes an increase in k*I of six percent. Experiments 103 and 110 of Table 6 show that further increasing (Ag^+) to 26×10^{-6} M causes no further change in k*I.

Reproduced with permission of the copyright owner. Further reproduction prohibited without permission.

More data on the dependence of k*I upon (Ag^+) are shown by experiments 83, 82, and 84 of Table 1 (Section C) and experiments 103 and 110 of Table 6. As (Ag^+) is increased at (ArH) = 4×10^{-6} M and (H^+) = 0.10 M from 4 to 27×10^{-6} M, k*I increases from 6.56 to 8.6×10^{-9} sec^{-1}. For a 6.75 fold change in (Ag^+), k*I changes only 1.3 fold. Above 15×10^{-6} M, (Ag^+) k*I appears to be constant and hence is described by equation (12).

When, for mesitylene, (ArH) is increased, k*I is expected to decrease according to equation (13). At 13.3×10^{-6} M the expected value for k*I from Figure 1, where (Ag^+) equals 4.25×10^{-6} M, is 4.34×10^{-9}. When (Ag^+) is then increased to 10×10^{-6} M, as in experiment 126, Table 6, k*I becomes $7.19 \pm 0.25 \times 10^{-9}$. At 13×10^{-6} M (ArH) then increasing (Ag^+) 2.35 fold causes an increase in k*I by a factor of 1.65. The same behavior is noted for m-xylene on comparing experiment 125 with experiments 101, 102, and 104 in Table 4. The increase of k*I by a factor of 1.56 in experiment 104 required an increase in (Ag^+) by 5.1.

The assumption of equilibrium in the precipitation of the silver iodide formed in the hydrolysis of I_2 has been of considerable interest in this study. If, in Mechanism V, it is assumed that the formation of AgI_2^+ is at equilibrium at all times, but that the rate of precipitation of I^- by Ag^+ is not, then the following mechanism can be considered, ignoring that part due to AgI_2^+

$$I_2 + H_2O \underset{k_{-1}}{\overset{k_1}{\rightleftharpoons}} H_2OI^+ + I^- \qquad K_1 = k_1/k_{-1}$$

$$I^- + Ag^+ \underset{k_{-7}}{\overset{k_7}{\rightleftharpoons}} AgI \qquad K_{sp} \equiv k_{-7}/k_7$$

Reproduced with permission of the copyright owner. Further reproduction prohibited without permission.

$$H_2OI^+ + ArH \underset{k_{-3}}{\overset{k_3}{\rightleftharpoons}} \sigma + H_2O$$

$$H_2O + \sigma \longrightarrow ArI + H_3O^+$$

If attention is focused upon the first three reactions of this mechanism and if the steady state assumption is made for H_2OI^+ and I^- then

$$(I^-) = \frac{k_1\ (I_2) + k_{-7}}{k_{-1}\ (H_2OI^+) + k_7\ (Ag^+)}$$

$$(H_2OI^+) = \frac{k_1\ (I_2) + k_{-3}\ \sigma}{k_{-1}\ (I^-) + k_3\ (ArH)}$$

Combining these two expressions and rearranging

$$(H_2OI^+) = \frac{k_1\ (I_2) + k_{-3}\ \sigma \left[1 + \dfrac{k_{-1}\ (H_2OI^+)}{k_7\ (Ag^+)}\right]}{k_{-1}\ \dfrac{k_{-7}}{k_7\ (Ag^+)} + k_3\ (ArH) \left[1 + \dfrac{k_{-1}\ (H_2OI^+)}{k_7\ (Ag^+)}\right]} \qquad (26)$$

Now if it is assumed that there is equilibrium between Ag^+ and I^-, then as previously shown

$$(H_2OI^+) = \frac{k_1\ (I_2) + k_{-3}\ \sigma}{k_{-1}\ \dfrac{K_{sp}}{(Ag^+)} + k_3\ (ArH)} \qquad (27)$$

where I^- has been replaced by $K_{sp}/(Ag^+)$. Comparing these two expressions for (H_2OI^+), then, shows that the requirement for equilibrium is that

Reproduced with permission of the copyright owner. Further reproduction prohibited without permission.

$$k_1 (H_2OI^+) \ll k_7 (Ag^+)$$

Equilibrium conditions thus require that the rate of precipitation of I^- by Ag^+ must be identical to that of formation of I^-. Even though equilibrium does not exist, it is assumed that the above inequality holds.

Using equation (27)

$$\frac{\partial (H_2OI^+)}{\partial (Ag^+)} = \frac{\{k_1 (I_2) + k_{-3}\ \sigma\}\ k_{-1}\ K_{sp}}{\{k_{-1}\ K_{sp} + k_3\ (ArH)(Ag^+)\}^2} \qquad (28)$$

This is positive at all values of (Ag^+). Increasing (Ag^+) in order to accelerate the rate of precipitation of AgI has a coincident effect of increasing (H_2OI^+). If the equilibrium associated with K_1 is met, then that associated with K_{sp} may also be maintained. Conversely, if the equilibrium related to K_{sp} is not maintained, then that for K_1 cannot be met.

Associated with the kinetic process of precipitation of AgI is an alternate interpretation. For slowly formed AgI which exists as large particles, the thermodynamic value of K_{sp} is 8.29×10^{-17}. For freshly formed AgI in the very dilute solutions here, there is a significant possibility that the AgI is predominately colloidal,[51] and that this form of AgI has an effectively larger K_{sp} than for aged AgI.[52] As a result, the calculated value of (I^-) based on the thermodynamic value of K_{sp} will be too small, and k*I will in turn be too small. If the major source of H_2OI^+ is from AgI_2^+, then the influence of K_{sp} will be found only in the effect on the numerical value of (HOI), which varies approximately in an inverse fashion with K_{sp}. See Appendix A for the functional dependence of

Reproduced with permission of the copyright owner. Further reproduction prohibited without permission.

HOI on K_{sp}.

Another possible complicating factor is consistent with the observed dependence of k*I on (Ag^+), and that is the adsorption of Ag^+ on the surface of AgI to cause a decrease in effective (Ag^+). The precedent of this proposed phenomenon is described as follows. The surface adsorption of Ag^+ on AgX where X = Cl^-, Br^-, and I^- is the important feature of the Mohr and Fajans methods of halide determination.[53] There is an increase in the importance of this adsorption which follows the above series.[54] The crystalline compound $AgNO_3$: AgCl is known.[55] Where solid AgBr is in the presence of 10^{-5} M $AgNO_3$, approximately one of every seven surface AgBr molecules has a silver ion associated with it.[56] Surface adsorption is of increased importance where colloidal AgX is formed, and colloid formation increases with the above halide series.[57]

Under kinetic conditions where H^+ = 0.1 M $HClO_4$, the addition of 6×10^{-6} M Ag^+ to 2×10^{-6} M NaI produces no visible clouding or precipitation. Over the range of 3000 to 5000 Å there is, however, using a 10 cm cell, an effective absorbance of approximately 0.1 absorption units which may be due to scattering of light by colloidal AgI. Colloid formation is favored where the rate of combination of Ag^+ with I^- is rapid. Under the common kinetic conditions employed,

$$(AgI) \approx 2.5 \times 10^{-6} \text{ M}$$

and

$$(Ag^+) \approx 3.4 \times 10^{-6} \text{ M}$$

such that a high ratio of $(AgI)/(Ag^+)$ exists, and surface adsorption can possibly be very important. The adsorption of 20 percent of Ag^+ to give

Reproduced with permission of the copyright owner. Further reproduction prohibited without permission.

Ag_2I^+ could then give a 20 percent error in the effective value of (Ag^+) used in the numerical determination of k*I. The correct value of k*I would be 8×10^{-9}. When (Ag^+) is larger, say near 15 to 20 $\times 10^{-6}$ M, the amount adsorbed on the surface of AgI would be much less significant and the value of k*I would increase to a maximum and remain constant. This is in fact what is observed. The largest value of k*I is 8.5×10^{-9} at (Ag^+) of 26.61×10^{-6} M.

The Effect of Temperature on Silver Ion Dependence. At 35°, Figure 1 shows a smaller slope, 3.22×10^{12} than at 25° for mesitylene; this may be understood in terms of the relative importance of k_1 to $k_2K(Ag^+)$. The interpretation of the slope at 35° is difficult, however. From equation (13) and the slopes at 25° and 35°, the apparent sum of the hydrolysis rate constants, $k_1 + k_2K(Ag^+)$ is smaller at the higher temperature, 3.60×10^{-3} sec^{-1}. Since k_1 and k_2 are rate constants, they must increase with T, but K and k_2K must decrease with T to satisfy the observed behavior. This implies that the sum of ΔH° for K and $\Delta H^\ddagger$ for k_2 is negative.

Another instance where a negative activation energy is obtained[57] is the HBr catalyzed bromination of mesitylene in CCl_4. The halogenating agent can be thought of as $Br^+(BrHBr)^-$. The negatively charged moiety decreases in stability with temperature.

The term $k_2K(Ag^+)$ will make a larger contribution to the sum, $k_1 + k_2K(Ag^+)$, at 25°. Insofar that k*I at 25° increases only six percent with a six-fold change of (Ag^+), as opposed to a predicted decrease if k_1 is important, $k_2K(Ag^+)$ must be the dominant term in the expression for the considered slope and thus equation (14) is applicable. The result is that at 25° k_2K is 1.39×10^3 sec^{-1}, determined from the slope of

Reproduced with permission of the copyright owner. Further reproduction prohibited without permission.

8.8×10^{12} ℓ-sec/m in Figure 1, $K_{sp} = 8.24 \times 10^{-17}$, and $(Ag^+)_o = 3.85 \times 10^{-6}$ M.

From the intercept for mesitylene at 25°,

$$k^*I = \frac{k_2 K k_3}{k_{-2}(1 + k_{-3}/k_5)}$$

Sullivan showed for the iodination of 2,4-dinitrophenoxide ion by H_2OI^+ that k_{-3}/k_5 had a value of 0.43 ± 0.04 sec^{-1}. Since the reactivity of 2,4-dinitrophenoxide ion was found to be similar to that of anisole, which is similar to mesitylene, and since the isotope effect determined for this halogenating agent is similar in magnitude, 2.3, the above reversibility ratio may be applicable here; therefore,

$$\frac{k_3}{k_{-2}} \approx 9.45 \times 10^4 \text{ ℓ/m}$$

This ratio combined with a value of (ArH) represents the ratio of (H_2OI^+) that goes to form sigma complex to that reverting to I_2. For (ArH) = 4×10^{-6} M

$$\frac{k_3}{k_{-2}}(ArH) = 3.78 \times 10^{-1}$$

whereas for (ArH) = 34×10^{-6} the product is 3.22. At 4×10^{-6} M (ArH) only one of every 3.5 H_2OI^+ molecules goes to give sigma complex while at the higher value three of every four H_2OI^+ molecules does so. In the latter case it is not difficult to see that equilibrium concentrations of H_2OI^+ cannot be maintained, and hence k*I can be very sensitive to changes in (ArH).

Reproduced with permission of the copyright owner. Further reproduction prohibited without permission.

The linear behavior at 35° in Figure 1 is interpreted in light of the temperature dependence of K. It is felt that at 35° a smaller amount of AgI_2^+ is formed at the same (I_2) and (Ag^+) than at 25°. The slope found in Figure 1 at 35° is 3.6×10^{12} ℓ-sec/mole. This numerical value along with 3.456×10^{-16} for K_{sp} and 4.0×10^{-16} M for (Ag^+) gives k_2K = 83 ℓ/m-sec (to be compared with value of 1.33×10^3 at 25°), if k_2K (Ag^+) is significantly greater than k_1 at 35°. The implied negative free energy of activation for k_2K may be understood in terms of the previous discussion of the relative temperature dependence of k_2 and K. The linearity of the plot at 35°, compared to that at 25°, is partially explained by the fact that the percent of I_2 existing as HOI at 35° is approximately one half that at 25° as determined by equilibrium calculations. This is due to the fact that, while K_{sp} increases from 8.3×10^{-17} to 3.456×10^{-16}, the hydrolysis constant K_h increases only from 5.4×10^{-13} to 1.365×10^{-12}. There is a much smaller correction necessary to get $(k^*I)_t$ than shown previously for 25°. This smaller value of (HOI), and hence of (H_2OI^+), at higher temperatures would explain the greater decrease in k*I with respect to (ArH); there is a smaller effective buffer of H_2OI^+. Also, all equilibria are probably more readily attained at 35° than at 25°.

The Effect of Silver Ion on the Isotope Effect. The fact that the isotope effect, determined from the ratio of intercepts in Figure 1 is 2.2 ± .3, which is within experimental error of the value determined at higher temperatures in the absence of Ag^+, suggests that there is no change in the overall process of proton loss in the presence of Ag^+. If there is increasing importance of the inorganic chemistry of Mechanism V in the rate determining process, however, then [according to equation (13)]

Reproduced with permission of the copyright owner. Further reproduction prohibited without permission.

the experimental isotope effect should decrease. At the intercept (Figure 1) at 25° for the two types of mesitylene the isotope effect is 2.2 while at (ArH) = 34 x 10^{-6} M the isotope effect is reduced to 1.37. At (ArH) = 50 x 10^{-6} M the isotope effect is expected to be 1.05 and clearly this is within the limit of an isotope effect of unity, where proton loss is no longer rate determining.

The Influence of Variations in Iodine Concentration

The dependence of k*I upon (I_2) for mesitylene is shown in Table 1 (Section B) and Figure 4. As (I_2) is decreased from 3.5 to 0.51 x 10^{-6} M, k*I decreases from 7.05 to 4.95 x 10^{-9} while (ArH) = 4.1 x 10^{-6} and (Ag^+) = 4.24 x 10^{-6} M. Figure 4 is understood in terms of the difficulty in attaining the form of AgI to which the thermodynamic value of K_{sp} pertains. At low values of (I_2), there may be insufficient AgI for nucleation and hence there may be either supersaturation of the solution with AgI or colloidal formation of a more soluble form of AgI. This would lead to a non-equilibrium value for HOI with respect to K_{sp}. Since a specific functional dependence of HOI on K_{sp} exists, k*I would then be in error. If (HOI) is in fact too large, then the calculated value of k*I would be too small.

The Influence of Variations of Ionic Strength

The effect of ionic strength upon the rate of iodination of hydrocarbons is also shown in Figure 2. The values of k*I where (Ag^+) = 0 at 25° and 35° at 10^{-5} M ionic strength are obtained by extrapolating the data from higher temperatures. The values are 1.49 x 10^{-8} and 5.79 x 10^{-8} sec^{-1}, respectively. Equation (25) gives 1.8 for the ratio $(\delta^{\ddagger})_{\ell}/(\delta^{\ddagger})_h$ where $((k^*I)_{obs})_h$ = 8.0 x 10^{-9} sec^{-1}. If $(\delta^{\ddagger})_{\ell}$ is unity for

Reproduced with permission of the copyright owner. Further reproduction prohibited without permission.

the low ionic case, then $(\delta^{\ddagger})_h$ must be less than unity. This might be interpreted by way of ordering of the solvent by the perchloric acid added to produce an ionic strength of 0.1 M. The more ordered solvent would not be as able to stabilize the transition state and hence the rate of the reaction would be smaller.

The disagreement in the rate constants at low and high ionic strength may also lie in the possibility that true AgI equilibrium is never attained at the Ag^+ and I_2 concentrations employed; there may not even be enough AgI to allow anything other than colloidal AgI to which K_{sp} does not refer.

Conclusions from the Study of Mesitylene, Anisole, and m-Xylene

In general, it appears that silver ion has the anticipated effect on the rate of reaction of mesitylene, anisole, and m-xylene with iodine in water. The rate varies inversely with the iodide ion concentration calculated from the AgI solubility equilibrium constant. Through the use of Ag^+ the iodide ion concentration range has been extended from 10^{-4} M down to 10^{-12} while the ionic strength was increased for 10^{-5} M to 10^{-1} M. The use of Ag^+, however, causes a deviation in the concentration of halogenating agent from that predicted for an equilibrium concentration, and the rate of reaction then becomes similar to the rate of formation of the halogenating agent. It is highly pleasing that only small deviations in k*I were found for such large variations in iodide ion concentration and ionic strength. To this writer's knowledge, this is the first instance where the kinetics of a compound have been studied in a quantitative manner over such large concentration variations.

Reproduced with permission of the copyright owner. Further reproduction prohibited without permission.

For slower reactions than those discussed here, it is felt that the K_{sp} equilibrium will be maintained and also that the halogenating agent will be formed rapidly enough so as not to be significant in the rate determining process.

Reproduced with permission of the copyright owner. Further reproduction prohibited without permission.

CHAPTER V

KINETICS AND RELATIVE REACTIVITIES OF BENZENE AND OTHER METHYLATED DERIVATIVES

Introduction

In the previous chapter, several mechanisms for iodination in the presence of Ag^+ were presented. Mechanism V was shown to be consistent with the data given for mesitylene, anisole, and m-xylene. While these studies were done near $(Ag^+) = 4 \times 10^{-6}$ M, with few exceptions most of the subsequent kinetic studies were done where $(Ag^+) \approx 10^{-5}$ M. At the (Ag^+) employed here, the source of H_2OI^+ is assumed to be AgI_2^+ as suggested for mesitylene. The purpose of the remainder of this work is to study the change in reactivity brought about by increasing the number of methyl groups of the benzene ring from one to five. Of particular interest is the comparison of the kinetics of iodination in water with those of bromination in water[29]; the rates of bromination by Br_2 increased by a factor of 10^9 on going from benzene to pentamethylbenzene.

Since an isotope effect of 1.5 has been found for the bromination[18] of sterically crowded 3-bromodurene and 3-methoxydurene in acetic acid while none has been found for benzene,[58] it is of interest to examine the effect of structure upon the isotope effect of iodination. In particular, does the isotope effect on iodination in water change as the number of methyl groups on the aromatic ring is increased? Coincident with this inquiry is the question of the effect of crowding on the overall rate of

Reproduced with permission of the copyright owner. Further reproduction prohibited without permission.

reaction. Does the rate of reaction increase in a predictable fashion as indicated by partial rate factors determined for less reactive, non-crowded molecules?

In Huckel calculations, the influence of methyl groups may be included by varying the matrix diagonal element corresponding to the substituted ring carbon. Using all valence electrons, a more exact quantum mechanical model of the methyl group and a quantitative description of the specific participation of the group in aromatic resonance is included in recent CNDO calculations.[59] It would be of interest to predict relative rates of electrophilic substitution of methyl bearing hydrocarbons using molecular orbital theory where the proton is used as the electrophile. Since the proton is considered to be significantly smaller than either Br_2 or H_2OI^+ correlation of the rate constants for these two reagents with CNDO calculations may give some information concerning steric hinderance in these reactions.

The correlation of rate data with theoretical calculations is possible from the following considerations. From absolute rate theory[60] a rate constant may be expressed as

$$k_r = \frac{\kappa kT}{h} \exp\left(-\Delta G^{\ddagger}/RT\right) \qquad (1)$$

where $\Delta G^{\ddagger}$ is the "free energy of activation," R is the gas constant, T is the absolute temperature, κ is the transmission coefficient, k is the Boltzman constant, and h is Planck's constant; thus

$$RT \ln (k_r) = RT \ln \left(\frac{\kappa kT}{h}\right) - \Delta G^{\ddagger} \qquad (2)$$

Reproduced with permission of the copyright owner. Further reproduction prohibited without permission.

Since $\Delta G^{\ddagger} = \Delta H^{\ddagger} - T\Delta S^{\ddagger}$, and if $T\Delta S^{\ddagger}$ is proportional to $\Delta H^{\ddagger}$, or perhaps constant and small compared to $\Delta H^{\ddagger}$, and further if $\Delta H^{\ddagger} = \Delta E^{\ddagger} + \Delta(PV)^{\ddagger} \approx 0$, then correlation of interest is $\ell n\ (k_r)$ versus $\Delta E^{\ddagger}$. It is expected that energy calculations using molecular orbital schemes refer to zero degrees Kelvin, but so far as correlations have been made, it has been successfully assumed that $\Delta E^{\ddagger}$ is proportional to $\Delta E_o^{\ddagger}$. The definition of $\Delta E_o^{\ddagger}$ is that of the difference in the energy between models representing the transition and ground states, respectively, at 10°K.

Experimental Results

The results of the remainder of the kinetic studies are presented in Tables 7-13 and include benzene, toluene, p-xylene, o-xylene, durene, prehnitene, and pentamethylbenzene. These compounds are listed in order of increasing reactivity as judged by the magnitude of k*I at 35°. Where the deuterated hydrocarbon was studied, the protium analogue was also studied and is noted by pairing of the two runs in the appropriate tables. The average value of the observed rate constants are computed and listed in each table. For benzene the high (Ag^+) used to make the reaction rate practical gives rise to a complicating conversion[61] of I_2 to HIO_3 according to the equilibrium

$$3H_2O + 3I_2 \rightleftharpoons IO_3^- + 6H^+ + 5I^-$$

$$K = \frac{(IO_3^-)(H^+)^6(I^-)^5}{(I_2)^3} \approx 4.5 \times 10^{-46} \quad \text{at } 35^\circ$$

While the thermodynamic parameters derived from the rate studies will be discussed in detail later, some consideration is given here to

Reproduced with permission of the copyright owner. Further reproduction prohibited without permission.

Table 7. Benzene Rate Constants Determined in the Presence of Ag^+ and $HClO_4$

Experiment No.	ArH $\underline{M} \times 10^3$	I_2 $\underline{M} \times 10^6$	Ag^+ $\underline{M} \times 10^6$	$k^*(I^-) \times 10^{14}$ sec^{-1}
Temperature = 25.0°				
(H^+) = 0.10 $\underline{M}$				
198	.7874	5.285	36.67	0.122 ± 0.018
Temperature = 30.0°				
(H^+) = 0.10 $\underline{M}$				
154	11.97	2.370	32.59	0.440 ± 0.015
156	13.66	2.368	31.52	0.438 ± 0.053
(H^+) = 0.20 $\underline{M}$				
162	12.16	2.145	31.87	0.402 ± 0.093
163	10.23	3.635	32.84	0.437 ± 0.019
Temperature = 35.0°				
(H^+) = 0.20 $\underline{M}$				
243	12.80	2.953	32.94	0.93 ± 0.13
244	13.12	2.429	22.58	0.89 ± 0.44
245	12.58	2.810	22.24	0.98 ± 0.05
			Average:	0.93 ± 0.03
250	12.07	5.206	25.16	1.65 ± 0.02
251*	18.12	8.330	25.79	0.72 ± 0.02
(H^+) = 0.30 $\underline{M}$				
207	5.998	5.648	34.21	1.68 ± 0.07
215	11.17	2.276	34.05	1.56 ± 0.12
217	11.79	2.317	27.57	1.93 ± 0.13
219	11.59	2.853	35.60	1.58 ± 0.13
			Average:	1.69 ± 0.12

*Benzene-$\underline{d}_6$ (99.5% $\underline{d}$)

Reproduced with permission of the copyright owner. Further reproduction prohibited without permission.

Table 8. Toluene Rate Constants Determined in the Presence of Ag^+ and 0.1 M $HClO_4$

Experiment No.	ArH M × 10^6	I_2 M × 10^6	Ag^+ M × 10^6	$k^*(I^-) \times 10^{13}$ sec^{-1}
Temperature = 25.0°				
70	800.6	6.120	18.00	3.01 ± 0.05
71	457.5	6.120	18.00	3.11 ± 0.05
72	773.2	6.730	10.00	2.90 ± 0.08
73	773.2	3.703	18.00	3.26 ± 0.33
87	705.3	7.214	18.00	3.50† ± 0.12
100	255.1	2.542	18.00	2.90 ± 0.09
101*	938.7	1.945	36.00	3.49† ± 0.18
106	1135.	2.247	35.30	3.24 ± 0.11
95	787.9	2.538	18.00	3.01 ± 0.09
93	883.8	1.987	5.678	3.13 ± 0.09
92**	758.4	1.987	5.678	1.61 ± 0.12
97	750.0	2.349	18.00	2.99 ± 0.27
96**	808.4	2.349	18.00	1.28 ± 0.13
			Average:	3.06 ± 0.09
Temperature = 35.0°				
89	680.2	5.938	18.00	22.1 ± 0.4
88***	647.5	5.938	18.00	11.7 ± 0.4
105	790.5	1.588	18.00	20.6 ± 1.8
104***	1571.	1.588	18.00	12.4 ± 0.6
			Average:	21.4 ± 0.7

*(H^+) = 0.20 M

**Toluene-d_5 (92% d)

***Toluene-d_5 (80% d)

†Not included in average

Reproduced with permission of the copyright owner. Further reproduction prohibited without permission.

Table 9. p-Xylene Rate Constants Determined in the Presence of Ag^+ and 0.1 M $HClO_4$

Experiment No.	ArH M × 10^6	I_2 M × 10^6	Ag^+ M × 10^6	$k^*(I^-) \times 10^{11}$ sec^{-1}
Temperature = 25.0°				
192	548.9	5.890	30.90	0.211 ± 0.007
196	713.1	5.597	27.01	0.191 ± 0.092
Temperature = 35.0°				
193	491.6	5.887	24.51	1.30 ± 0.03*
194	495.2	5.537	23.97	1.17 ± 0.02
195	243.4	5.765	28.59	1.11 ± 0.03
197	579.1	5.277	14.71	1.07 ± 0.11
200	693.3	5.828	23.70	1.13 ± 0.03
201	603.8	2.867	4.371	1.19 ± 0.12
202	317.2	6.068	22.26	1.02 ± 0.07
246	396.0	2.685	23.01	1.02 ± 0.05
247**	671.8	2.685	23.01	0.517 ± 0.009
248	350.2	2.924	23.56	1.13 ± 0.02
249**	609.7	2.924	23.56	0.551 ± 0.02
			Average:	1.11 ± 0.05

*Not included in average

**p-Xylene-d_4 (92.3% d)

Reproduced with permission of the copyright owner. Further reproduction prohibited without permission.

Table 10. o-Xylene Rate Constants Determined in the Presence of Ag^+ and 0.1 M $HClO_4$

Experiment No.	ArH M x 10^6	I_2 M x 10^6	Ag^+ M x 10^6	$k^*(I^-)$ x 10^{12} sec^{-1}
Temperature = 25.0°				
228	679.0	3.222	24.68	2.61 ± 0.18
230	679.0	3.119	24.57	2.68 ± 0.09
232	679.0	2.995	25.30	2.50 ± 0.07
			Average:	2.60 ± 0.06
Temperature = 35.0°				
229	339.5	3.088	32.91	12.9 ± 0.9
231	338.5	2.891	24.57	14.0 ± 0.4
233	339.5	2.891	25.30	12.2 ± 0.4
			Average:	13.0 ± 0.6

Reproduced with permission of the copyright owner. Further reproduction prohibited without permission.

Table 11. Durene Rate Constants Determined in the Presence of Ag^+ and 0.1 M $HClO_4$

Experiment No.	ArH M x 10^6	I_2 M x 10^6	Ag^+ M x 10^6	$k^*(I^-)$ x 10^{10} sec^{-1}
Temperature = 25.0°				
186	4.707	5.702	13.53	1.16 ± 0.06
179	9.264	5.675	13.41	1.16 ± 0.04
180	15.44	5.309	14.66	1.11 ± 0.05
181	15.44	5.608	14.71	1.14 ± 0.02
187	24.34	5.325	15.49	1.07 ± 0.03
184	25.31	5.211	15.07	1.16 ± 0.03
185	9.737	5.299	18.96	1.06 ± 0.03
188	21.19	4.832	27.69	1.12 ± 0.03
			Average:	1.13 ± 0.03
Temperature = 35.0°				
182	6.176	5.338	14.77	4.64 ± 0.32
183	6.176	5.289	26.85	4.63 ± 0.15
263	11.19	3.044	27.40	4.88 ± 0.15
262*	13.64	2.892	27.40	2.05 ± 0.10
265	5.209	2.479	27.49	5.21 ± 0.08**
264*	11.93	2.396	27.49	2.29 ± 0.04
			Average:	4.72 ± 0.11

*Durene-d_2 (90.6% d)

**Not included in average

Reproduced with permission of the copyright owner. Further reproduction prohibited without permission.

Table 12. Prehnitene Rate Constants Determined in the Presence of Ag^+ and 0.1 M $HClO_4$

Experiment No.	ArH M x 10^6	I_2 M x 10^6	Ag^+ M x 10^6	$k^*(I^-)$ x 10^9 sec^{-1}
Temperature = 25.0°				
235	11.49	2.535	4.183	1.03 ± 0.05
237	11.44	2.790	3.965	1.06 ± 0.05
			Average:	1.05 ± 0.02
Temperature = 35.0°				
236	11.49	2.306	4.183	4.36 ± 0.28
238	11.49	2.712	3.965	4.83 ± 0.27
			Average:	4.60 ± 0.23

Reproduced with permission of the copyright owner. Further reproduction prohibited without permission.

Table 13. Pentamethylbenzene Rate Constants Determined in the Presence of Ag^+ and 0.1 M $HClO_4$

Experiment No.	ArH M x 10^6	I_2 M x 10^6	Ag^+ M x 10^6	$k^*(I^-)$ x 10^9 sec^{-1}
Temperature = 25.0°				
223	11.07	2.911	5.418	4.32 ± 0.14
224	10.62	2.937	4.939	4.01 ± 0.28
225	10.39	2.732	4.671	4.02 ± 0.16
			Average:	4.12 ± 0.13
Temperature = 35.0°				
220	1.672	2.463	4.477	16.7 ± 1.2
221	8.359	2.434	5.036	16.9 ± 1.7
222	8.359	2.412	4.936	16.8 ± 0.7
227	8.359	2.988	4.377	17.4 ± 0.3
261	5.956	2.603	14.38	16.8 ± 0.5
260*	6.397	2.603	14.38	6.52 ± 0.42
267	6.728	2.731	13.94	16.0 ± 0.4
266*	5.956	2.731	13.94	6.41 ± 0.23
			Average:	16.8 ± 0.3

*Pentamethylbenzene-d (92% d)

Reproduced with permission of the copyright owner. Further reproduction prohibited without permission.

these parameters for benzene. The rate constant k*I appears to increase by a factor 13.3 for a 10° change in temperature. This in turn implies that $\Delta H^{\ddagger}$ for benzene is ca. 72.5 kcal/mole. This is an unusually large value. Immediately suspect is the rate constant at 25°. The single value for 25° cited in Table 7 is the only result of the one successful effort among some ten experiments to obtain data with sufficiently small scatter to determine a rate constant. The high degree of irreproducibility at 25° is consistent with the aforementioned iodate formation. If there is an "iodate problem," there is raised some question as to the validity of the experiments done at 30°. Varying (H^+) should cause some change in (k*I) if there is a problem, but there is essentially no difference in k*I when (H^+) is either 0.1 M or 0.2 M. For $(I^-) = 2 \times 10^{-11}$ M, $(H^+) = 0.2$ M, and $(I_2)_0 = 1.8 \times 10^{-6}$ M and the equilibrium concentration of (IO_3^-) is calculated to be 1×10^{-6} M neglecting HOI formation. This is 55 percent of the iodine present initially. If $(H^+) = 0.3$ M then (IO_3^-) is reduced to 0.088×10^{-6} M and the effect of this amount would be hard to detect. As no indication of complication exists at this iodide concentration for faster reactions of more reactive hydrocarbons the rate of formation of IO_3^- must be comparable to the rate of iodination of benzene. The mean activity coefficients[62] of the two acid concentrations differ by less than two percent and cannot be the cause of the rate difference. The values of k*I at 0.3 M H^+ are therefore considered the more reliable for benzene.

Not only must the equilibrium concentration of IO_3^- be considered but also the rate of formation. At 25° and (H^+) of 0.1 M the activation energy for the formation of IO_3^- is approximately 38 to 40 kcal/mole.[63]

Reproduced with permission of the copyright owner. Further reproduction prohibited without permission.

On consideration of some of the other kinetic studies in this thesis, in particular toluene, the activation energy for benzene is anticipated also to be 38 to 40 kcal/mole. If the entropies for the two reactions are ignored for the moment, it is fairly clear that the rates of formation of IO_3^- and the rate of reaction of H_2OI^+ and benzene are similar. The large uncertainty in these values for both processes does not allow a prediction of the predominate process at 35°, or any other temperature for that matter.

In Table 14 is found a summary of all the kinetic studies, including k*I at 25° and 35°, the enthalpy and entropy of activation, $\Delta S^{\ddagger}$ and $\Delta H^{\ddagger}$, and the observed relative reactivities at 25° and 35°.

Now $\Delta G^{\ddagger}$ may be readily obtained from an observed constant via equation (1) rewritten in the fashion

$$\Delta G^{\ddagger} = - RT \ln \left(\frac{hk_r}{\kappa kT}\right) \qquad (3)$$

where the transmission coefficient κ is assumed to be 1.0. It is possible to calculate $\Delta H^{\ddagger}$ by plotting $\ln \left(\frac{k_r}{T}\right)$ versus $\frac{1}{T}$ for which the slope is $- \Delta H^{\ddagger}/R$. The entropy of activation, $\Delta S^{\ddagger}$, was determined as $\frac{\Delta H^{\ddagger} - \Delta G^{\ddagger}}{T}$. It is noted that if $\Delta H^{\ddagger}$ is independent of temperature, then so is $\Delta S^{\ddagger}$.

Errors in k*I are with respect to the average of each set of kinetic runs.

The percent errors in $\Delta H^{\ddagger}$, P.E., were determined[64] as the absolute value of

$$100 \left[1/\ln (k_2/k_1)\right] \left[\left(\frac{\Delta k_1}{k_1}\right)^2 + \left(\frac{\Delta k_2}{k_2}\right)^2\right]^{\frac{1}{2}} \qquad (4)$$

Reproduced with permission of the copyright owner. Further reproduction prohibited without permission.

Reproduced with permission of the copyright owner. Further reproduction prohibited without permission.

Table 14. Thermodynamic Properties of Kinetic Studies Done in the Presence of Ag^+

Hydrocarbon	25° (k*I) x 10^x	35°	x	$\Delta H^\ddagger$ kcal/m	$\Delta S^\ddagger$ cal/deg	$\Delta G^\ddagger$ kcal/m	$(\Delta S^\ddagger)^*$ cal/deg	$(\Delta G^\ddagger)^*$ kcal/m	α
Benzene		1.61 ± 0.11	14						
Toluene	3.06 ± 0.09	21.4 ± 0.7	13	34.9 ± 0.8	- 3.02 ± 2.7	34.48	- 0.84 ± 2.7	35.16	3**
p-Xylene	2.01 ± 0.10	11.1 ± 0.5	12	30.6 ± 0.8	-15.8 ± 2.6	33.48	-13.1 ± 2.6	34.33	4
o-Xylene	2.60 ± 0.06	13.0 ± 0.6	12	28.8 ± 0.9	-17.7 ± 2.9	33.39	-16.3 ± 2.9	33.21	2
Durene	1.13 ± 0.03	4.72 ± 0.11	10	25.5 ± 0.6	-21.2 ± 1.9	31.19	-19.8 ± 1.9	31.61	2***
m-Xylene	1.06 ± 0.05	6.59	10	32.8 ± 1.2	+ 2.1 ± 4.5	30.99	+ 4.5 ± 4.5	31.41	2***
Prehnitene	1.05 ± 0.02	4.60 ± 0.23	9	26.4 ± 1.0	-13.8 ± 3.4	28.80	-12.4 ± 3.4	30.22	2
$C_6H(CH_3)_5$	4.12 ± 0.13	16.8 ± 0.3	9	25.1 ± 0.6	-12.7 ± 1.9	29.00	-12.7 ± 1.9	29.00	1
Mesitylene	8.0 ± 0.4	32.2 ± 1.5	9	24.8 ± 0.89	-16.8 ± 3.0	28.60	-14.55 ± 3.0	29.28	3

The number of equivalent sites per molecule are noted as α.

*For a specific reaction site

**The 2,4,and 6 positions are equated

***The 2,4 position considered only

where Δk is the mean deviation in $(k*I)_i$ at T_i. The error in $\Delta S^{\ddagger}$ was determined from

$$R \frac{\Delta k_i}{k_i} + \frac{\delta(\Delta H^{\ddagger})}{T_i} \tag{5}$$

where R is the gas constant and $\delta(\Delta H^{\ddagger}) = \text{P.E.}\ (\Delta H^{\ddagger})$. The mean value of the first term was employed. Errors in T were ignored by comparison with errors in k.

The equation for the error in $\Delta S^{\ddagger}$ is derived in the following manner. Assuming negligible errors in T, a small change in $\Delta S^{\ddagger}$ may be written

$$\delta(\Delta S^{\ddagger}) = \frac{\delta(\Delta H^{\ddagger})}{T} - \frac{\delta(\Delta G^{\ddagger})}{T} \tag{6}$$

The quantity $\delta(\Delta H^{\ddagger})$ is known from above. Now the errors in $\Delta G^{\ddagger}$ may be expressed from equation (3) as

$$\delta \Delta G_i^{\ddagger} = RT\ \delta\ \ell n\ k_i$$

but for small changes in k_i

$$\delta\ \ell n\ k \approx \frac{\Delta k_i}{k_i} .$$

A true isotope effect may be determined from an observed one where the deuterium labeled substate has some of the protium analogue as a contaminant in small amounts by the relationship

$$(\text{I.E.})_{\text{corr}} = \frac{f(\text{I.E.})_{\text{obs}}}{1 - (1 - f)(\text{I.E.})_{\text{obs}}}$$

Reproduced with permission of the copyright owner. Further reproduction prohibited without permission.

where

$$(I.E.)_{obs} = \frac{\{(k^*I)_{obs}\}_h}{\{(k^*I)_{obs}\}_d}$$

and f is the mole fraction of deuterium content. The errors in the isotope effect were estimated from the sum of the percent error for each of the isotopically labeled molecules. In Table 15 are listed the isotope effects.

Discussion

Isotope Effects

Before considering in detail the relative reactivities of the hydrocarbons, attention is first directed toward the isotope effect with some mention of relative reactivities. In the previous chapter the details of Mechanism V give the following expression for the case where all the equilibria related to H_2OI^+ are maintained.

$$k^*I = \frac{k_2 K k_3 k_5}{k_{-2}(k_{-3} + k_5)} \tag{7}$$

Now k_2, k_{-2}, and K are constant with respect to varying the structure of the hydrocarbon. If the rate constant k_3 for the attack of H_2OI^+ on the aromatic substrate has no isotope effect, then on considering k*I for protium and deuterium bearing compounds

$$\frac{(k^*I)_h}{(k^*I)_d} = \frac{(1 + k_{-3}/k_5)_d}{(1 + k_{-3}/k_5)_h} \tag{8}$$

Insofar as k_3 is isotopically independent, then so is k_{-3}. As stated

Reproduced with permission of the copyright owner. Further reproduction prohibited without permission.

Table 15. Isotope Effects Determined in 0.1 M $HClO_4$

Compound	Temperature	Number of Determinations	$(I.E.)_{obs}$	$(I.E.)_{corr}$
Benzene*	35	1	2.36	2.4 ± 0.3
Toluene	25	2	2.14	2.4 ± 0.3
	35	2	1.78	2.0 ± 0.1
p-Xylene	35	2	2.03	2.2 ± 0.1
Mesitylene	25	**	2.2	2.2 ± 0.2
Durene	35	2	2.33	2.7 ± 0.2
Pentamethylbenzene	35	2	2.51	2.9 ± 0.3

*(H^+) = 0.20 M

**From the appropriate intercepts in Figure 1 as discussed in the previous chapter

Reproduced with permission of the copyright owner. Further reproduction prohibited without permission.

earlier, Sullivan found that $(k_5)_h/(k_5)_d$ increased monotonically with $k_{-3}/(k_5)_h$ for phenoxide ion, p-nitrophenoxide ion, and 2,4-dinitrophenoxide ion at very high iodide concentration. If it is assumed momentarily that the C-H(D) bond in the sigma complex intermediate is the same in all three intermediates, then on the Bell-Evans-Polanyi (BEP) principle[65] one could explain the decrease in isotope effect on going from phenoxide to the dinitrophenoxide ion. This principle states that the activation free energy for the forward rate of an equilibrium process varies inversely with the overall enthalpy of that equilibrium process. The activation free energy for the formation of the quinoid intermediate of phenol should be smaller than for the analogous intermediate of 2,4-dinitrophenoxide ion due to the destabilization effect of the addition of nitro groups to the intermediate. It appears that k_{-3}/k_5 should then decrease from phenoxide to the dinitrophenoxide ion; this is what was observed. The reversibility ratios decrease from 1.4×10^6 to 4.2×10^3. On consideration of equation (8) and the fact that k_{-3}/k_5 are very large compared to unity, the variance in the observed isotope effect from 6.5 to 4.5 for these compounds must reside in the ratio $(k_5)_h/(k_5)_d$ and hence reflects only losses in vibrational energy in the C-H(D) bond in the transition state. It is also noted that the implied relative loss in vibrational energy in the transition state parallels the stabilities of the related sigma complexes.

When H_2OI^+ is the halogenating agent for 2,4-dinitrophenoxide ion, the observed isotope effect is 2.3, but this occurs only when the iodide ion concentration is very low. Sullivan showed that the reversibility ratio k_{-3}/k_5 was only 0.44. This is a case where the relative rates of

Reproduced with permission of the copyright owner. Further reproduction prohibited without permission.

the sigma complex reverting to H_2OI^+ and ArH, versus that of losing a proton are comparable. The isotope effect in the proton loss step must be the same regardless of the halogenating agent, I_2 or H_2OI^+, as they both give the same sigma complex. For H_2OI^+ k_{-3} refers to the reaction of the complex with water to give H_2OI^+ and ArH whereas when I^- is the nucleophile in the case of the I_2 mechanism the products are the reactants, I_2 and ArH. Water is only 2×10^{-6} as efficient as I^- in removing I^+ from the sigma complex and hence the isotope effect is controlled by the efficiency of a reagent to remove I^+ from the intermediate complex.

Since at low iodide concentration 2,4-dinitrophenoxide ion, and mesitylene are of comparable reactivity at 50°, 7.15×10^{-6} sec^{-1} and 3.8×10^{-7} sec^{-1}, respectively, and since the halogenating agent and observed isotope effects are the same, it is thought that the isotope effect for mesitylene is controlled by the same factor as for 2,4-dinitrophenoxide ion at low iodide, the near equality of activation energies of k_{-3} and k_5.

It is conceivable that $(k_5)_h/(k_5)_d$ for mesitylene, if measurable, could be as large as the value for the dinitrophenoxide ion, 4.5, based on the above discussion of the similarities and the fact that the observed isotope effects are the same.

From CNDO calculations, the proton complex of mesitylene, where $k_{-3} \approx k_5$ is less stable by 180 kcal than the quinoid intermediate of phenol where $k_{-3} >> k_5$, and hence from the BEP principle the free energy of activation for k_3 is expected to be much larger for mesitylene and the dinitrophenoxide ion than for phenoxide ion.

On comparing benzene and mesitylene, the apparently constant isotope

Reproduced with permission of the copyright owner. Further reproduction prohibited without permission.

effect of about 2.2 at 35° over a reactivity range varying by a factor of 10^6 suggests that the reversibility ratio k_{-3}/k_5 is approximately the same throughout the methylated series and hence a constant fraction of the sigma complex formed goes on to product.

The isotope effect for durene and pentamethylbenzene are 2.7 and 2.9, respectively, as compared to 2.2 for the other hydrocarbons studied. On bromination in acetic acid these two isotope effects are thought to differ from unity[18] due to steric crowding and the same cause is thought to be responsible for the above increase in the isotope effect in iodination. The bromination isotope effect values above differ from the "standard" value of unity by 10.0 and 20.0 percent, respectively, while for iodination the deviations from the "standard" value of 2.2 are 23 and 32 percent, respectively. Steric crowding in the transition state is thought to be the cause of the amplification of the apparent characteristic isotope effect of iodination by H_2OI^+. It is noted that due to the large size of the iodine atom the transition state for pentamethylbenzene might be very similar in structure to hexamethylbenzene which has S_6 symmetry,[66] not D_{6h}, due to crowding among the methyl groups. It would appear that this crowding would increase k_{-3}; that is, if the sigma complex is more difficult to form in the hindered case, then its reversion to H_2OI^+ and ArH should be facilitated. Perhaps k_5 might be the same for mesitylene and pentamethylbenzene and k_{-3}/k_5 would then be larger for pentamethyl benzene and the isotope effect would then be larger for the latter compound. The magnitude of k_{-3}/k_5 for durene is probably inter mediate between the two cases considered above.

Reproduced with permission of the copyright owner. Further reproduction prohibited without permission.

Product Isolation and Partial Rate Factors

At commonly employed ArH concentrations the relative rates of reaction of the hydrocarbons studied span a range of approximately 10^6, as indicated by the largest and smallest values for k*I observed. The accurate relative reactivities of specific reaction sites as well as the relative reactivities of each of the hydrocarbons is somewhat more complex, however, and required knowledge of the product distribution as well as accurate values of relative rate constants. Gnanapragasam isolated 2,4,6-trimethyliodobenzene as the only reaction product of mesitylene with iodine. In this study the reaction products were isolated from reactions of iodine with toluene and o-xylene in the presence of silver ion.

For toluene 1.20 g (0.013 m) was added to three liters of purified water in a black ground glass stoppered bottle. After three hours on a mechanical shaker the solution was made 24×10^{-6} M in Ag^+, and 0.1 M in $HClO_4$ by the addition of appropriate amounts of stock solutions of known concentration. After equilibrating in a constant temperature bath at 35° for three hours, 12.0 cc of 1.3×10^{-3} M (15.6×10^{-6} moles) of iodine solution was added. After shaking vigorously the flask was allowed to stand at 35° for 12 hours, then an aliquot was quenched with Na_2CO_3 and one gram of NaI was added. The optical density at 3530 Å showed no detectable I_2 remaining. The remaining portion was extracted three times with 300 ml of hexane with mechanical shaking. The extracts were combined, washed with aqueous NaOH, water, and dried over Dierite. The solution was then reduced to 10.5 ml on a spinning-band column.

Standard solutions of the three possible reaction products, ortho, meta, and para-iodotoluene showed on gas chromatographic analysis that the

Reproduced with permission of the copyright owner. Further reproduction prohibited without permission.

meta and para isomers as one peak, could be differentiated from the ortho isomer. The chromatographic analysis was carried out on an F & M gas chromatograph, model 810. The column used was prepared by Mosher[67] and was of DEGA/H_3PO_4 on silanized glass beads. The substrate was 0.15 percent DEGA and 0.06 percent H_3PO_4. The oven temperature was 90° and the flow rate of the carrier gas, N_2, was 22 cc/min. Using synthetic reaction products, it was determined that greater than 90 percent of the reacted iodine could be recovered as iodotoluenes.

The separation of the ortho isomer peak from the meta-para peak was completed by decomposing the chromatogram into two Gaussian components[68] via a least squares fit.[69] The Gaussian functions g(t) used were of the form

$$g(t) = \alpha \exp [- (\beta - t)^2/\gamma^2]$$

where α is the maximum amplitude, where $\beta = t$, β is the position of the maximum on the chromatograph time scale, t, and γ is the peak half-width at the height α/e where e is the base of the natural log. The values of the variables for the ortho isomer are 37.79, 2.529, and 0.673, respectively, while for the composite meta-para isomer peak they are 57.099, 3.600, and 0.674. The Gaussian components of the product mixture show an identical relative height ratio and relative area ratio, 0.66, and this value is considered an accurate representation of the ratio of the product distribution, (ortho)/(meta + para). Forty percent of the total product was the ortho isomer and 60 percent a mixture of meta and para isomers. For the moment it will be assumed that 60 percent of the total rate constant for toluene will give the rate constant for the para position,

Reproduced with permission of the copyright owner. Further reproduction prohibited without permission.

and 20 percent will give the rate constant for the ortho position. Since there are two equivalent ortho positions in toluene, this leads to a value of 3.0 for the ratio of rate constants for the para and ortho position. The ratio is similar to that determined for the iodination of toluene by I_2 in an acetic acid - peracetic acid[14] medium, 2.7.

In the case of o-xylene, the above reaction conditions were employed, except that 0.4575 g (4.32×10^{-3} moles) of the hydrocarbon was added. The product was isolated and the hexane extract reduced to 10 ml and analyzed as above. The pure components did not give symmetric peaks, but they were of the same shape and the apparent product ratio of 2,3-dimethyliodobenzene to 3,4-dimethyliodobenzene was much less than unity. The chromatogram was then resolved visually and showed nine percent of 2,3-dimethyliodobenzene and 91 percent of the 3,4-dimethyliodobenzene. Due to the method for resolution of the peak, the error may be as large as 50.0 percent for the lesser component.

The question of relative reactivity of methyl substituted benzene substrate as a function of the reactivity of the parent molecule depends upon a reliable value of the rate constant for benzene. In Table 7 it is seen that the benzene rate constant at 35° is dependent upon (H^+), and that the variations are assumed to be dependent upon the amount of HIO_3 formed, which is smaller at higher (H^+). At 35° the observed rate constant for toluene is 2.14×10^{-12} sec^{-1} and when divided by the rate constant for one position in benzene, it becomes 797. When the rate constant for a position is divided by the rate constant for a single position in benzene, the ratio is then known as a partial rate factor, P_u, where u denotes the position, ortho, meta, or para relative to the methyl group.

Reproduced with permission of the copyright owner. Further reproduction prohibited without permission.

We have seen that the ratio of partial rate factors P_p/P_o is 3.0 if it is assumed that P_m is negligible in comparison to either P_p or P_o. The value for P_o is just 0.20 times 797; thus P_o = 160 and P_p is 0.60(797) or 479. Now P_m can be evaluated on comparing P_o and the rate constant for p-xylene divided by that of one position in benzene (26.6) to give

$$26.6 = \frac{4P_o P_m}{P_o} = 4P_m$$

or P_m = 6.67. Now the initial value of P_p determined from the product ratio is in error to the extent that the para product peak contains the meta product also; thus a more accurate value of the para partial rate factor is 479 - 2(6.67) = 466. This new value will be assigned to P_p for all further discussion for iodination in water.

According to the "additivity principle," the reactivity of a position in a poly-methyl substituted hydrocarbon relative to a position in benzene can be described as the product of each of the appropriate toluene partial rate factors relative to the reaction center appropriate for the position of methyl substitution. The total reactivity of the molecule will in turn be the sum of the reactivity of each individual position. For example, the relative rate constant for m-xylene which has two positions with one ortho and one para activating methyl group, one with two meta activating methyl groups, and one with two ortho methyl groups is

$$k_{rel} = 2P_o P_p + P_m^2 + P_o^2$$

To assume that the meta product isomer in toluene is negligible compared to the para product seems to be quite valid on consideration of

Reproduced with permission of the copyright owner. Further reproduction prohibited without permission.

the values of P_p and P_m, 465 and 6.67, respectively. In m-xylene the question is raised as to what is the accurate partial rate factor for the 2,4-dimethyl activated position. The data in Table 16 suggest that only 14.5 percent of the total product for m-xylene should be the 2,6-dimethyl isomer and 85.5 percent the 2,4-dimethyl isomer. It will be assumed for comparative purposes that the entire product is 2,4-dimethyl iodobenzene. Since rate constants are generally compared on a log scale, the above assumption leads to an approximate error of only 0.07 log units, which is negligible compared to the log of the total relative rate constant, 4.6. It is thus suggested that, if there is crowding in the transition state at the 2,6 position, the effect of it on the rate of m-xylene would be difficult to detect on a comparative basis. Mesitylene also has such a position, that is, one flanked on either side by methyl groups, but also has a methyl group in the 4-position. The deviation of the calculated mesitylene rate constant from the experimental one is a factor of 3.0. This suggests that, for mesitylene, the experimental rate might be represented as $3(P_o')^2P_p$ where P_o' is peculiar to the environment of mesitylene. The new value P_o' is 92.0. Thus the steric effect of two ortho methyl groups is to reduce that contribution by $(P_o')^2/(P_o)^2$ or 0.33.

The use of the alternate value P_o' gives 3.17×10^5 for the calculated rate for prehnitene, compared to 2.87×10^5 determined experimentally. This is very good agreement. To a first approximation it appears that 2,3,4,5-tetramethyl substitution has a bulking effect of the same magnitude as two ortho methyl groups. The ortho steric effect of two adjacent methyl groups might be estimated by comparing the product analysis of o-xylene and the relative rates predicted from partial rate factors.

Reproduced with permission of the copyright owner. Further reproduction prohibited without permission.

Reproduced with permission of the copyright owner. Further reproduction prohibited without permission.

Table 16. Observed and Calculated Rate Constants Relative to Benzene

Hydrocarbons	Legend	$(k*I)_{obs} \times 10^{14}$	Observed Relative Rate	Calculated Partial Rate Factor Contributions**	Calculated Total Relative Rate**
Benzene	(1)	1.61	1	6(1)	1
Toluene	(2)	2.14×10^{2}*	1.33×10^{2}*		1.33×10^{2}
2-Di-Me				2(159.5)	
3-Di-Me				3(6.7)	
4-Di-Me				465.4	
p-Xylene	(3)	1.14×10^{3}	7.08×10^{2}	4(1070)	7.08×10^{2}
o-Xylene	(4)	1.33×10^{3}*	4.97×10^{3}*		1.38×10^{3}
2,3-Di-Me		1.20×10^{2}	4.47×10	2(1070)	
3,4-Di-Me		1.21×10^{3}	4.52×10^{3}	2(3110)	
Durene	(5)	4.72×10^{4}	2.93×10^{4}	$2(1068)^{2}$	3.77×10^{5}
m-Xylene	(6)	6.58×10^{4}	4.08×10^{4}		2.88×10^{4}
2,4-Di-Me				$2(7.4 \times 10^{4})$	
2,6-Di-Me				2.50×10^{4}	
3,5-Di-Me				8.90×10	
Prehnitene	(7)	4.60×10^{5}	2.87×10^{5}	$2(2.75 \times 10^{5})$	5.50×10^{5}
Pentamethylbenzene	(8)	1.68×10^{6}	1.04×10^{6}	8.78×10^{7}	8.78×10^{7}
Mesitylene	(9)	3.16×10^{6}	1.97×10^{6}	$3(1.97 \times 10^{6})$	5.91×10^{6}

*Total rate for compound

**Based on toluene and p-xylene

The observed 2,3-dimethyl product was 9.1 ± 5.0 percent while the predicted value is 25.0 percent. Since the observed and calculated total rates agree so well, 1.33×10^3 versus 1.38×10^3, respectively, and since the error in the 2,3-dimethyl substituted product may be even larger than estimated, the steric effect of adjacent methyl groups may not be significant.

On comparison of durene with o-xylene, however, one has a situation similar to that of one ortho methyl versus two, except that in durene one is comparing one "ortho-dimethyl" versus two "ortho-dimethyl" groups. Such a steric effect appears to be to reduce the rate for durene by a factor of 12.9. If P_o' is used in the calculation for the rate of durene, the rate constant is 1.26×10^5 versus 2.93×10^4 determined experimentally; the steric factor is only reduced from 12.9 to 4.3. It appears then that 2,3,5,6-tetramethyl substitution in the transition state gives rise to steric problems other than those found for mesitylene as based on the comparison of P_o with P_o'.

The use of P_o' for pentamethylbenzene reduces the apparent steric factor from 84.2 only to 28.1, the rate constant being 2.92×10^7. The unaccounted-for steric factor is increased significantly on going from four non-adjacent methyl groups to five methyl groups. It is quite possible that the remaining factor is due to the out of plane deformations of methyl groups in the transition states. This would raise the activation energy.

Figure 6 shows a plot of the observed relative rates and the relative rates calculated using the toluene partial rate factors. A slope of unity is arbitrarily drawn. No correlation coefficient has been considered.

Reproduced with permission of the copyright owner. Further reproduction prohibited without permission.

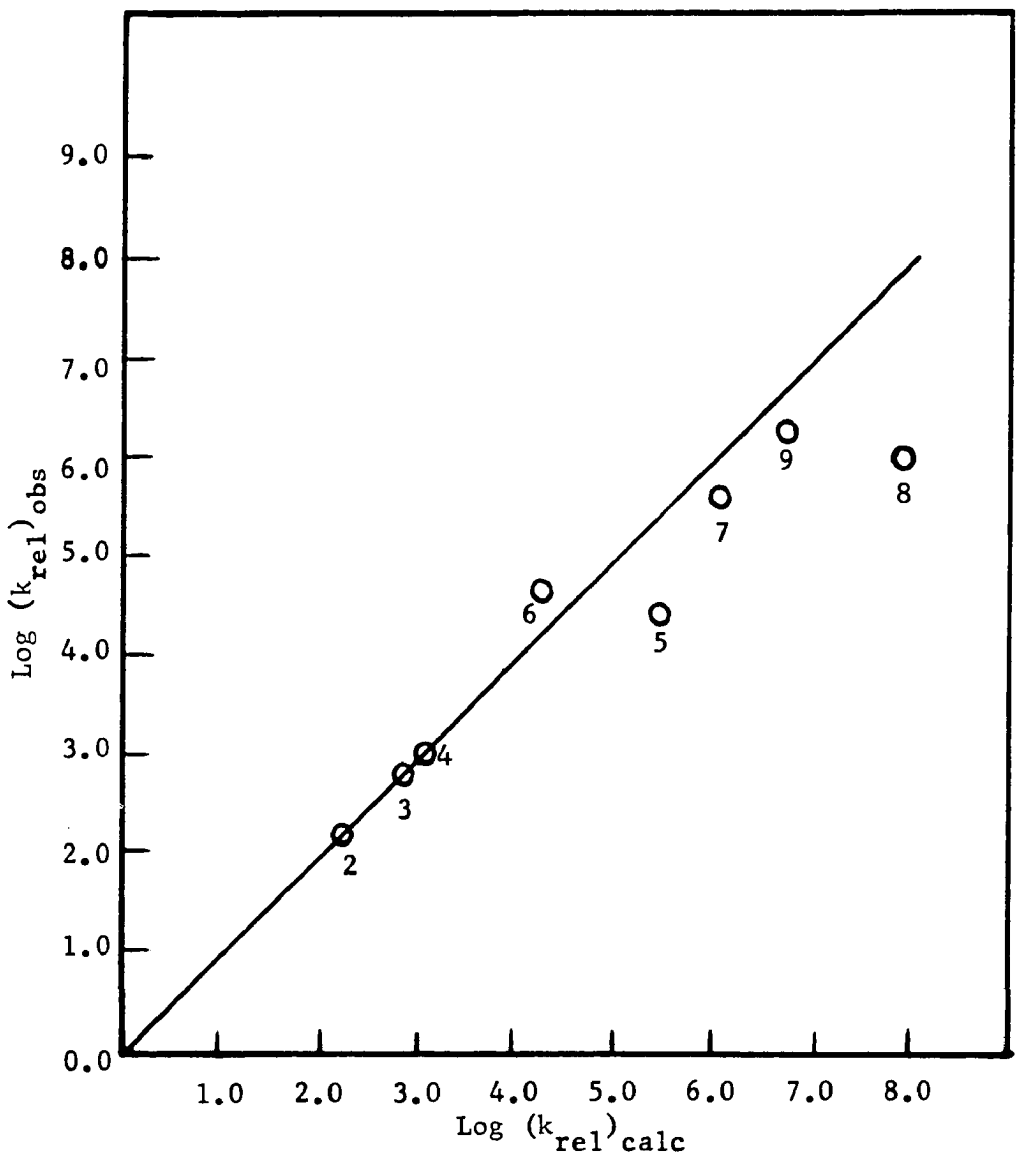

Figure 6. Plot of Observed Relative Rates for Iodination in H_2O Versus Those Calculated from Partial Rate Factors. (See Table 16 for legend.)

Reproduced with permission of the copyright owner. Further reproduction prohibited without permission.

Figure 7 and Table 17 show the results of Ogata and Aoki, for iodination of some of the same hydrocarbons in acetic acid in the presence of peracetic acid. The partial rate factors here are 55, 2.5, and 150 for P_o, P_m, and P_p, respectively. These authors state that the rate of iodination was almost independent of hydrocarbon concentration; thus the relative rates were determined by competitive methods. The explanation of the relative rates being zero order in (ArH) is very similar to the effect already discussed for the drop in rate constants for mesitylene, the relatively slow rate of formation of halogenating agent. For aromatics more reactive than benzene the rate of reaction becomes that of the slower rate of formation of halogenating agent, CH_3CO_2I. The rate of formation of the intermediate sigma complex is not significant in the rate determining process for kinetics involving this halogenating agent. It would appear then that the relative rates of formation of H_2OI^+ versus CH_3CO_2I is 10^5 to 10^6 since for both reagents the relative rate constant of mesitylene to that of benzene is near 10^6. From the linearity of the comparison of iodination in the two media, it appears that the major difference is the relative reactivity of the halogenating agents. It appears that CH_3CO_2I is more reactive and less selective than H_2OI^+.

Hammett Correlations

For comparative purposes the $\log_{10}$ of a partial rate factor is assumed on some theoretical bases to be proportional to the sum of the contributions to the rate of reaction of substituents at various positions relative to the reaction center. Where strong resonance interaction in the transition state electronic charge is thought to be donated to the aromatic π system by a substituent at position u, the Hammett equation

Reproduced with permission of the copyright owner. Further reproduction prohibited without permission.

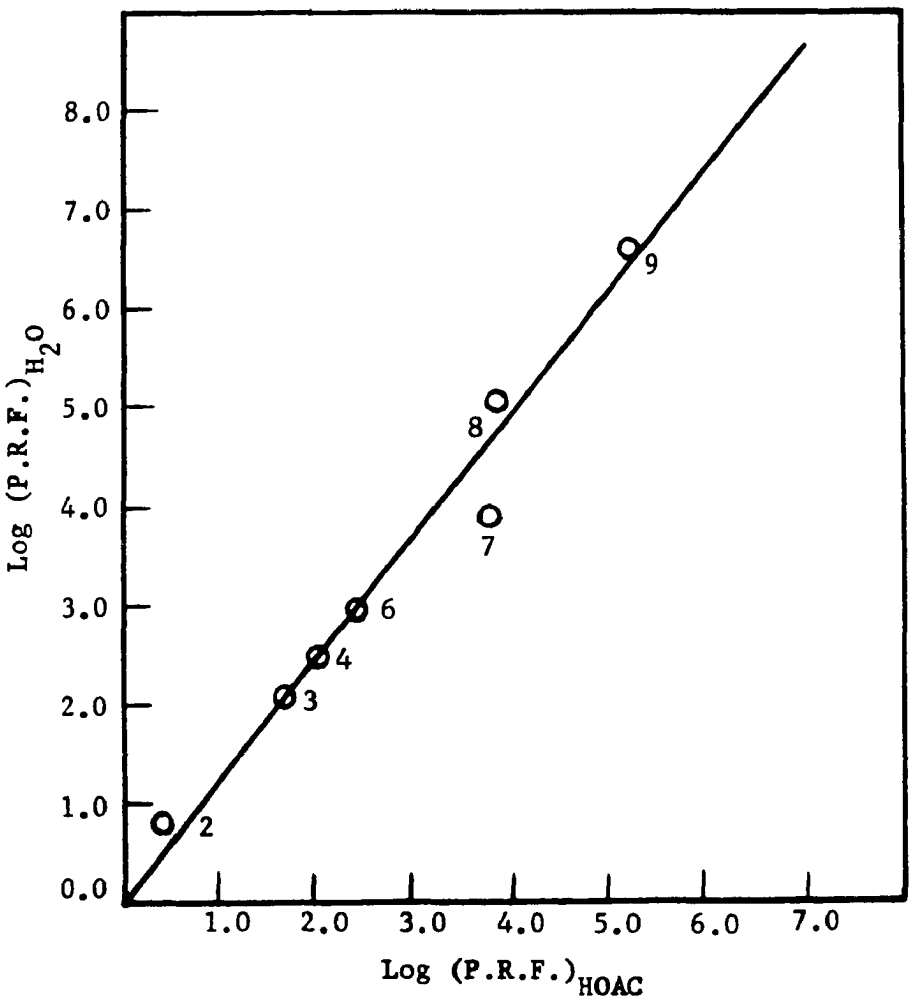

Figure 7. Comparison of Partial Rate Factors Determined in H_2O and HOAC-HO_2AH. (See Table 18 for legend.)

Reproduced with permission of the copyright owner. Further reproduction prohibited without permission.

Table 17. Comparison of Observed and Calculated Rate Constants at 60° Calculated from Partial Rate Factors of Ogata and Aoki, $P_o = 55$, $P_m = 2.5$, and $P_p = 150$

Hydrocarbon	Legend	Total Relative Rate (Observed)*	Total Relative Rate (Calculated)*	Partial Rate Factors
Benzene	1	1*	1*	1
Toluene	2	43.3	43.3	**
p-Xylene	3	90.5	90.5	136
o-Xylene	4	106	84.3	319†
m-Xylene	5	2.08×10^3	4.72×10^3	6.25×10^3††
Durene	6	2.45×10^3	6.08×10^3	7.35×10^3
Mesitylene	7	8.15×10^4	2.27×10^5	1.63×10^5

*Relative to benzene

**See Table Title

†Product assumed to be 3,4-dimethyliodobenzene

††Product assumed to be 2,4-dimethyliodobenzene

Reproduced with permission of the copyright owner. Further reproduction prohibited without permission.

may be written

$$\log \text{(Partial Rate Factor)} = \rho \sum_{u} \sigma_{u}^{+}$$

where ρ is the constant of proportionality and of which the magnitude gives some indication of the sensitivity of the speed of the reaction to the substituents, to the nature of the solvent. If ρ is negative and since all σ^{+} being used here[71] are negative, then the reaction rate will be enhanced by increased substitution in the reactant. The correlation of the rate constants for specific positions for iodination and bromination with Hammett σ^{+} values appears in Figure 8 and Table 18. The σ^{+} values used are -0.276, -0.067, and -0.297 for ortho, meta, and para positions, respectively. The correlation for the six rate constants for iodination noted in Table 18 are characterized by having no steric difficulties near the reaction center under consideration and have a least squares slope of -8.55 (r=0.996) while the slope, determined from all the data is -6.95 (r=0.98). From the aqueous bromination data for all compounds but pentamethyl benzene, the value of ρ is -11.5 (r=0.992) while for the entire series it is -10.7 (r≠0.998).

Figure 8 suggests that bromination in water has a detectible steric effect only for pentamethylbenzene while for iodination the ortho-meta activated position of o-xylene, durene, mesitylene, and pentamethylbenzene have significant steric effects. It must be remembered that errors in σ_{o}^{+}, since it is the least well known of the three σ^{+} values, may contribute to the apparent steric effect. Figure 9 correlates directly the bromination and iodination data and for prehnitine, mesitylene, and pentamethylbenzene. There appears to be more steric hinderance for iodination

Reproduced with permission of the copyright owner. Further reproduction prohibited without permission.

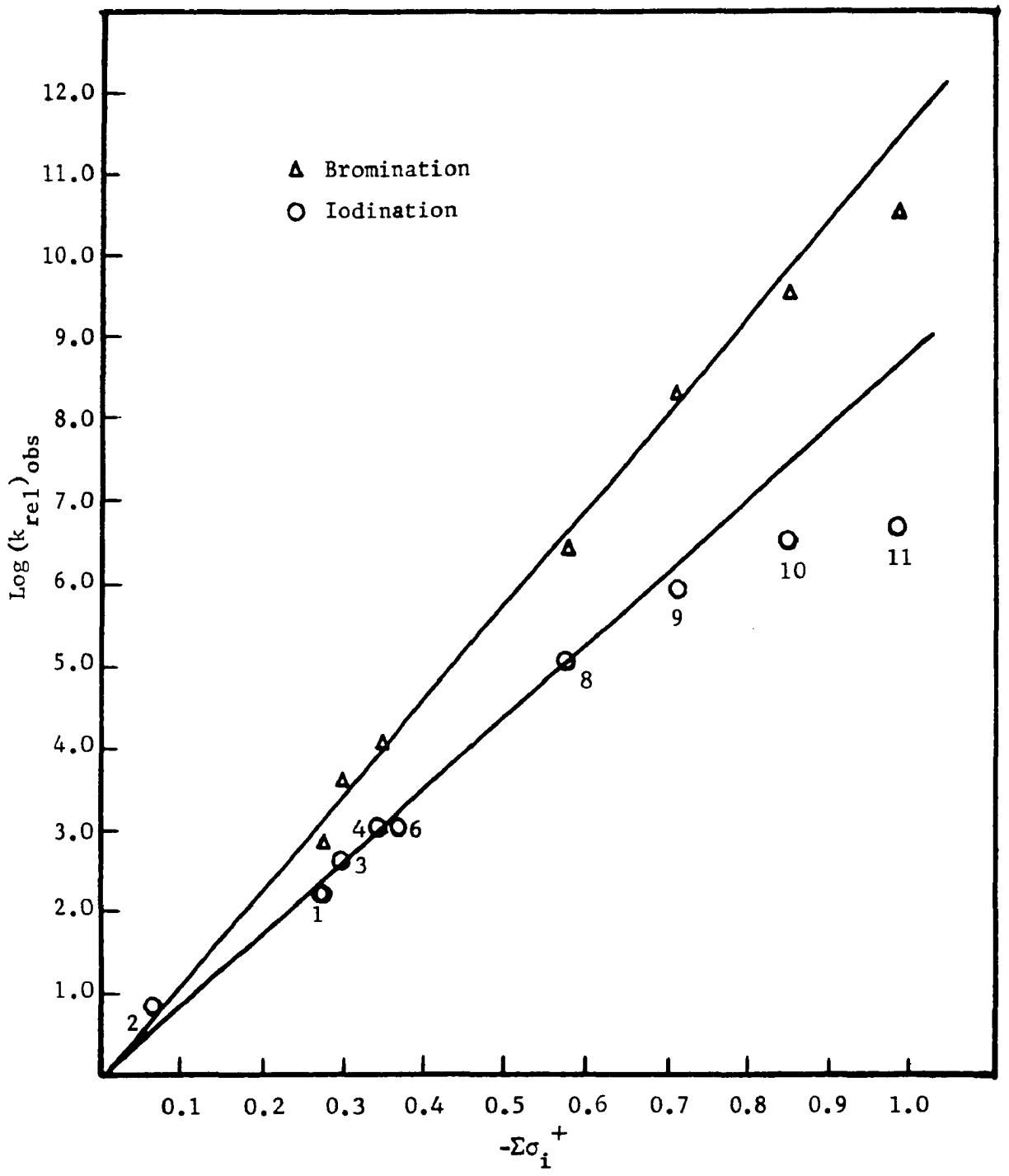

Figure 8. Hammett Plots for Iodination and Bromination in H_2O. (See Table 18 for legend.)

Reproduced with permission of the copyright owner. Further reproduction prohibited without permission.

Table 18. Hammett Data for Iodination and Bromination in H_2O

Hydrocarbon Isomer	Legend	log (Partial Rate Factor) I_2	log (Partial Rate Factor) Br_2	$\Sigma\sigma_i^+$
Benzene		0	0	0
Toluene 2-Me	1	2.20*	2.84	-0.276
3-Me	2	0.82*	--	-0.067
4-Me	3	2.68*	3.63	-0.297
p-Xylene	4	3.03*	4.10	-0.343
o-Xylene 2,3-Di-Me	5	2.06	--	-0.343
3,4-Di-Me	6	3.06*	--	-0.364
Durene	7	3.94	--	-0.686
m-Xylene**	8	5.09*	6.48	-0.573
Prehnitene	9	5.93	8.24	-0.707
Mesitylene	10	6.59	9.52	-0.849
Pentamethylbenzene	11	6.79	10.52	-0.983

*ρ for these values is -8.55 ($r = 0.996$)

**2,4-Di-Me isomer only

Reproduced with permission of the copyright owner. Further reproduction prohibited without permission.

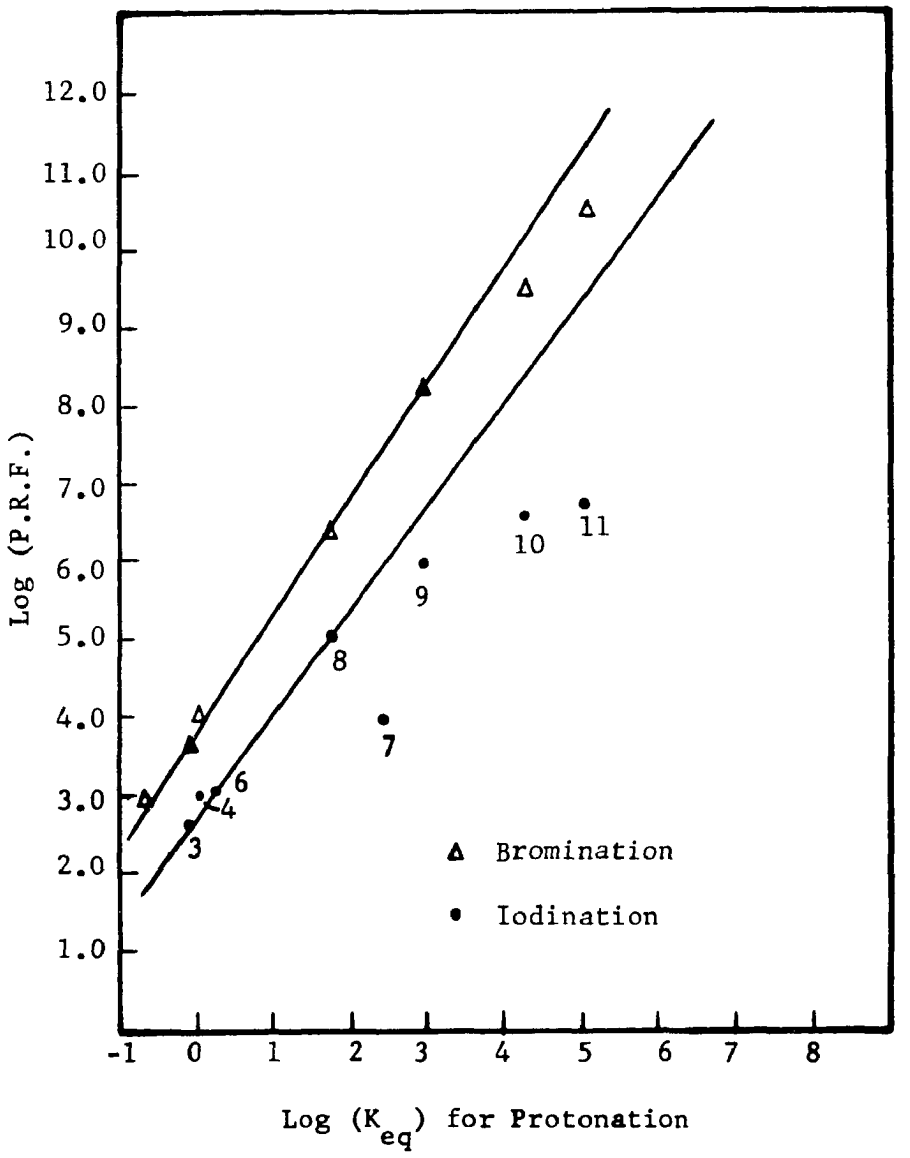

Figure 9. Comparison of Partial Rate Factors for Iodination and Bromination with Equilibrium Constants for Proton Complex Formation. (See Table 18 for legend.)

Reproduced with permission of the copyright owner. Further reproduction prohibited without permission.

than bromination. In terms of relative rates, iodination for these latter compounds is slower by factors of 3.5, 10, and 55, respectively, than predicted from toluene partial rate factors.

To get an absolute magnitude of the relative steric problem for iodination and bromination, perhaps the best correlation is that of these rates with the equilibrium constant[17] for proton complex formation with the aromatic hydrocarbon, since the proton is much smaller than either Br or I. Figure 9 shows these comparisons. It is immediately seen that, for the most unfavorable case, pentamethylbenzene, there appears to be a "steric inhibition of rate" by a factor of 500 for iodination, but only by a factor of 5.0 for bromination. All the previous arguments concerning steric crowding in the transition state are accounted for here. Bromination appears to be nearly free of crowding while iodination shows significant crowding as indicated by the large decrease in rate compared to that predicted from less reactive compounds.

Thermodynamic Parameters

The interpretation of the thermodynamic data of Table 14 may now have some microscopic meaning. Except for pentamethylbenzene the order of reactivity for iodination in water at 25° is the same as for chlorination, bromination, and deuteration. In these latter reactions there is approximately an order of magnitude difference in the rate of reaction of durene over m-xylene and pentamethylbenzene over mesitylene. In this study, however, these pairs of compounds differ by a factor of 2.0, at most, at both 25° and 35°. Further, durene is slightly less reactive than m-xylene at 35°, and mesitylene is slightly more reactive than pentamethylbenzene at both 25° and 35°. The overall observed relative order

Reproduced with permission of the copyright owner. Further reproduction prohibited without permission.

of reactivity for iodination is similar to that of mercuration.[72] In particular, m-xylene and durene are very similar in observed reactivity as well as the pair mesitylene and pentamethylbenzene. For benzoylation[73] the latter pair immediately above are of similar reactivity whereas in the former pair durene is the more reactive by an order of magnitude. Except for the study of mercuration, the observed relative rate constant for pentamethylbenzene deviates in a negative direction from that calculated from toluene partial rate factors.

The activation parameters, $\Delta S^{\ddagger}$, are negative except for m-xylene. In terms of partial rate factors for toluene it is hard to understand why the rate constant for m-xylene increases some sixfold for a change of 10° in temperature. No experimental explanation for this behavior has been uncovered so far. The 25° value was determined as an average of eight points while the 35° value was determined from only two, and is thus suspect. The value of $\Delta G^{\ddagger}$ does not vary as rapidly with changes in k*I as does $\Delta H^{\ddagger}$ and, if k*I for m-xylene changes by a factor of 5 for a 10° change in temperature, then $\Delta S^{\ddagger} \approx 0$. For smaller changes in k*I, $\Delta S^{\ddagger}$ is negative. It is estimated that $\Delta H^{\ddagger}$ should be between 26.4 and 29.8 kcal/mole, the values for prehnitene and o-xylene, respectively. A range of 2.5 kcal for $\Delta H^{\ddagger}$ would give an uncertainty in $\Delta S^{\ddagger}$ near 8.3 cal/deg.

For the remaining compounds the value of $\Delta H^{\ddagger}$ decreases from near 35 kcal/mole for toluene to near 25 to 26 kcal/mole for compounds having a reactivity greater than o-xylene. The apparent leveling off effect in $\Delta H^{\ddagger}$ is of interest. Increasing the number of methyl groups from two to five brought about a change in rate of 10^3 but $\Delta H^{\ddagger}$ changes only ca. 3.0 kcal. In all these cases the entropy of activation is unfavorable except

Reproduced with permission of the copyright owner. Further reproduction prohibited without permission.

for m-xylene.

Since the methyl groups of o-xylene are probably in the plane of the aromatic ring, then durene is probably planar also. Pentamethylbenzene, however, may not be planar and may have the methyl groups alternately above and below the ring plane. On going around the ring the first and last groups would be on the same side of the ring plane. The interpretation of the entropies of activation of these five hydrocarbons is enlightening. The planarity of durene allows the attack of H_2OI^+ to occur from either side of the aromatic ring. On pentamethylbenzene the attack by H_2OI^+ is more favored from the side of the ring opposite the numbers 2 and 6 methyl groups. The resulting geometry of the transition state could then be similar to that of hexamethylbenzene. If the adjacent methyl groups of pentamethylbenzene are already deformed from the ring plane in the reactant, then there may be more room for attack by H_2OI^+. Compared to the planar reactant, durene, however, the transition state may be puckered like pentamethylbenzene and the transition state may be less favored from an entropy argument. These arguments are offered as a rationalization of the values of $\Delta S^{\ddagger}$, -12.7 and -19.8 for pentamethylbenzene and durene, respectively. Since there is postulated a preferred side of attack for pentamethylbenzene, there will be an effect on the entropy of $R \ln(1/2) = -1.4$ cal/deg, and the entropy for attack on the preferred side may be somewhat the smaller, perhaps near -14.1 cal/deg. Prehnitene may also be considered using similar entropy arguments as the four adjacent methyl groups can also be puckered. The entropy value of -12.4 is very similar to that of the observed value for the penta substituted hydrocarbon previously discussed. The magnitude of the entropy

Reproduced with permission of the copyright owner. Further reproduction prohibited without permission.

for mesitylene is interesting in comparison to the first two cases discussed for the values of $\Delta S^{\ddagger}$ lie between the associated values of those two cases. The reaction site is bordered on either side by single methyl groups. The reactivity is very similar to that of pentamethyl benzene and more reactive than durene. It is suggested then that the single bordering methyl groups in mesitylene do not interfere greatly in the course of the reaction; the relative rate constant calculated from the toluene partial rate factor differs from the experimental value only by a factor of 3.0. Pentamethylbenzene differs by a factor of 84, durene by 12.7, and prehnitene by 1.9.

The entropy of activation of o-xylene is smaller than that for pentamethylbenzene. It is noted that the product isolation showed 10 to 15 percent of the 2,3-dimethyl product and 85 to 90 percent of the 3,4-dimethyl product. The toluene partial rate factors predict 25.9 percent of the 2,3-dimethyl product. If the difference in the observed and calculated product is in fact real, then perhaps the value for the total entropy change for o-xylene may also be rationalized in terms of a crowded transition state.

The specific contributions to $\Delta G^{\ddagger}$ are difficult to assess theoretically because of the complexity of the transition state and reactant molecules. However, a means of correlating $\Delta S^{\ddagger}$ in an elementary fashion has been proposed. When the reaction under consideration occurs between polar molecules to give a polar transition state, then $\Delta S^{\ddagger}$ may be associated with the polar properties of the reactants (r) and transition state from the relation[74]

Reproduced with permission of the copyright owner. Further reproduction prohibited without permission.

$$(\Delta S)_{el} = -\left[\sum_r \frac{\mu_r^2}{(R_r)^3} - \frac{(\mu^{\ddagger})^2}{(R^{\ddagger})^3}\right] \frac{3D}{(2D+1)^2} \left(\frac{\partial \ell n\ D}{\partial T}\right)$$

where $(\Delta S)_{el}$ is the entropy change on transferring the reactants and transition state dipole, μ, from a vacuum to a medium of constant dielectric D. The dipole moments and radii of the reactants are noted by the subscript r.

In the case of concern the halogenating agent, H_2OI^+, makes the same contribution to $(\Delta S^{\ddagger})$ for all molecules and hence is ignored. Further, the dipole moment of all the hydrocarbons is less than 0.5 Debeye, and these contributions will be ignored. From Table 19, however, it is seen that the proton model for the transition states shows much larger dipole moments. Since Figure 11 shows a good correlation between calculated and observed relative rates, perhaps the calculated dipole moments of the proton complex can be used in the above correlation. Now the cube of the radius of the transition states are not known but are estimated in terms of the molar volume of the parent hydrocarbon. These approximations result in Figure 10 which shows a correlation (r=0.86) of $(\Delta S^{\ddagger})$ versus $\left(\frac{\mu^2}{V}\right)_{calc}$. The proton complex μ and the molar volume V, as determined from the hydrocarbon densities are given in Table 20. It is difficult to say what can be deduced from Figure 10 but perhaps it says that nothing unusual appears to occur when a nonpolar hydrocarbon reacts with a polar halogenating agent to give a very polar transition state in water. The slope of the plot is of the sign predicted by theory as $\partial\ \ell n(D)/\partial T$ for water is negative. The values of $\Delta S^{\ddagger}$ for iodination of meta-xylene, toluene, mesitylene, and para-xylene parallel the experimental values[15]

Reproduced with permission of the copyright owner. Further reproduction prohibited without permission.

Table 19. Correlation of $(\Delta S^{\ddagger})_{obs}$ with a Dipole Model

Hydrocarbon	Legend	Dipole Moment (Debeyes)	Molar Volume cc/m*	$\left(\frac{\mu^2}{V}\right)$	$(\Delta S^{\ddagger})_{obs}$
m-Xylene	1	15.8	124	2.0	+ 4.5 ± 4.5
Toluene	2	15.0	106	2.12	- 0.84 ± 2.7
Mesitylene	3	16.4	139	1.95	-14.6 ± 3.0
p-Xylene	4	12.1	123	1.2	-13.1 ± 2.6
Prehnitene	5	12.7	150	1.1	-12.4 ± 3.4
Pentamethylbenzene	6	13.3	161**	1.1	-12.7 ± 1.9
o-Xylene	7	6.7	121	0.37	-16.3 ± 2.9
Durene	8	8.5	144***	0.50	-19.8 ± 1.9

*Determined from hydrocarbon densities.[75]

**Determined by the density given for hydrocarbon in the solid state.

***Determined by taking 0.90 times the value (160) determined at 81°.

Reproduced with permission of the copyright owner. Further reproduction prohibited without permission.

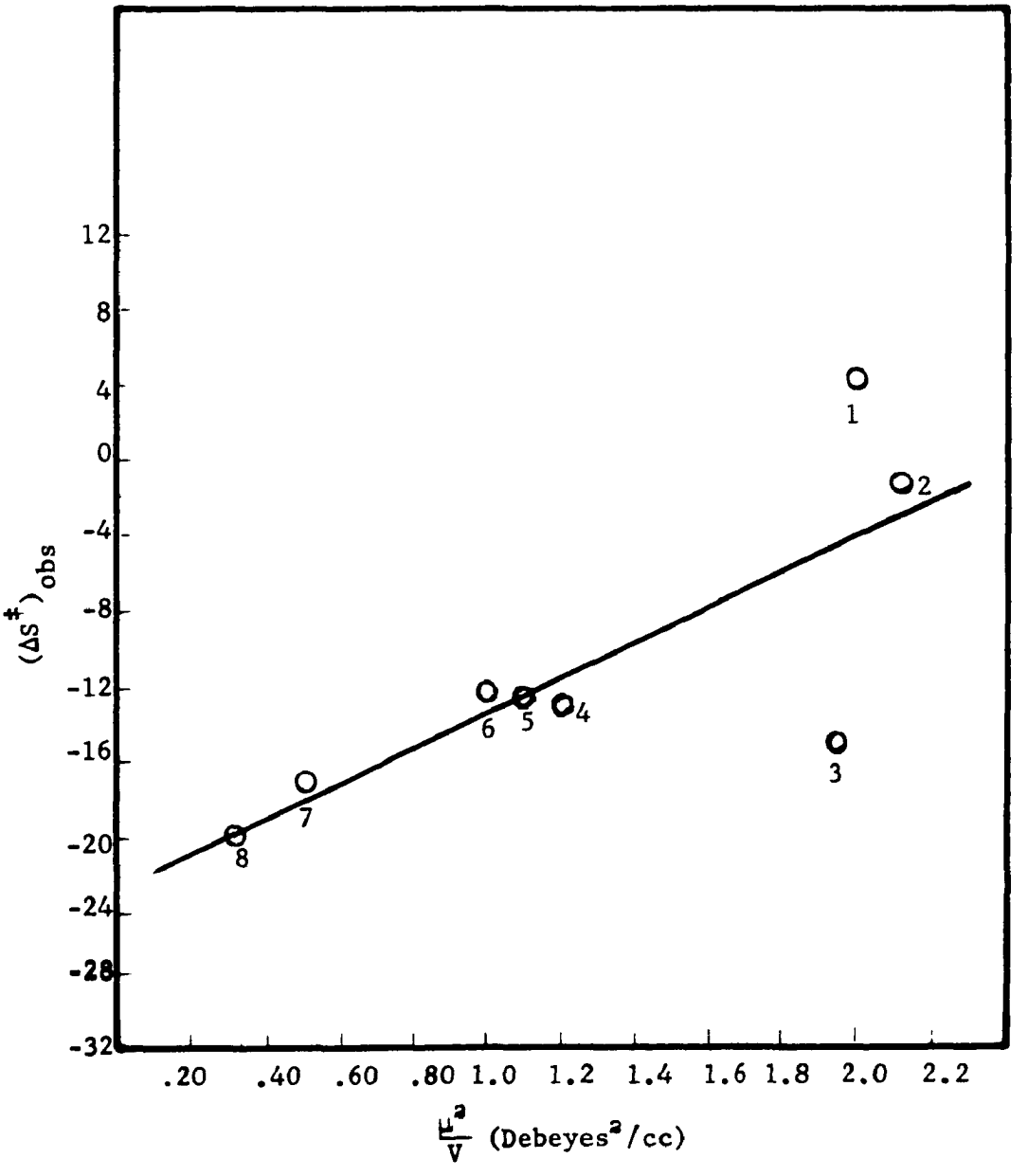

Figure 10. Correlation of $(\Delta S^{\ddagger})_{obs}$ with Dipole Model. (See Table 19 for legend.)

Reproduced with permission of the copyright owner. Further reproduction prohibited without permission.

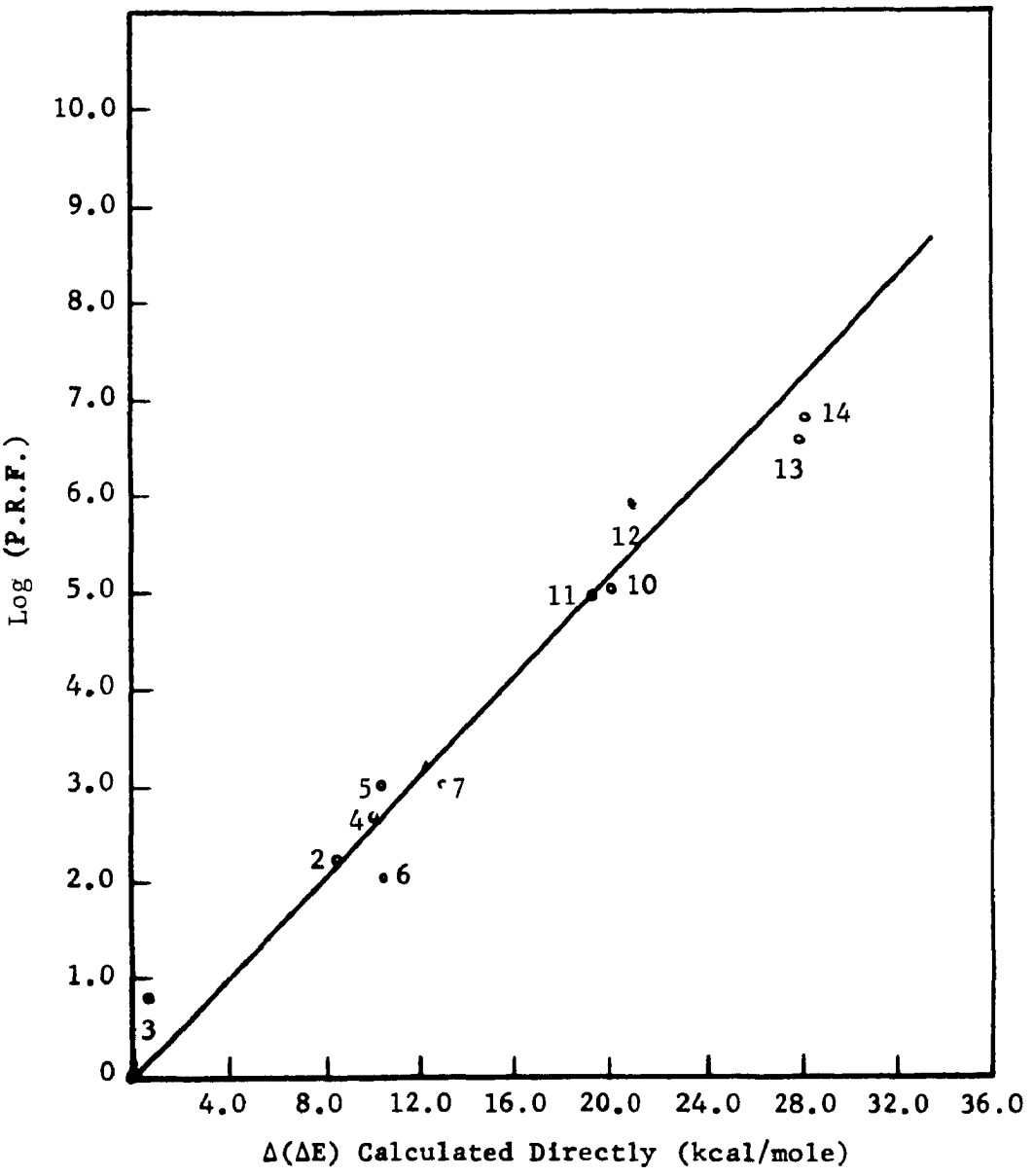

Figure 11. Plot of Log (Partial Rate Factors) for Iodination in H_2O Versus Calculated Proton Affinities. (See Table 20 for legend.)

Reproduced with permission of the copyright owner. Further reproduction prohibited without permission.

Reproduced with permission of the copyright owner. Further reproduction prohibited without permission.

Table 20. Relative Proton Affinities and Relative Rates of Iodination in H_2O

	Proton Complex Methyl Position(s)	Legend	$\Delta(\Delta E)$ kcal/mole	log(Partial Rate Factors)*	$\Delta(\Delta E)$ Calculated from Toluene kcal/mole
Benzene		1**	0	0	0
Toluene	2	2	- 8.51	2.20	- 8.51
	3	3	- 0.69	0.82	- 0.69
	4	4	-10.16	2.68	-10.16
p-Xylene	2	5	-10.44	3.00	- 9.20
o-Xylene	2,3	6	-10.52	2.06	- 9.20
	3,4	7	-13.08	3.06	-10.85
m-Xylene	2,6	8	-17.23	--	-17.0
	3,5	9	- 3.94	--	- 1.40
	2,4	10	-20.45	5.09	-18.67
Durene	2,3,5,6	11	-19.35	4.94	-18.4
Prehnitene	3,4,5,6	12	-21.13	5.94	-20.1
Mesitylene	2,4,6	13	-27.85	6.60	-27.28
Pentamethylbenzene	2,3,4,5,6	14	-28.0	6.79	-28.68

*Statistically corrected

**Legend for Figure 10 and Figure 11

of ΔS° for proton complex formation of these same compounds, -15.6, -16.7, -20.2, and -20.8 cal/deg, respectively.

Insofar that $\Delta S^{\ddagger}$ is the derivative of $\Delta G^{\ddagger}$ with respect to temperature, and since Figure 8 is approximately linear, then it is suggested that $\Delta H^{\ddagger}$ be proportional to $\Delta S^{\ddagger}$. A plot of $\Delta H^{\ddagger}$ versus $\Delta S^{\ddagger}$ gives a slope of 370°K (r=0.80). Since the correlation coefficient is so low, the correlation may not be considered significant[78] and the plot is not given.

Molecular Orbital Calculations

Since the purpose of this study is primarily the study of the influence of methyl substituents on the reactivity of benzene, perhaps the most meaningful correlation using molecular orbital calculations will be one that refers specifically to the effects of methyl substituents; therefore, the correlation given in Table 19 and Figure 11 is

$$\Delta(\Delta E) \equiv \Delta E\,[C_6H_{6-n}\,(CH_3)_n] - \Delta E(\text{benzene})$$

versus

$$\log (\text{Partial Rate Factor})$$

where ΔE is the change in energy calculated for the reaction

$$ArH + H^{+} \rightleftarrows ArH_2^{+}$$

The CNDO calculations were carried out using the CNINDO program[76] of Pople and Dobosh. This program is also capable of performing INDO (Intermediate Neglect on Differential Overlap) calculations. The Cartesian coordinates of the atoms were calculated from the input values of the molecular geometry in terms of the molecular bond distances and angles using the program COORD.[77] These two programs were combined such that input

Reproduced with permission of the copyright owner. Further reproduction prohibited without permission.

coordinates could be either in terms of (x,y,z) or (r,θ,∅). If the latter parameters were used, the former could then be punched out by the computer if desired.

The model for the ground state is basically the structure of benzene with methyl groups attached in appropriate positions. The aromatic ring in both the ground state and the transition state[25] models is assumed to be a regular hexagon with C-C bond distances of 1.395 Å. The $C\text{-}CH_3$ bond distance is 1.52 Å, and the $C\text{-}C\text{-}CH_3$ bond angle is 120°. The C-H bond distance for the sp^3 methyl group is 1.093 Å, and for the ring protons is 1.083 Å. The geometry at the reaction center in the transition state model has been given a C-H bond distance of 1.10 Å and an HCH bond angle of 110°. The effect of the relative configuration of the methyl group protons with respect to the ring plane and other methyl groups has not been found to be important so long as the same relative methyl group geometries are the same in both models and if the reaction center is symmetrically substituted. On considering three configurations of the methyl groups of o-xylene

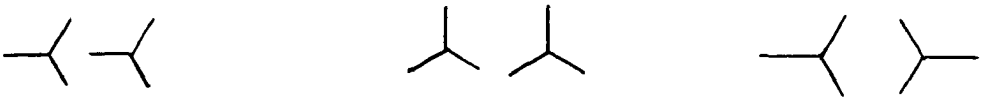

(1) (2) (3)

where (1), (2), and (3) represent the proton positions relative to the horizontal ring plane the largest deviation in ΔE, for the 3,4-dimethyl proton complex isomer is 0.1 percent, or 250 calories, and the average deviation is 0.05 percent. The configurations used for all the calculations

Reproduced with permission of the copyright owner. Further reproduction prohibited without permission.

are given in Appendix D. The use of a proton as a model atom for I^+ is predicated by the above requirements and substantiated by the successful correlation of proton-type reactions with other substitution reactions such as chlorination, bromination, and deuterium exchange mentioned earlier.

The energies listed, $\Delta(\Delta E)$, or relative proton affinity, are the differences between the energy difference on protonation of various positions of the substrates studied and the energy difference on protonation of benzene. These differences in "proton affinity" are plotted versus the observed relative rates of iodination in Figure 11 and are listed in Table 20. The energy of the position of greatest proton affinity is used in the plot where rate constants for specific positions are not determined experimentally. The correlation coefficient of the plot in Figure 10 is 0.996. It appears that the proton model proposed is a good one for electrophilic reactions. The model thus handles well methyl group interactions with the aromatic ring in the proton complex. The points of major deviation from the line are for the sterically hindered positions of o-xylene, mesitylene, and pentamethylbenzene. Such behavior helps to justify the assumption that there should be no steric problems for protonation equilibria.

That the Hammett relationship should hold for polymethylbenzene molecules is given some foundation by the CNDO calculations. The relative proton affinities calculated from the appropriate sum of proton affinities for the three positions in toluene are given in Table 20. In Figure 12 is a plot of the proton affinity calculated directly for each hydrocarbon versus that derived from the toluene values. The agreement appears to be

Reproduced with permission of the copyright owner. Further reproduction prohibited without permission.

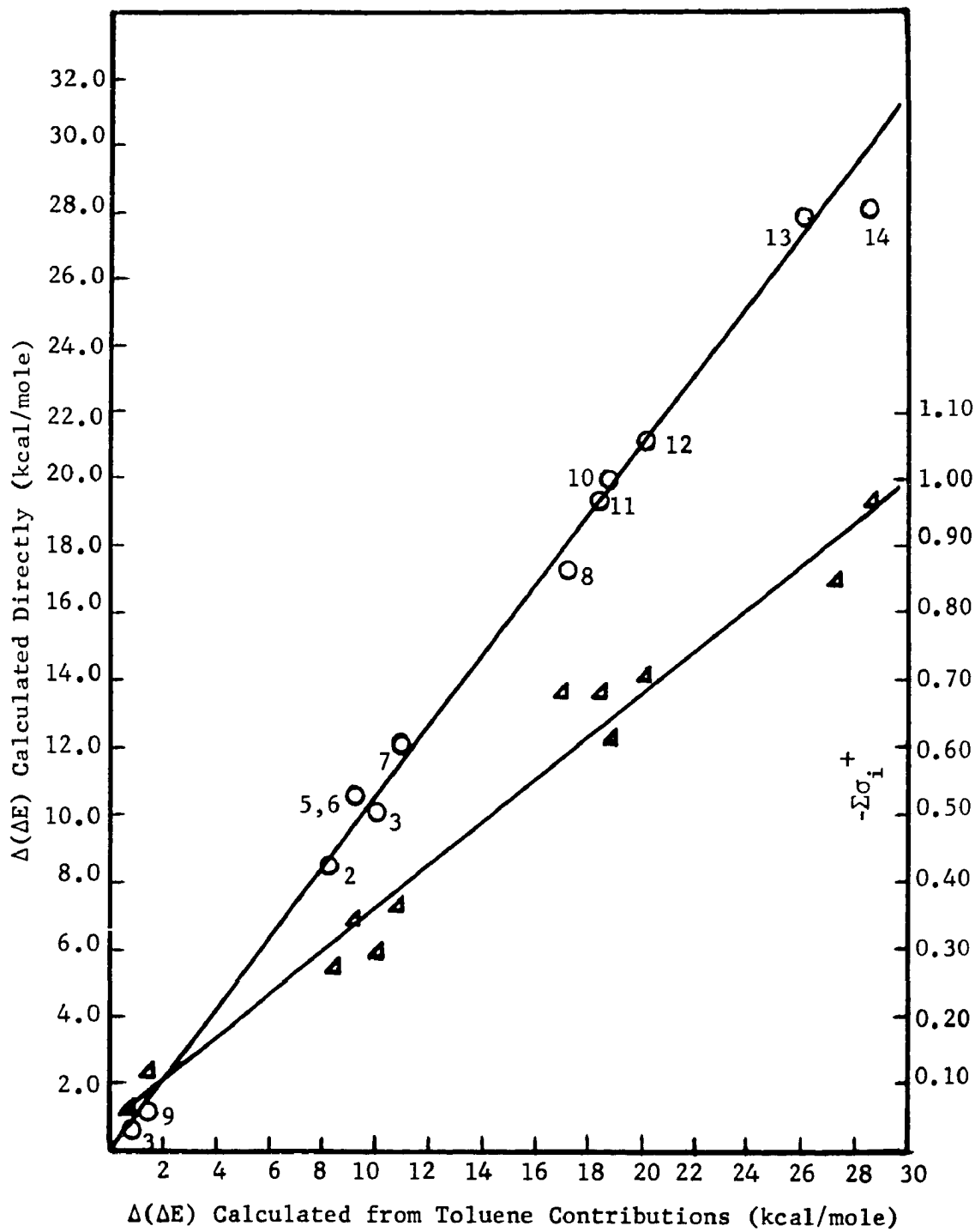

Figure 12. Additivity Principle Correlations.
(See Table 20 for legend.)

Reproduced with permission of the copyright owner. Further reproduction prohibited without permission.

very good. The slope is 1.03 (r=0.994). Since the slope is so near unity at least from CNDO calculations, the increase of the number of substituent methyl groups from one to five increases the proton affinity of benzene in a regular manner; there does not appear to be a "saturation point" beyond which increasing the number of methyl groups causes no change in the proton affinity. CNDO calculations have been often criticized, but as long as they work their use is justified! In this study they give a good account of the ability of methyl group to stabilize a positively charged closed shell system.

For direct comparison both proton affinities calculated directly and the Hammett parameters, $\Sigma\sigma_i^+$, for each hydrocarbon position are plotted in Figure 11 versus the respective proton affinities calculated from the toluene values. The correlation with both ordinate and abscissa is linear, showing that on a relative basis $\Sigma\sigma_i^+$ values parallel proton affinities. The slope of the plot is 0.032 (r=0.989).

In Table 21 are the valence shell atom electron populations resulting from the calculations for the ground state and proton complex of pentamethylbenzene, toluene, and the para-toluene proton complex. The indices, i, refer to the carbon atoms and the numbers quoted for the hydrogen atoms are the total electron density for all the hydrogen atoms attached to carbon atom i. The differences in the electron densities on going from the ground state to the proton complex are noted as Δ.

Some comment is necessary on comparing calculations of molecular properties other than energy. While ΔE may be essentially invariant to the methyl group's configuration, there is no requirement that the density matrix should be. As a result it will be assumed that the differences in

Reproduced with permission of the copyright owner. Further reproduction prohibited without permission.

Table 21. Ground State (G.S.) and Proton Complex (P.C.) Properties from CNDO Calculations

	Carbons			Hydrogens		
No.	G.S.	P.C.	Δ	G.S.	P.C.	Δ
			Pentamethylbenzene			
1	4.0433	4.0712	-0.0279	2.9652	2.8265	+0.1387
2	3.9698	3.8489	+0.1209	--	--	--
3	3.9974	4.0411	-0.0637	--	--	--
4	4.0451	4.0450	+0.0001	2.9665	2.8511	+0.1154
5	3.9770	3.8322	+0.1448	--	--	--
6	4.0482	4.0739	-0.0257	2.9603	2.8202	+0.1401
11	4.0309	4.0820	-0.0511	1.0089	1.7342	-0.7253
			Toluene			
1	4.0445	4.0756	-0.0311	2.9588	2.7309	+0.2279
2	3.9545	3.7908	+0.1637	--	--	--
3	4.0152	4.0572	-0.0480	1.0063	0.9437	+0.0626
4	3.9863	3.8461	+0.1227	1.0063	0.9432	+0.0640
5	4.0072	4.0786	-0.0714	1.0063	1.6880	-0.6817

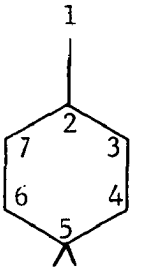

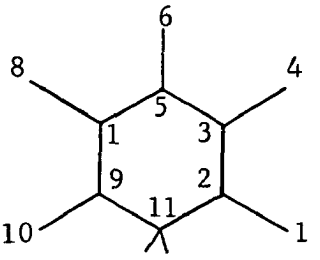

Reproduced with permission of the copyright owner. Further reproduction prohibited without permission.

electron densities and bond orders for particular atoms and bonds will be the chemically significant numbers. It is noted that the fact that a molecule bears a positive charge does not mean that all atoms in a charge molecule will have lower electron densities than in the parent molecule. In the pentamethylbenzene case, C_1 and C_6 have larger electron densities in the complex than in the parent hydrocarbon, while C_4 shows essentially no change. The methyl group in toluene shows behavior similar to C_1 and C_6 of pentamethylbenzene.

Two factors commonly are thought to directly affect the stability of a conjugated system bearing a formal charge, the ability of a substituent to stabilize the system by direct resonance interaction and an empirical rationalization that trisubstituted carbons bear a positive charge more readily than disubstituted carbons, and hence are better able to stabilize such a system. The comparison of the calculation of distribution of the charge in pentamethylbenzene and toluene on protonation to give a sigma complex shows that there is a theoretical justification for the two arguments above. On protonation of toluene the percent of a whole positive charge induced on the H_3 group is $100(\Delta) = 22.8$, and on the tertiary carbon 16.4 percent. This accompanied by an increase in the C_1-C_2 π bond order between C_4 and C_5 must be significant. Calculation shows that the methylene protons bear 31.8 percent of the charge and the C_4-C_5 π bond order is 0.364, significantly larger than the C_1-C_2 value, as well as the zero value for the C_4-C_5 π bond order implicated in the above structure. The charge in the toluene proton complex is 71.4 percent accounted for on considering the charge changes in the methyl group, the tertiary carbon, and the methylene group. Of the 71.4 percent, con-

Reproduced with permission of the copyright owner. Further reproduction prohibited without permission.

sidering the tertiary carbon and the methyl group as a charge absorbing unit accounts for 36.1 percent of the charge. Of the remaining 28.6 percent change of the total molecular charge, 24.5 percent is located on the carbon meta to the tertiary carbon.

It is interesting to note that, in the proton complex of toluene, the change in charge density on the hydrogens of positions 3 and 4 are the same, ca. +0.064, but that the difference on the associated ring carbons changes magnitude by 0.17 electrons. The cause of this may be the "completeness" of σ-π separability in the CNDO calculations or it may lie in the fact that the repulsion integrals used in the calculations have no directional character; they are a function of internuclear distance only.

In the pentamethylbenzene complex changes in electron density on an ortho, meta, and para position CH_3 group account, respectively, for 11.1, 11.5, and 11.4 percent of the formal charge. This shows about the same amount of charge on each CH_3 group regardless of the position! The charge picture changes somewhat when the ortho, meta, and para tertiary carbon changes are added to the above values. The ortho and para tertiary carbons have positive changes in charge of 0.120 and 0.144, respectively, while the meta tertiary carbon has a negative change of 0.0637. These numbers result in gross changes in charge for the tertiary carbon-methyl group units of 0.258, 0.232, and 0.052 for para, ortho, and meta, respectively. This order is the same as that expected by elementary resonance theory. To isolate so called inductive effects from resonance effects in the methyl group of the complex requires a comparison of the net change of charge on the methyl group with the change in the ring-methyl-carbon bond order. The C-CH_3 π bond orders change significantly on formation of

Reproduced with permission of the copyright owner. Further reproduction prohibited without permission.

the proton complex. For the para position the change is from 0.197 to 0.249, for the ortho 0.192 to 0.238, and for meta 0.192 to 0.186. These changes are +0.052, +0.046, and -0.006, respectively. Since the change in charge on each methyl group is the same within 2.0 percent, it is suggested that the inductive effect of each methyl group in stabilizing the sigma complex is the same. The changes in bond orders differ significantly for the three ring positions and have the same relative order of magnitude as the positive charges on the associated tertiary carbons. It is thus suggested that the resonance of the methyl group is accounted for by the change in the $C\text{-}CH_3$ π bond order.

Conclusions

The kinetics of the iodination of methyl-substituted benzene are very similar in general nature to other electrophilic reactions involving the same aromatic substrates and other halogens. In general, the reactivity of the hydrocarbon increases as the number of methyl groups is increased.

Using water as solvent, a numerical treatment of the thermodynamics of the inorganic portion of the mechanism is possible. It has been established that the halogenating agent is H_2OI^+ and that this reagent evolves from the hydrolysis of AgI_2^+. Of prime importance in the halogenation reaction studied here is the appearance of a primary proton isotope effect of approximately constant magnitude, 2.2 to 2.9, throughout the series of hydrocarbons studied. Insofar as it may be assumed that this isotope effect is approximately constant, then the relative rates of reactivity found reflect the relative rate of formation of sigma complexes; to wit,

Reproduced with permission of the copyright owner. Further reproduction prohibited without permission.

for compounds i and j

$$\frac{(k^*I)_i}{(k^*I)_j} = \frac{\left[\frac{k_2 K k_3 k_5}{k_{-2}(k_{-3} + k_5)}\right]_i}{\left[\frac{k_2 K k_3 k_5}{k_{-2}(k_{-3} + k_5)}\right]_j} \approx \frac{(k_3)_i}{(k_3)_j}$$

as a nearly constant isotope effect implies that $k_5/(k_{-3} + k_5)$ is approximately the same for all hydrocarbons studied. In light of the behavior of the mesitylene kinetics then, it is demonstrated that the kinetics of iodination of methyl substituted benzene by H_2OI^+ have some of the same specific properties of kinetic studies of chlorination and bromination. The presence of an isotope effect for these simply substituted hydrocarbons makes this halogenation study unique while at the same time, for all the compounds studied here, sigma complex formation is partially determining and the formation of halogenating agents can also be partially rate determining.

Another unique facet of this study is the quantitative treatment of the presence of Ag^+ and the effect of Ag^+ on the kinetics of iodination. The similarities between the relative rate of reaction among all the halogenation kinetics then, in conjunction with the good agreement of the rate constants for mesitylene determined both in the presence and absence of Ag^+, suggests that the behavior of Ag^+ is to affect only the inorganic portion of the reaction in a known, quantitative way. It may be stated that, on comparing kinetics at 10^{-6} M (I^-) and 10^{-11} M (I^-) effectively, Ag^+ serves solely to regulate the iodide concentration.

The variance of the ionic strength over a large range, from 10^{-5} M to $10^{-0.52}$ M has no adverse effect on the reaction and the major function

Reproduced with permission of the copyright owner. Further reproduction prohibited without permission.

of perchloric acid that controls the ionic strength at the higher ionic strength is to suppress the hydrolysis of I_2 to HOI, a reaction which is significant in the presence of Ag^+.

Not only have the kinetics of the hydrocarbons been studied, but a means was developed to study the activity, or ideality, of the hydrocarbons in aqueous media and it is verified experimentally that the hydrocarbons obey Henry's law in aqueous media over the ionic strength range used in this study.

Another area of investigation that is important to kinetic studies is the semiempirical molecular orbital calculations used to correlate the rate data obtained. It is found that a proton complex (sigma complex) model in conjunction with the CNDO/2 scheme is a useful combination with which to augment the understanding of the kinetic studies herein. Not only do the molecular orbital calculations correlate with the rate data well, but the dipole moment of the proton complex model serves to correlate the entropy of activation when used with a dipole model for the transition state.

Further, the "additivity principle" is accurately verified on comparing proton affinities for polymethyl-substituted benzenes.

Finally, it is not necessary to be skeptical about using pure water (as long as it is pure!) as a solvent for kinetic studies of reactions of nonpolar hydrocarbons.

Reproduced with permission of the copyright owner. Further reproduction prohibited without permission.

CHAPTER VI

RECOMMENDATIONS FOR FUTURE WORK

The techniques developed in the course of this work make possible kinetic studies of halogenation of aromatic molecules of reactivity comparable to benzene. Low solubilities of hydrocarbons in water do not present difficulties in the presence of a reactive halogenating agent such as H_2OI^+. Naphthalene and naphthalene-$\underline{d}_8$ can be studied, as well as 1-methylnaphthalene and its perdeutero analogue.

The bromination of relatively unreactive hydrocarbons dissolved in water in the presence of silver ion may also be studied. The unreacted bromine may be determined spectroscopically after reacting with an excess of iodide ion according to the equilibrium reaction

$$3I^- + Br_2 \rightleftarrows 2Br^- + I_3^-$$

As a result of the silver ion adsorption on AgI, it is suggested that possible association of silver ion with the iodine atom of iodobenzene may be studied by measuring the solubility of iodobenzene in aqueous silver nitrate solutions. After equilibration with iodobenzene, the aqueous layer may be quenched with iodide ion and extracted with isooctane. The optical density can be determined and compared to that of standard solutions. It is proposed that there may be strong adsorption of silver ion on the iodine atom due to the high polarizability of iodobenzene.

Reproduced with permission of the copyright owner. Further reproduction prohibited without permission.

APPENDICES

Reproduced with permission of the copyright owner. Further reproduction prohibited without permission.

APPENDIX A

SOLUTION TO GENERAL RATE EQUATION

In this appendix is given the solution in closed form for the general rate equation

$$\frac{-d(I_2)}{dt} = \frac{dx}{dt} = \frac{k^*I}{K_{sp}} \{(ArH)_o - x\} \{(I_2)_o - x - HOI\} \{(Ag^+)_o - x - HOI\}$$

where x is the product formed, HOI is the amount of I_2 that exists as HOI, and K_{sp} is the solubility product for AgI. In the remainder of the appendix, Ag^+ will appear without the charge sign and all concentrations will correspond to zero time, which is denoted above as ( ). Now HOI is related to x by

$$K' = \frac{K_h}{K_{sp}} = \frac{(HOI)(H^+)(I^-)}{(I_2) - x - HOI} \gamma_{\pm}^2 / (Ag^+)(I^-)\gamma_{\pm}^2$$

$$= \frac{(HOI)(H^+)}{\{(I_2) - x - HOI\}\{Ag) - x - HOI\}}$$

where $\gamma_{\pm}$ is the mean activity coefficient.

If

$$K \equiv (H^+)/K'$$

then

$$HOI = -x + \frac{(Ag + I_2 + K) - [(Ag + I_2 + K)^2 - 4K - 4(Ag)(I_2)]^{\frac{1}{2}}}{2}$$

Reproduced with permission of the copyright owner. Further reproduction prohibited without permission.

Defining the discriminant as W^2 gives

$$x = \frac{(Ag + I_2 + K)^2 - W^2}{4K}$$

and

$$dx = - \frac{WdW}{2K}$$

It will be useful to have the following definitions

$$\alpha \equiv Ag - I_2 - K$$

$$\gamma \equiv I_2 - Ag - K$$

$$\beta \equiv 4\{K(ArH) + (Ag)(I_2)\} - (Ag + I_2 + K)^2$$

It can be shown that the rate equation is now

$$\frac{-WdW}{dt} = \frac{k^*I}{K_{sp}} \frac{(\alpha+W)(\beta+W^2)(\gamma+W)}{8}$$

Defining the right side as

$$\frac{k^*I}{K_{sp}} \left(\frac{AW+B}{\beta+W^2} + \frac{C}{\alpha+W} + \frac{D}{\gamma+W} \right)$$

the new constants are

$$B \equiv \frac{\beta(\alpha+\gamma)}{(\alpha^2+\beta)(\gamma^2+\beta)}$$

$$C \equiv \frac{-\alpha}{(\alpha-\gamma)(\alpha^2+\beta)}$$

Reproduced with permission of the copyright owner. Further reproduction prohibited without permission.

$$D \equiv \frac{-\gamma}{(\alpha-\gamma)(\gamma^2+\beta)}$$

$$A \equiv -(C+D)$$

and

$$\frac{-k^*I}{8K_{sp}} \int dt = \int \frac{WdW}{(\alpha+W)(\beta+W^2)(\gamma+W)} \equiv \int \frac{(AW+B)dW}{(\beta+W^2)} + \int \frac{CdW}{(\alpha+W)} + \int \frac{DdW}{(\gamma+W)}$$

The sum of the second and third integrals is

$$C\ \ell n\ (\beta+W^2) + D\ \ell n\ (\gamma+W)$$

and the first part of the first integral is

$$\frac{A}{2}\ \ell n\ (\beta+W^2)$$

The second part of the first integral is dependent on the algebraic sign of β and

$$\int \frac{BdW}{\beta+W^2} = \begin{cases} \beta^{-\frac{1}{2}} \arctan\ (\beta+W^2) & \text{for } \beta > 0 \\ -(-\beta)^{-\frac{1}{2}}\ \ell n \left|\frac{(-\beta)^{\frac{1}{2}}+W}{(-\beta)^{\frac{1}{2}}-W}\right| & \text{for } \beta < 0 \end{cases}$$

The limits of integration for W are W evaluated for x at t=T and for x=t=0.

Reproduced with permission of the copyright owner. Further reproduction prohibited without permission.

APPENDIX B

SOLUTION TO BLANK REACTION EQUATION

The rate equation for blank reactions is

$$\frac{-d(I_2)}{dt} = \frac{dx}{dt} = \frac{k}{K_{sp}} \{(I_2) - x - HOI\} \{(Ag^+) - x - HOI\}$$

Utilizing some of the identities found in Appendix A, as well as the same method of solution, the rate equation becomes

$$\frac{-WdW}{dt} = \frac{k}{K_{sp}} \frac{(\alpha+W)(\gamma+W)}{2}$$

or

$$\frac{-kdt}{2K_{sp}} = \int \frac{WdW}{(\alpha+W)(\gamma+W)} \equiv \int \frac{AdW}{\alpha+W} + \int \frac{BdW}{\gamma+W}$$

for which

$$A \equiv -\frac{\alpha}{\gamma-\alpha}$$

$$B \equiv \frac{\gamma}{\gamma-\alpha}$$

Thus

$$\frac{-k}{2K_{sp}} \int_o^T dt = \frac{1}{\alpha-\gamma} [\alpha \ \ell n \ (\alpha+W) - \gamma \ \ell n \ (\gamma+W)]$$

The integration limits for W and t are the same as in Appendix A.

Reproduced with permission of the copyright owner. Further reproduction prohibited without permission.

APPENDIX C

SAMPLE CALCULATION

This appendix contains the contents of the computer printout for experiment 154 in which it was necessary to correct for a blank reaction. The formulae in Appendices A and B were employed.

Reproduced with permission of the copyright owner. Further reproduction prohibited without permission.

Rate Constants for Experiment #154

Stochiometric	ArH = 1.197 @ -02 M/L
Stochiometric	I_2 = 2.370 @ -06 M/L
Stochiometric	Ag^+ = 3.259 @ -05 M/L
Initial	H^+ = 1.0 @ -01 M/L
Initial	HOI = 1.413 @ -06 M/L
Initial	I_2 = 9.574 @ -07 M/L
Initial	Ag^+ = 3.118 @ -05 M/L
Initial	I^- = 8.546 @ -12 M/L

Blank Drop Slope = 1.065 @ -16
Error in Blank Drop Slope = 2.856 @ -19
Rate Constant Correction = 8.894 @ -15
Error in Rate Correction = 2.386 @ -17

Time (sec)	k*I (obs)	k*I (corr)	% Reaction
36570	1.317 @ -14	4.274 @ -15	34.40
43870	1.303 @ -14	4.137 @ -15	39.36
48070	1.296 @ -14	4.067 @ -15	42.02
56170	1.355 @ -14	4.653 @ -15	48.58
69335	1.356 @ -14	4.666 @ -15	56.03
84200	1.330 @ -14	4.411 @ -15	62.41
88429	1.349 @ -14	4.597 @ -15	64.72

Average = (4.40 ± 0.17) @ -15 sec^{-1}

Reproduced with permission of the copyright owner. Further reproduction prohibited without permission.

APPENDIX D

METHYL GROUP GEOMETRIES

The dihedral angles of the methyl group protons used in the molecular orbital calculation are presented here. The angles listed are defined with respect to counterclockwise rotation of the group about the ring-CH_3 bond. When viewed from the center of the aromatic ring, zero degrees is found in the ring plane to the right of the methyl carbon. Protons above the ring have angles between zero and 180°, and those below the plane have angles greater than 180° but less than 360°.

The locations of the methyl bearing carbons are found by counting around the ring counterclockwise from the reaction center, which is carbon number one.

Reproduced with permission of the copyright owner. Further reproduction prohibited without permission.

Methyl Group Geometries Used in Molecular Orbital Calculations

Hydrocarbon	Isomer	Methyl Group Locations	Methyl Hydrogen Angles (°)
Toluene	2-Me	2	60,180,300
	3-Me	3	60,180,300
	4-Me	4	60,180,300
o-Xylene	2,3-Di-Me	2	60,180,300
		3	60,180,300
	3,4-Di-Me	3	60,180,300
		4	60,180,300
m-Xylene	3,5-Di-Me	3	0,120,240
		5	60,180,300
	2,6-Di-Me	2	60,180,300
		6	0,120,240
	2,4-Di-Me	2	0,120,240
		4	60,180,300
p-Xylene		2	60,180,300
		4	60,180,300
Durene		2	0,120,240
		3	60,180,300
		5	0,120,240
		6	60,180,300
Prehnitene		3	60,180,300
		4	60,180,300
		5	60,180,300
		6	60,180,300
Mesitylene		2	60,180,300
		4	60,180,300
		6	60,180,300
Pentamethylbenzene		2	0,120,360
		3	0,120,360
		4	90,210,330
		5	60,180,300
		6	60,180,300

Reproduced with permission of the copyright owner. Further reproduction prohibited without permission.

BIBLIOGRAPHY*

1. E. Berliner, J. Chem. Educ., 43, 124 (1966).

2. U. Berglund-Larson and L. Melander, Arkiv Kemi, 6, 219 (1953).

3. E. Grovenstein, Jr. and U. V. Henderson, J. Am. Chem. Soc., 78, 569 (1956).

4. E. Grovenstein, Jr. and D. C. Kilby, ibid., 79, 2972 (1957).

5. E. Grovenstein, Jr. and N. S. Aprahamian, ibid., 84, 212 (1962).

6. R. J. Sullivan, "The Kinetics and Mechanism of the Iodination of Anisole, Phenol, p-Nitrophenol, and 2,4-Dinitrophenol," Ph.D. Thesis, Georgia Institute of Technology, 1968.

7. N. S. Gnanapragasam, Unpublished work done in the laboratories of Dr. E. Grovenstein, Jr., 1963-1965.

8. R. J. Sullivan, loc. cit., p. 150.

9. E. Baciocchi, Ric. Sci., 33 (II-A), 1121 (1963).

10. H. C. Brown and L. M. Stock, J. Am. Chem. Soc., 79, 5175 (1957).

11. Ibid., p. 1421.

12. E. Grovenstein, Jr. and A. J. Mosher, ibid., 92, 3810 (1970).

13. E. L. Mackor, P. J. Smit, and J. H. van der Waals, Trans. Faraday Soc., 53, 1309 (1957).

14. Y. Ogata and K. Aoki, J. Am. Chem. Soc., 90, 6187 (1968).

15. E. L. Mackor, A. Hofstra, and J. H. van der Waals, Trans. Faraday Soc., 53, 186 (1957).

16. D. A. McCauley and A. P. Lien, J. Am. Chem. Soc., 73, 2013 (1951).

17. M. Kilpatrick and F. Luborsky, ibid., 75, 577 (1953).

---

*Abbreviations used herein follow the form employed by Chemical Abstracts, Access 1 (1969).

Reproduced with permission of the copyright owner. Further reproduction prohibited without permission.

BIBLIOGRAPHY (Continued)

18. E. Baciocchi, G. Illuminati, G. Sleiter, and F. Stegel, ibid., 89, 125 (1967).

19. R. M. Keefer and L. J. Andrews, ibid., 79, 4348 (1957).

20. R. M. Keefer, A. Ottenberg, and L. J. Andrews, ibid., 78, 255 (1956).

21. M. J. S. Dewar, Tetrahedron, 19, Supp. 2, 89 (1963).

22. L. Salem, "The Molecular Orbital Theory of Conjugated Systems," W. A. Benjamin Inc., New York, 1966, p. 280.

23. J. A. Pople and G. A. Segal, J. Chem. Phys., 43, Supp. 136 (1965).

24. M. J. S. Dewar and E. Hasselbach, J. Am. Chem. Soc., 92, 590 (1970).

25. A. Streitweiser, Jr., P. C. Mowery, R. G. Jesaitis, and A. Lewis, ibid., 92, 6529 (1970).

26. G. Klopman, ibid., 86, 1463 (1964).

27. P. B. D. De La Mare and J. H. Ridd, "Aromatic Substitution," Butterworths Scientific Publications, London, 1959.

28. E. Berliner and F. Gaskin, J. Org. Chem., 32, 1660 (1966).

29. P. Alcais, F. Rothenberg, and J. DuBois, J. Chim. Phys., 63, 1443 (1966).

30. H. C. Brown and L. M. Stock, J. Am. Chem. Soc., 79, 1421 (1957).

31. R. A. Wirkkla and H. C. Brown, ibid., 88, 1447 (1966).

32. K. B. Wiberg, ibid., 90, 59 (1967).

33. N. S. Gnanapragasam, Unpublished data, 1964.

34. H. J. Lucas and E. R. Kennedy, "Organic Synthesis," Coll. Vol. II, John Wiley and Sons, Inc., New York, 1943, p. 351.

35. E. Baciocchi, G. Illuminati, G. Sleiter, and F. Stegel, loc. cit., p. 128.

36. R. J. Sullivan, loc. cit., p. 26.

37. Ibid., p. 25.

Reproduced with permission of the copyright owner. Further reproduction prohibited without permission.

BIBLIOGRAPHY (Continued)

38. Ibid., p. 26.

39. Ibid., p. 36.

40. Ibid., p. 41.

41. Ibid., p. 42.

42. C. McAuliffe, J. Phys. Chem., 70, 1267 (1966).

43. Chia-chi Yang, "The Solubilities of Benzene and Other Related Hydrocarbons in H_2O and D_2O," M.S. Thesis, Georgia Institute of Technology, 1967.

44. F. C. Schmalsteig, Private communication on work done in laboratories of Dr. E. Grovenstein, Jr., 1966.

45. R. J. Sullivan, loc. cit., p. 42.

46. N. S. Gnanapragasam, Unpublished data, 1965.

47. B. B. Owen and S. R. Brinkley, Jr., ibid., 60, 2233 (1938).

48. A. A. Frost and R. G. Pearson, "Kinetics and Mechanism," John Wiley and Sons, Inc., New York, 1961, p. 123.

49. R. Keefer, J. Blake, and L. Andrews, J. Am. Chem. Soc., 76, 3062 (1954).

50. I. M. Kolthoff and I. H. Elving, "Volumetric Analysis," Vol. I, John Wiley and Sons, Inc., New York, 1928, p. 153.

51. R. A. Durst, Editor, "Ion Selective Electrodes," National Bureau of Standards Special Publications 314, Washington, 1969, p. 417.

52. I. M. Kolthoff and I. H. Elving, loc. cit., p. 167.

53. Ibid., p. 162.

54. Karl Hellwig, Z. Anorg. Chem., 25, 183 (1900).

55. W. Frankenburger, Z. Physik Chem., 105, 225, 273 (1923).

56. I. M. Kolthoff and I. H. Elving, loc. cit., p. 167.

57. T. L. Allen and R. M. Keefer, J. Am. Chem. Soc., 77, 2957 (1955).

58. P. B. D. De La Mare, T. M. Dunn, and J. T. Harvey, J. Chem. Soc., 923 (1957).

Reproduced with permission of the copyright owner. Further reproduction prohibited without permission.

BIBLIOGRAPHY (Continued)

59. J. A. Pople and David Beveridge, "Approximate Molecular Orbital Theory," McGraw-Hill Book Company, Inc., New York, 1970, p. 163.

60. S. W. Benson, "The Foundations of Chemical Kinetics," McGraw-Hill Book Company, Inc., New York, 1960, p. 250.

61. I. W. Kolthoff and I. H. Elving, "Volumetric Analysis," Vol. II, John Wiley and Sons, Inc., New York, 1928, p. 233.

62. Elsevier Publishing Co., "Electrochemical Data," Amsterdam, 1952, p. 75.

63. G. R. Zolkind and S. I. Yavorskii, Izv. Akad. Nauk Turkm. SSR, Ser. Fiz-Teklin. Khim. i Geol. Nauk, 56 (1964); Chem. Abst., 62, 13899d (1965).

64. S. W. Benson, loc. cit., p. 91.

65. M. J. S. Dewar, "The Molecular Orbital Theory of Organic Chemistry," McGraw-Hill Book Company, Inc., New York, 1969, p. 284.

66. O. Schnepp and D. S. McClure, J. Chem. Phys., 26, 83 (1957).

67. A. J. Mosher, "The Reaction of Atomic Oxygen with Organic Compounds," Ph.D. Thesis, Georgia Institute of Technology, March, 1970, p. 33.

68. A. B. Littlewood, "Gas Chromatography," Academic Press, New York, 1970, p. 11.

69. V. Schievelbein, "The Electronic Structure of Square Nickel (II) and Copper (II) Complexes," Ph.D. Thesis, Georgia Institute of Technology, 1969, Chap. III.

70. Francis E. Condon, J. Amer. Chem. Soc., 70, 1964 (1948).

71. J. Dubois, P. Alcais, and F. Rothenberg, J. Org. Chem., 33, 439 (1968).

72. H. C. Brown and C. W. McCrary, J. Am. Chem. Soc., 77, 2310 (1955).

73. H. C. Brown, R. A. Balto, and F. R. Jenson, J. Org. Chem., 23, 417 (1958).

74. A. A. Frost and R. G. Pearson, loc. cit., p. 141.

Reproduced with permission of the copyright owner. Further reproduction prohibited without permission.

BIBLIOGRAPHY (Concluded)

75. "Handbook of Chemistry and Physics," The Chemical Rubber Co., Cleveland, 1966, p. C75-C601.

76. J. A. Pople and Paul Dobosh, Program No. 141, Quantum Chemistry Program Exchange, University of Indiana, Bloomington, Indiana.

77. N. C. Baird and M. J. S. Dewar, Program No. 136, Quantum Chemistry Program Exchange, University of Indiana, Bloomington, Indiana.

78. H. H. Jaffe, Chem. Rev., 53, 191 (1953).

Reproduced with permission of the copyright owner. Further reproduction prohibited without permission.

VITA

John Murray McKelvey, Jr. was born to John Murray and Joyce (Cates) McKelvey in Stanley, North Carolina on November 1, 1937. He attended public schools in Rome, Georgia and graduated from Rome High School in 1955. He received his A.B. degree in Spanish from Mercer University, and an M.S. degree in Chemistry from the University of Georgia. During his studies at the Georgia Institute of Technology, he was a research assistant and a teaching assistant. He was also an American Chemical Society Petroleum Research Foundation Fellow and was elected to membership in Sigma Xi. He was a member of the Atlanta Symphony Chamber Chorus, directed by Robert Shaw, for three years during his doctoral studies. He was chosen to participate in a National Science Foundation -- Centre Nationale de la Rechèrche Scientifique (France) Postdoctoral Exchange Program and will study in Paris, France.

Reproduced with permission of the copyright owner. Further reproduction prohibited without permission.